THE UNIVERSITY *of* EDINBURGH

The Novel Functions of Tribbles 1 in Macrophages

Yi-Hsia Liu

PhD Thesis

The University of Edinburgh

2012

Declaration

I, hereby, declare that the work presented in this thesis is the product of my own efforts, and the practical research on which it is based on my own except where stated in the text and in the acknowledgement section. This work has not been submitted in any other application for a higher degree.

Yi-Hsia Liu

Oct 2012

Acknowledgements

I would like to express my great gratitude to my supervisor Prof. David Argyle for the two great years being a member of his research group since my original supervisor left; for his encouragement, understanding, caring, and for his inspiring me to the field of inflammatory signalling pathways. Great thanks to Prof. Jonathan Lamb who is leading me to the field of Immunology. Great thanks to Dr. Darren Shaw for help with statistical analysis. To Rhona, who always helps me sort out my lab costs and gives me a warmly smile every day. To Dr. Karen Tan and Dr. Matylda Sczanieckato who always gives me a hand when I need help. I'd like to express my gratitude to my colleagues in the David's group, most notably Hannah, Thalia, Karen, Tom, Tina, Chen and Alex. Moreover, I also thank Prof. Morrison and his group members for giving me not only technical support but also emotional help. In addition, I would also like to thank my best friends from Taiwan and Robert Chou, Sophia Hsieh and Miray Tonk for their friendship and support.

Finally, I would like to thank my parents for their unconditional support both in emotional and in financial aspects, Yu-Hao and Chih-Chung for their endless support.

This is for you.

Abstract

Tribbles (Trib) protein was first described in *Drosophila* as a regulator of proliferation, later being implicated as a G_2/M modulator. In mammalian systems, three Trib gene family members have been identified, which share a conserved motif similar to the catalytic domain of serine/threonine kinases. However, they lack several conserved residues in the ATP-binding pocket and the core motif of the catalytic domain necessary for catalytic function. Tribbles 1 (Trib1) is involved in inflammation through its ability to regulate MAPK, NF-κB and the CCAAT Enhancer Binding Protein (C/EBP). Moreover, Trib1 is associated with human disease, such as atherosclerosis and acute myeloid leukaemia. In this thesis, I investigated the functional role of Trib1 in Toll-like Receptor (TLR)-induced inflammatory responses together with pro- or anti-inflammatory cytokines. The RAW264.7 myeloid cell line was stimulated with TLR2/9 ligands in the presence or absence of IFN-γ or IL-10. I observed a high level of Trib1 expression in the presence of IFN-γ and TLR2 ligands, but weak Trib1 expression following treatment with IL-10 and TLR9 ligands. In gene knock-down experiments using small interfering RNAs (siRNA) to reduce Trib1 expression, C/EBPβ was up-regulated in both stimulated (by IFN-γ and TLR2 ligands) and resting macrophage populations. TNF-α production was increased following Trib1 knockdown after treatment with IFN-γ and/or TLR2 ligands but IL-6 secretion remained unchanged. Furthermore, ERK1/2 expression was reduced in Trib1 siRNA-treated cells and failed to induce chemokinesis in macrophages. Finally, Trib1 was demonstrated to act as a modulator of cell cycle (G_2/M) transition and displays a delayed apoptotic phenotype.

The work in this thesis demonstrates that mammalian Trib1 contributes to the pro-inflammatory response and functions as a regulator of the ERK1/2 and C/EBPβ pathways following TLR ligand-mediated activation. Its novel functions include acting as a modulator of G_2/M arrest and suppressing macrophage migration.

Abbreviations

ACC	acetyl CoA carboxylase
AML	acute myeloid leukaemia
APC	antigen presenting cell
ATF4	activation transcription factor 4
ATP	adenosine triphosphate
BLP	bacterial lipoprotein
BM	bone marrow
BMM	Bone marrow derived macrophages
BSA	bovine serum albumin
C/EBP	CCAAT enhancer binding protein
COP-1	constitutive photomorphogenesis 1
COX-2	cyclo-oxygenase-2
Ct	cycle threshold
DC	dendritic cell
ddCt	delta-delta Ct
DMEM	Dulbecco's Modified Eagle Medium
DMSO	dimethylsulphoxide
DNA	deoxyribonucleic acid
dNTP	deoxynucleotide triphosphates
DTT	dithiothreitol
EMT	epithelial to mesenchymal transition
ERK	extracellular signal-regulated kinase
FACS	fluorescent-activated cell sorting

FAM	carboxyfluorescein
FBS	foetal bovine serum
FITC	fluorescein isothiocyanate
FOXO	forkhead box protein O
GAS	gamma-activated sequence
GAPDH	glyceraldehyde 3-phosphate dehydrogenase
GLME	generalised linear mixed effect
GFP	green fluorescent protein
GSK	glycogen synthase kinase
HRP	horseradish peroxidase
ICAM	intercellular adhesion molecule
IFN	interferon
iNOS	inducible nitric oxide synthase
IRAK	IL-1R-assaociated kinase
IRF	IFN gene regulatory factor
JAK	Janus kinase
JNK	c-Jun N-terminal kinase
kDa	kilo Dalton
LAM	lipoarabinomannan
LAP	liver activating protein
LDL	low density lipoprotein
LIP	liver inhibitory protein
LME	linear mixed effect
LPS	lipopolysaccharide

LTA	lipoteichoic acid
MAPK	mitogen-activated protein kinase
MAPKK	MAP kinase kinase
MCP	monocyte chemoattractant protein
MD2	myeloid differentiation 2
MIP	macrophage inflammatory proteins
MyD88	myeloid differentiation primary response protein 88
NF-κB	nuclear factor kappa B
ODN	oligodeoxyribonucleic acid
ox-LDL	oxidized low-density lipoprotein
PAMPs	pathogen-associated molecular patterns
PBS	phosphate buffered saline
PBST	phosphate buffered saline Tween 20
PCR	polymerase chain reaction
PGN	Peptidoglycans
PI	Propidium iodide
PI3K	Phosphatidylinositol 3-kinase
PMN	polymorphonuclear leukocyte
PPARα	peroxisome proliferator activated receptor-α
PRR	pattern recognition receptor
RA	retinoic acid
RNA	ribonucleic acid
RNAi	RNA interference
RNase	ribonuclease

RT	room temperature
RT-PCR	reverse transcription-polymerase chain reaction
SD	standard deviation
SDS	sodium dodecyl sulphate
SDS-PAGE	sodium dodecyl sulphate polyacrylamide gel electrophoresis
siRNA	small interfering RNA
SR	scavenger receptor
STAT	signal transduction and activation of transcription
TAE	tris acetate ethylenediaminetetraacetate
TAM	tumour-associate macrophages
TBS	tris-buffered saline
TBST	tris-buffered saline Tween-20
TEMED	tetramethylethylenediamine
TIR	Toll/IL-1 receptor
TIRAP	TIR domain-containing adaptor protein
TLR	Toll-like receptor
TNF	tumour necrosis factor
TRAF6	TNF receptor associated factor-6
Trib	Tribbles
TRAM	TRIF-related adapter molecule
TRIF	TIR domain-containing adaptor- inducing IFN-
VCAM	vascular cell adhesion molecular
WAT	white adipose tissue

Table of Contents

Index of Figures

Index of Tables

Chapter 1: General introduction

Failure to control inflammatory responses leads to many kinds of diseases. Inflammation is triggered not only in response to exogenous stimuli, such as pathogens, but also by chronic processes arising from tissue stress and malfunction, which now appear to be associated with the pathology of a number of modern diseases, including metabolic diseases and atherosclerosis. Innate immunity is the first line of host defence against pathogens, and many types of immune cells are implicated in this response, such as neutrophils, macrophages and dendritic cells. Among these cells, macrophages and dendritic cells are the key components of early inflammatory responses of the innate system and control the subsequent activation of adaptive immunity. Innate immunity involves not only cellular responses but also cytokine families, such as the interferon (IFN) family. Moreover, Toll-Like receptors (TLRs) play essential roles in activating downstream components to trigger inflammatory responses and then to activate the adaptive immune system. A recently discovered gene family, *Tribbles*, is involved in inflammation, and reports indicate that the encoded proteins contribute to chronic inflammatory responses, including those associated with atherosclerosis and cancers. However, their functions remain ill-defined and research findings are contradictory. Details of the function of Tribbles proteins will be presented in the following sections. The goals of this thesis are to discover novel roles for Tribbles in macrophages. This introduction provides a current review of the literature, and is followed by the general materials and methods section and three result chapters containing separate introduction, methods and discussion sections. The final chapter summarises and critically reviews the findings of this study and indicates future areas of research.

1.1 The innate immune system

Immunity is defined as resistance to disease, specifically infectious diseases (Murphy *et al.*, 2011). Host immune defence consists of two major interacting elements, the innate (non-specific) and adaptive (specific) immune systems. Innate immunity is the first line of defence against pathogens, including elements such as epithelial barriers, and provides protection mediated by both soluble (lysozymes) and cellular components (macrophages and neutrophils). Induced innate responses either succeed in clearing the infection (by phagocytosis) or hold it until an adaptive response develops (through antigen presenting cell (APC)-mediated T cell activation) (Boldrick *et al.*, 2002; Janeway *et al.*, 2001; Murphy *et al.*, 2011).

1.1.1 Induced responses of the innate immune system

Principle parts of the innate immune response are the cellular components. The main cell types involved in this process are macrophages or dendritic cells (DCs) and polymorphonuclear leukocytes (PMNs) (Dalton *et al.*, 1993; Janeway *et al.*, 2001). Macrophages are continuously differentiated by maturation of circulating monocytes. They are attracted by local innate inflammatory mediators and can cross the vascular endothelial barrier and migrate to sites of infection. After macrophages, neutrophils are the second most important family of phagocytes. Both types of phagocytic cells have important direct roles in the innate response because they recognise, ingest and destroy pathogens (Gordon, 2003; Janeway *et al.*, 2001). Macrophages migrate to areas with active phagocytosis, such as the skin, pulmonary alveoli, lymph node sinuses, connective tissues and hepatic sinusoids (Gordon and Taylor, 2005). Activated macrophages kill intracellular pathogens by generating nitric oxide and

reactive oxygen species. Natural killer (NK) cells develop in the bone marrow from the same progenitor cells as T and B lymphocytes and circulate in the blood. They do not express T or B cell antigen-specific cell surface receptors, but instead contribute to innate host defences through killing virus-infected cells and intracellular pathogen by releasing cytotoxic granules, without specific receptor binding (Janeway *et al.*, 2001).

Interactions between pathogens or pathogen products and pattern recognition receptors (PRRs), including TLRs, activates various signalling pathways that control the response to infections. Subsequently, cells of the innate immune system are activated and induce adaptive immune responses, for example T cell responses (Mills *et al.*, 2000). Therefore, the innate immune system plays a role in controlling and activating the adaptive immune system (Akira *et al.*, 2001; Janeway *et al.*, 2001; Murphy *et al.*, 2011).

Other components of the humoral innate response provide direct antimicrobial or antiviral effects. For example, lysozymes damage bacterial cell walls and type I IFNs reduce viral replication within cells. These functions will be addressed in section 1.2.2 (Janeway *et al.*, 2001; Ubol and Halstead, 2010).

1.1.2 Effector cells involved in the innate immune response: monocytes, macrophages and dendritic cells

Monocytes differentiate from myeloid lineage progenitor cells in the bone marrow before being released into bloodstream. After their release from bone marrow, monocytes differentiate into macrophages and migrate into tissues. Many reports indicate that IFN-γ is involved in the macrophage cell cycle and provides a cell

survival signal (Gordon, 2003).

Migration of macrophages into tissue occurs in response to inflammatory stimuli. Tissue resident macrophages generally differentiate from a Gr-1^{low} CX_3CR1^{high} $CCR2^-$ $CD62L^-$ subpopulation of murine monocytes, which are analogous in function to $CD14^+$ $CD16^+$ CX_3CR1^{high} $CCR2^-$ $CD62L^-$ human monocytes (Zhang and Mosser, 2008). During the inflammatory response, the dynamics of macrophage accumulation dramatically change. A substantial expansion of tissue macrophages results from the migration of immature blood monocytes into tissues, where they rapidly differentiate into macrophages. These migratory inflammatory macrophages typically form a Gr-1^{high} CX_3CR1^{low} $CCR2^+$ $CD62L^+$ subpopulation in mice, with a similar function to $CD14^{high}$ $CD16^-$ CX_3CR1^{low} $CCR2^+$ $CD62L^+$ human cells (Zhang and Mosser, 2008) (Fig. 1.1).

The heterogeneity of monocytes reflects their function specialisation in different anatomical locations. For example, macrophages from the alveolar region are distinct from thymic macrophages. There is a high level of pattern recognition receptor and scavenger receptor (SR) expression by alveolar macrophages, which are involved in clearing microorganisms, viruses and environmental particles within the lungs, whereas thymic macrophages function in the germinal centre to clear apoptotic lymphocytes generated during development of an acquired immune response (Gordon and Taylor, 2005).

Many transcription factors are involved in monocyte–macrophage differentiation. For example, PU.1 induces expression of the macrophage colony-stimulating factor receptor (Valledor *et al.*, 1998). Monocytic precursor cells recognizing macrophage colony-stimulating factor survive, proliferate and mature into monocytes. Moreover,

mature monocyte or macrophage phenotypes, such as the expression of CD11b, CD14 and CD18 and scavenger receptors, are regulated by PU.1 (Valledor *et al.*, 1998). In addition, macrophages express many cell surface receptors, such as SRs, which internalise modified low-density lipoprotein (LDL); mannose receptors, which recognise sugar components; and β-glucan receptors, which bind to apoptotic cells and invading pathogens and internalise them by phagocytosis (Gordon, 2003).

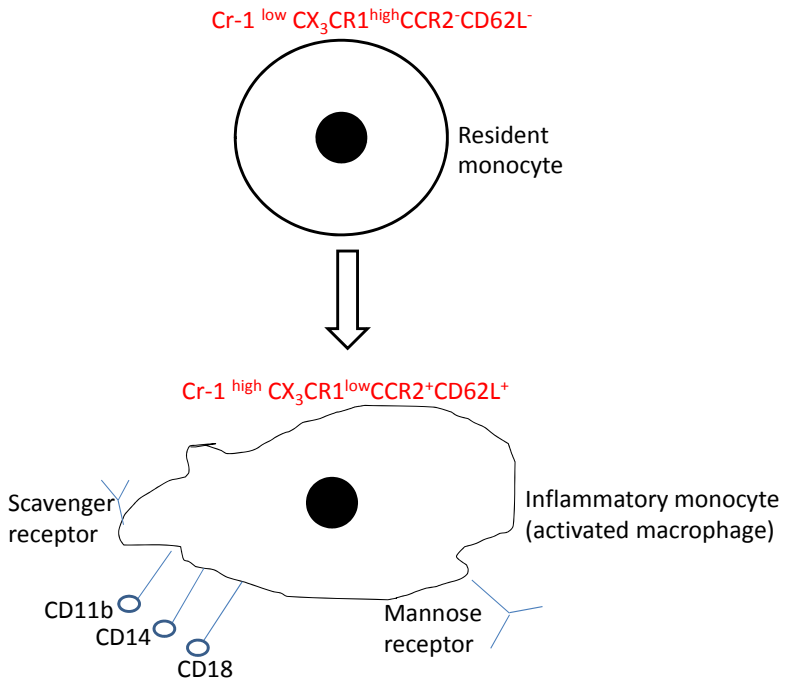

Figure 1.1. Development and function of monocyte subpopulations in mice. Resting monocytes, Gr-1^{low} CX_3CR1^{high} $CCR2^{-}$ $CD62L^{-}$, originate from the bone marrow. After stimulation by antigens, most inflammatory monocytes differentiate into macrophages, characterised as Gr-1^{high} CX_3CR1^{low} $CCR2^{+}$ $CD62L^{+}$. Mature monocytes express CD11b/CD14/CD18 and SRs.

DCs were discovered in 1973 by Steinman and Cohn, and were later identified as a group of immune cells important for both innate and adaptive immunity (Steinman and Cohn, 1973). DCs derive from both myeloid and lymphoid progenitors within the bone marrow and migrate via blood to tissues throughout the body and to peripheral lymphoid organs. Immature DCs reside in the epithelia of skin and mucosal tissues. They are characterised by a high endocytic function and low levels of surface histocompatibility complex class (MHC) and co-stimulatory molecules. Immature DCs do not directly kill microbes. During pathogen stimulation of immature DCs, surface MHC and co-stimulatory molecules are up-regulated. Two types of DCs exist: conventional and plasmacytoid. The main role of conventional DCs is to generate antigens that activate T cells, while plasmacytoid DCs are the main producers of antiviral interferons (Banchereau and Steinman, 1998).

Therefore, macrophages and DCs work to link innate and adaptive immunity.

1.1.3 Macrophage classification

The inflammatory environment affects macrophage differentiation, and the presence of certain cytokines regulates the phenotype and function of differentiated macrophages. Macrophages activated by TLRs and by IFN-γ induction are termed M1-type cells (Farrar and Schreiber, 1993; McCoy and O'Neill, 2008; Medzhitov, 2001). In contrast, macrophages exposed to Th2 cytokines, such as IL-4 and IL-13, or IL-10 and glucocorticoids have an alternatively activated phenotype (M2-type), characterised by a reduced ability to destroy intracellular bacteria. However, M2-type macrophages appear to function in the resolution of infection and in wound healing (Mantovani *et al.*, 2002; Mills *et al.*, 2000; Mosser, 2003; Sica *et al.*, 2008; Solinas *et*

al., 2009) (Fig. 1.2). IL-10 inhibits the production of pro-inflammatory cytokines, such as TNF-α, IL-6 and IL-12, in macrophages and inhibits antigen presentation by monocytes or macrophages by down-regulation of MHC II and co-stimulatory molecules (Haddad *et al.*, 2003; Moore *et al.*, 2001).

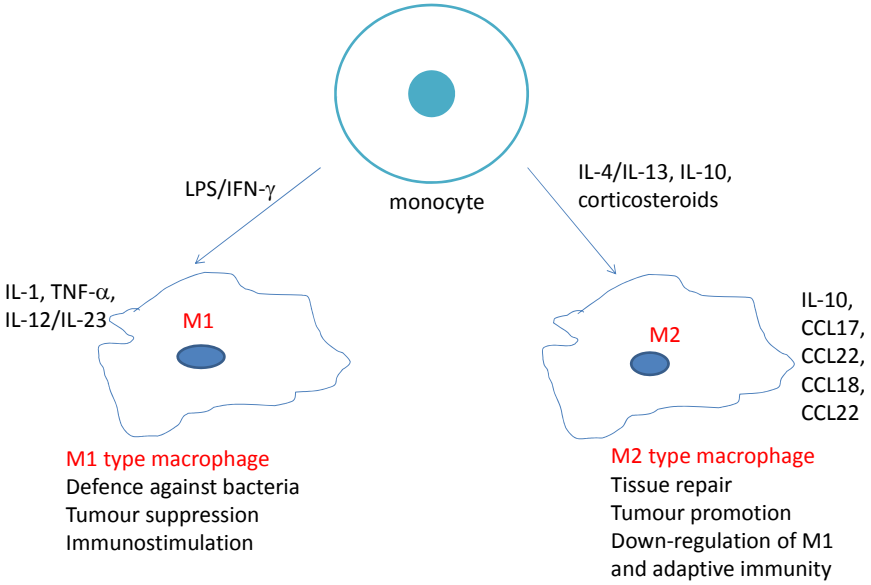

Figure 1.2. Polarisation of macrophage functions. Macrophages constitute an extremely heterogeneous cell population, which can be divided into two main classes: M1 and M2. M1 macrophages function in bacterial defence, tumour suppression and immunostimulation, whereas M2 macrophages are important in tissue repair and tumour progression.

1.1.4 Tumour-associated macrophages

In recent years, evidence has accumulated that macrophages play an important role in promoting tumour growth, progression and metastasis (Pollard, 2004). Indeed, similar to the different subtypes of resident tissue macrophages, macrophages residing in the tumour microenvironment exhibit distinct phenotypes and have been named tumour-associated macrophages (TAMs) (Gordon, 2003; Pollard, 2004). They have M2-phenotypes and contribute to a general suppression of antitumor activities (Martinez *et al.*, 2008; Pollard, 2004).

1.1.5 Potential functions of monocytes, macrophage and dendritic cells

The recruitment of monocytes and neutrophils from the blood to sites of inflammation is one of the most important functions of innate immunity. Recruitment of these cells takes place as part of the inflammatory response and is mediated by the expression of cell adhesion molecules on the surface of the endothelial cells of local blood vessels. Tissue macrophages provide an immediate defence against foreign pathogens and coordinate leukocyte infiltration (Martinez *et al.*, 2008). Adhesion and migration characterise both monocytes and macrophages. During inflammation, monocytes and neutrophils bind to adhesion molecules on endothelial cells and migrate into inflamed tissues where monocytes differentiate into macrophages (Juliano and Haskill, 1993). Intercellular adhesion molecule-1 (ICAM-1) is expressed on endothelium, epithelium and APCs (Janeway *et al.*, 2001). In addition to its role in cell adhesion, ICAM-1 contributes to monocyte–macrophage differentiation in inflamed tissues (Coccia *et al.*, 1999).

Monocytes can differentiate into either macrophages or DCs, both of which are professional APCs (Janeway *et al.*, 2001; Zhang and Mosser, 2008). DCs are more efficient APCs than macrophages because they constitutively express higher levels of cell surface markers than macrophages do. As a result, they rapidly capture antigens and transport them to lymph nodes. In addition, DCs are the major providers of MHC molecules required to activate T cells (Murphy *et al.*, 2011).

1.2 Signalling pathways in innate immunity

Cells of the immune system sense their environment and communicate with other cells using many different types of cell surface receptors. For example, Toll-like receptors (TLRs) detect microbial infection: pathogens ligate to immune TLRs present on the cell surface (TLR4) or on intracellular endosomes (TLR3). Interferons are produced by virus infected cells in response to viral infection and contribute to the innate antiviral defence mechanism.

1.2.1 Toll-like receptors (TLRs)

The involvement of Toll receptors in innate immunity was first described in the fruit fly, *Drosophila melanogaster*. *Drosophila* Toll was originally reported to establish dorso–ventral polarity during embryonic development but is also known to function in immunity (Belvin and Anderson, 1996; Medzhitov, 2001; O'Neill, 2004; Takeda *et al.*, 2003). Hultmark first identified Toll as an activator of the immune response in a *Drosophila* cell line (Rosetto *et al.*, 1995). *Drosophila* uses the Toll pathway to respond to Gram-positive bacterial and fungal infection (Belvin and Anderson, 1996). In contrast to *Drosophila* Toll, mammalian TLRs are not thought to be involved in development (Kimbrell and Beutler, 2001). Mammalian TLRs are type I transmembrane proteins that recognise most pathogenic microbes and are characterised by an extracellular domain containing leucine-rich repeats, a transmembrane region and an intracellular Toll/IL-1 receptor homology domain. TLRs are expressed by innate immune cells (dendritic cells, macrophages, NK cells), cells of the adaptive immune response (B lymphocytes) and non-immune cells (epithelial and endothelial cells, fibroblasts) (Medzhitov, 2001; Takeuchi and Akira, 2010). However, TLRs have limited specificity compared with antigen receptors of

the adaptive immune system. Stimulation of TLRs on cells of the innate immune system activates signalling pathways that initiate immune responses and inflammation as part of the antimicrobial response.

TLRs can bind to different ligands, including bacterial cell wall components, viral double-stranded RNA and immunomodulatory compounds (Takeda *et al.*, 2003). Based on their primary sequences, TLRs can be further classified into several categories depending on their recognition of pathogen-associated molecular patterns (PAMPs): the TLR1, TLR2 and TLR6 subfamily recognises lipoproteins; the closely related TLR7, TLR8 and TLR9 subfamily recognises nucleic acids (Akira *et al.*, 2006). TLR1, TLR2, TLR4, TLR5 and TLR6 are expressed on the cell surface and TLR3, TLR7, TLR8 and TLR9 are expressed exclusively in intracellular compartments, such as endosomes, and their ligands, mainly nucleic acids, require internalisation to the endosome before TLR binding can be achieved (Krishnan *et al.*, 2007). Ten TLRs have been reported in humans and 11 in mice. However, the ligand for TLR10 has not yet been identified (Takeuchi and Akira, 2010); Table 1.1).

Table 1.1. TLRs and their ligands

TLR	Location	Ligand and its origin	Cellular distribution
TLR1–TLR2 heterodimer	Plasma membrane	Triacyl lipoprotein / bacteria	Monocytes/macrophages, DCs, mast cells, eosinophils
TLR2–TLR6 heterodimer	Plasma membrane	Diacyl lipoprotein / bacteria, viruses, parasites	Monocytes/macrophages, DCs, mast cells, eosinophils
TLR3	Endosome	dsRNA / virus	DCs, NK cells
TLR4	Plasma membrane	LPS / bacteria, viruses	Macrophages, DCs, mast cells, eosinophils
TLR5	Plasma membrane	Flagellin / bacteria	Macrophages, DCs, intestinal epithelium
TLR7, TLR8	Endosome	ssRNA/ virus, bacteria	Plasmacytoid DCs, NK cells, eosinophils, B cells
TLR9	Endosome	CpG DNA / virus, bacteria, protozoa	Plasmacytoid DCs, eosinophils, B cells
TLR10	Endosome	Unknown	Plasmacytoid DCs, eosinophils, B cells
TLR11 (mouse only)	Plasma membrane	Profiling-like molecule / protozoa	Macrophages, DCs, liver, kidney, bladder epithelial cells

This table was modified from Janeway's Immunobiology (Murphy *et al.*, 2011).

1.2.1.1 TLRs and innate immunity

TLRs play a central role in the immune response by detecting invading pathogens, triggering the initiation of innate immunity and helping to strengthen adaptive immunity (Akira *et al.*, 2006; Medzhitov, 2001; Takeuchi and Akira, 2010). Innate recognition of PAMPs by TLRs initiates a signalling cascade that results in transcription of many immune and inflammatory genes. As well as initiating an innate immune response, there is increasing evidence to suggest that TLRs also play a role in other macrophage functions, such as phagocytosis, antigen processing, presentation and initiating the adaptive immune response (McCoy and O'Neill, 2008; Pasare and Medzhitov, 2004; Schnare *et al.*, 2001). Macrophages express most of the ten TLRs (summarised in Table 1.1; (McCoy and O'Neill, 2008). In an early study,

mRNA expression of TLRs 1–5 was analysed in a human leukocyte population containing monocytes, T lymphocytes, NK cells, DCs and granulocytes (Alan, 2001; McCoy and O'Neill, 2008). TLR1 was expressed on all of these cell types, whereas TLR2, TLR4 and TLR5 were expressed on monocytes or macrophages, DCs and granulocytes (Alan, 2001; McCoy and O'Neill, 2008). In contrast, TLR3 is expressed on DCs, NK cells and plays an important role in the antiviral immune responses by producing type I IFNs (Funami *et al.*, 2004; Muzio *et al.*, 2000). TLR4 is expressed on monocytes and macrophages in both humans and mice. TLR9 is constitutively expressed on DCs and has an essential role in antiviral immunity (Ashkar and Rosenthal, 2002; Kato *et al.*, 2005; Wan *et al.*, 2011). Sequence analysis indicates that TLR10 is related to TLR1 and TLR6. Mice do not express TLR10, but they express additional TLRs that are absent in humans, such as TLR11 (Takeuchi and Akira, 2010), which is similar to TLR5 and is expressed in response to protozoan infection (Pifer *et al.*, 2011).

Among TLR family members, TLR2 and TLR4 have been most intensely studied as they are regarded to be the major transmembrane TLRs. TLR2 identifies lipoteichoic acid (LTA) and lipoproteins from a variety of Gram-positive and Gram-negative bacteria, mycobacteria and fungi. Stimulation through TLR2 induces the expression of specific transcripts for pro-inflammatory cytokines. Moreover, TLR2 forms heterodimers with TLR1 or TLR6 detect specific lipid components of lipoproteins. For instance, TLR2–TLR1 heterodimers recognise triacyl lipopeptides, whereas TLR2–TLR6 heterodimers recognise diacyl lipopeptides (Kaisho and Akira, 2006; Liu *et al.*, 2006; Santos-Sierra *et al.*, 2009; Takeuchi *et al.*, 2001). Stimulation of TLR2 by, for example, diacyl lipoproteins in macrophages and DCs, induces the

production of pro-inflammatory cytokines. TLR2 expression has been reported to induce type I IFNs in monocytes in response to viral infection (Barbalat *et al.*, 2009). Therefore, the cellular responses to TLR2 differ depending on cell type. Furthermore, TLR2 plays a key role in the macrophage response to streptococcus species and *Mycobacterium tuberculosis* in mouse disease models and in humans (Draper *et al.*, 2006; McBride, 2010; Sabroe *et al.*, 2008). The C-terminus of TLR2 also participates in anti-fungal and anti-protozoan immunity (Gazzinelli *et al.*, 2004; Simitsopoulou *et al.*, 2008).

TLR4 is the best-studied TLR and was the first to be identified (Akira, 2003; Kaisho and Akira, 2001). TLR4 recognises LPS and the myeloid differentiation 2 (MD2) adaptor protein and its co-receptor CD14 (Kaisho and Akira, 2001). Stimulation with LPS activates macrophages and triggers downstream production of inflammatory cytokines, such as IL-1, IL-6 and TNF-α (Kaisho and Akira, 2001). Interestingly, TLR4 recognises not only bacterial components but also viral proteins such as a fusion protein from the Respiratory syncytial virus (Kurt-Jones *et al.*, 2000; Uematsu and Akira, 2007). Additionally, TLR4 was reported to regulate the pathogenesis of Influenza virus (H5N1)-induced acute lung injury (Imai *et al.*, 2008).

1.2.1.2 TLR signalling pathways

TLR signalling, regardless of which receptor is stimulated, results in the activation of NF-κB and downstream regulatory responses (Fig. 1.3). TLR3, TLR7 and TLR8 also mediate the activation of IFN gene regulatory factor-3 (IRF3) and IRF7 to trigger type 1 IFN induction (Akira *et al.*, 2006; Kaisho and Akira, 2001). The signalling events initiated by TLR activation are mediated by a unique interaction

between Toll/IL-1 receptor (TIR) domain-containing cytosolic adaptors, including myeloid differentiation primary response protein 88 (MyD88), the TIR domain-containing adaptor protein (TIRAP), the TIR domain-containing adaptor-inducing IFN-β (TRIF) and the TRIF-related adapter molecule (TRAM) (Akira *et al.*, 2006; Kaisho and Akira, 2001). MyD88 is the central adaptor protein associated with IL-1R-assaociated kinase (IRAK) 4, which in turn recruits and phosphorylates IRAK1 and IRAK2. Following interaction with TNF receptor associated factor-6 (TRAF6), the activated IRAK complex phosphorylates TAB1 and TAK1, which then activate NF-κB and mitogen-activated protein kinase (MAPK) pathways that mediate inflammatory responses through expression of pro-inflammatory cytokines (IL-1β, IL-6, IL-8, IL-12 and TNF-α) and macrophage inflammatory proteins (MIPα and MIPβ) (Akira, 2003; Takeuchi and Akira, 2010).

Recently, two CCAAT/enhancer-binding proteins (C/EBPs) family members have been reported to have roles in TLR-induced downstream signalling. In addition to their roles in conventional MyD88/TRAF/NF-κB signalling, C/EBPs β and δ are important transcription factors in a MyD88-dependent pathway that regulates the induction of pro-inflammatory cytokines, i.e. TNF-α production (Lu *et al.*, 2009) (Fig. 1.4).

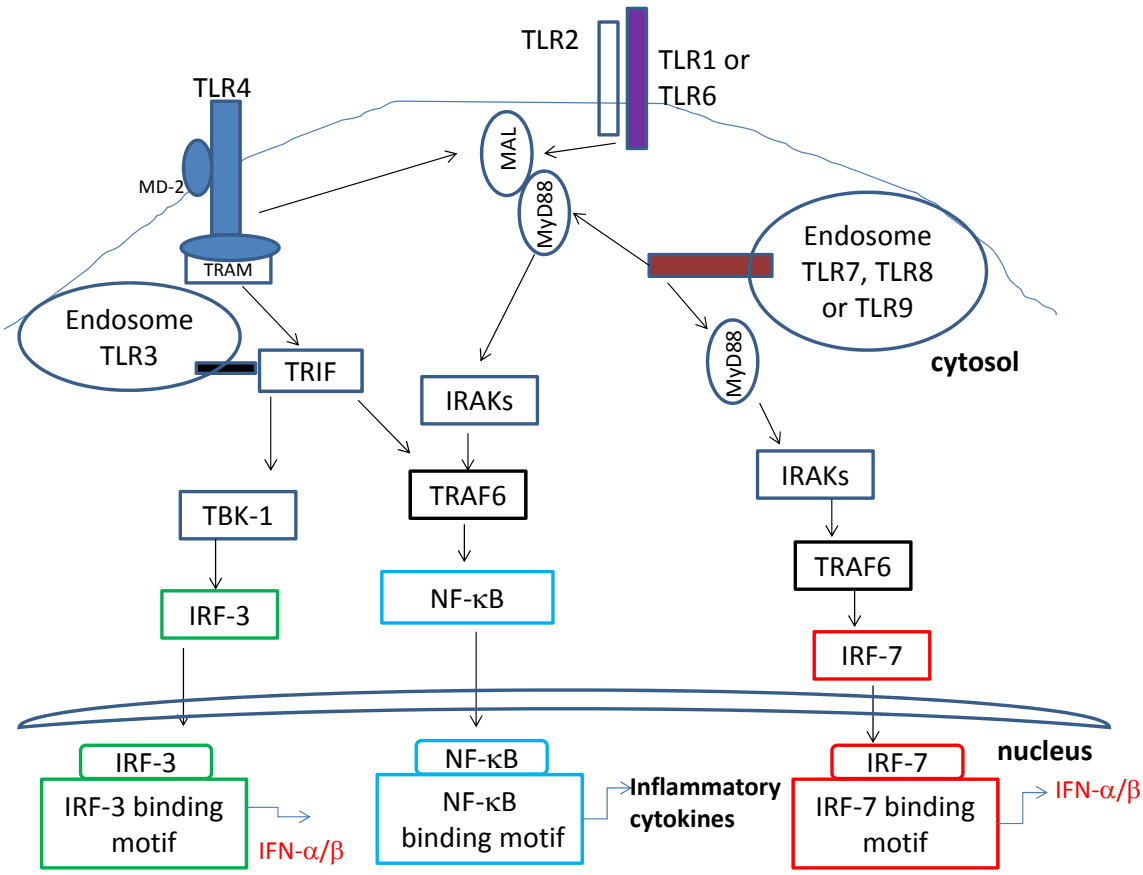

Figure 1.3. TIR-containing adaptors in TLR signalling. TLR signalling is divided into two main pathways: MyD88-dependent and MyD88-independent. Therefore, the MyD88 adaptor molecule is the key mediator of TLR signalling. The MyD88-dependent pathway is used by all TLRs except for TLR3. TLR7, TLR8 and TLR9 interact directly with MyD88 following ligand binding, while TLR4 and TLR2 (which forms a heterodimer with either TLR1 or TLR6) bind to the bridging adaptor Mal in order to recruit MyD88. Following MyD88 recruitment to activated TLRs stimulates the binding of IRAKs (IRAK1/4). IRAKs then activate TRAF6, which in turn activates the IKK complex, leading to phosphorylation and subsequent degradation of IκB. This process induces nuclear translocation of NF-κB and the induction of inflammatory cytokines. Activation of TLR7, TLR8 and TLR9 lead to the nuclear translocation of IRF-7, resulting in type I IFN expression. In contrast, the MyD88-independent pathway is only used by TLR3 and TLR4, and involves the TIR-adaptor molecule, TRIF. TRIF activates TBK1, which causes activation and nuclear translocation of IRF-3, resulting in type I IFN production. Similar to the MyD88-dependent pathway, TLR4 signalling via the MyD88-independent pathway requires a bridging adaptor, in this case TRAM. The MyD88-independent pathway leads to NF-κB activation via TRIF activation (adapted from Jenkins *et al.*, 2010).

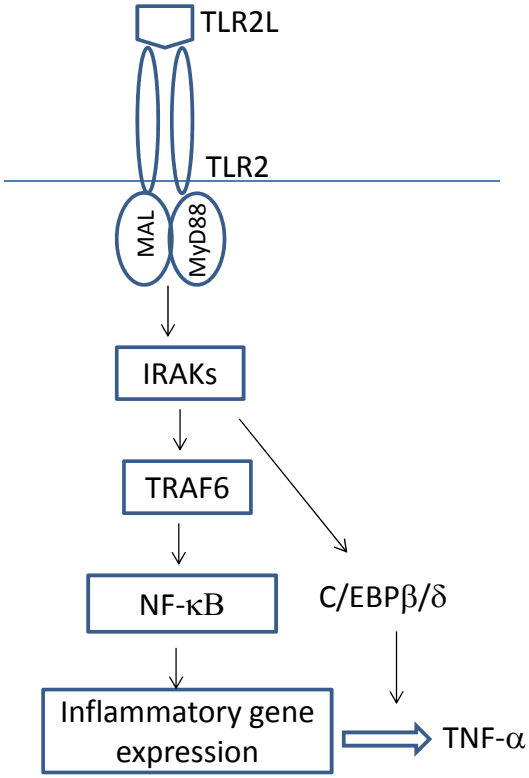

Figure 1.4. The TLR2 signalling pathway is regulated by C/EBPs β and δ. In addition to the well-known TLR2 signalling cascade (MyD88/TRAF/NF-κB), CEBPs β and δ transcription factors can mediate pro-inflammatory cytokine production. MyD88 recruited to activated TLRs binds to IRAK4, which then activates C/EBPs β and δ that induce inflammatory gene expression.

1.2.2 Type I and type II IFNs

Viral infection induces the expression of interferon proteins (IFNs), which interfere with viral replication. There are two types of IFNs: IFNs-α and β are type I IFNs and were first described over 50 years ago, while IFN-γ is a type II IFN. IFN-α and IFN-β are produced at the early stages of viral infection and have important roles in the response to intracellular pathogens (Murphy *et al.*, 2011; Trinchieri, 2010). Most type I IFNs are believed to be secreted by plasmacytoid DCs. Plasmacytoid DCs express the intracellular endosomal receptors TLR7 and TLR9 in response to single-stranded RNA and DNA viruses, respectively, by triggering signal transduction through MyD88 and inducing the downstream production of IFN-α/β via IRF7 (see Fig. 1.3) (Colonna *et al.*, 2004; Trinchieri, 2010). Therefore, IFN-α/β plays a key role in DC maturation and differentiation, and in B cell activation (Christian, 2000; Montoya *et al.*, 2002). Later studies indicated that IFN-α/β directly suppress viral replication and protect APCs from viral infections (Zhang *et al.*, 2008).

IFN-γ is distinct from type I IFNs at both the genetic and protein levels (Farrar and Schreiber, 1993). IFN-γ is secreted by $CD4^+$ T helper cell type 1 (Th1) lymphocytes, $CD8^+$ cytotoxic lymphocytes and NK cells. Recent evidence indicates that other cells, such as B cells and NKT cells, also produce IFN-γ (Murphy *et al.*, 2011). IFN-γ secretion by APCs is likely to be an important early host defence against infection. For instance, IFN-γ secretion results in increased expression of MHC class I and II molecules on APCs, whereas T cells are the major source of IFN-γ in the adaptive immune response (Farrar and Schreiber, 1993; Janeway *et al.*, 2001).

1.2.2.1 IFNs and activated macrophages

Macrophages are an important cellular source of IFNs in the immune system. Previous studies indicated that low level constitutive expression of IFN-α/β occurs in resting macrophages, and that macrophage IFN-α/β expression is up-regulated following viral infection and is stimulated by dsRNA or exposure to microbial products (Christian, 2000). In contrast, IL-4 and IL-10 suppress the production of IFN-α/β in mouse and human macrophages (Christian, 2000).

More importantly, pathogen-induced IFN-γ is a potent macrophage activator that orchestrates leukocyte recruitment and regulates the growth, maturation and differentiation of many cell types (Christian, 2000; Farrar and Schreiber, 1993). Classical activation of macrophages by IFN-γ is mediated by Signal Transduction and Activation of Transcription-1 (STAT1) signalling and comprises two essential aspects of macrophage function, antigen processing and presentation, as well as antimicrobial and antiviral effector mechanisms. For instance, the transporter associated with antigen processing (TAP) gene and the MHC heavy chains (β2-microglobulin) are direct up-regulated during antigen presentation mediated by STAT-1 (Briscoe *et al.*, 1996; Pestka *et al.*, 1997; Schroder *et al.*, 2006). To efficiently kill intracellular pathogens, such as mycobacteria, macrophages need help from the adaptive immune system, mainly in the form of IFN-γ provided by T cells (Hickman *et al.*, 2002; Lang, 2005).

1.2.2.2 General principles of IFN signalling pathways

IFN-γ and IFN-α/β both initiate the Janus kinase (JAK)–STAT signalling pathway, but involve different components (Briscoe *et al.*, 1996; Ramana *et al.*, 2001); (Figs.

1.5 and 1.6). The IFN-γ-induced JAK–STAT1 signalling regulates macrophage activation and function. IFN-γ binding to the IFNGR cell surface receptor leads to tyrosine phosphorylation and activation of JAK kinases 1 and 2, which facilitates transphosphorylation of both JAKs and receptor subunits. STAT1 is then recruited to the receptor and becomes phosphorylated on Tyrosine^{701}, enabling STAT1 to homodimerise (Briscoe *et al.*, 1996; Wen *et al.*, 1995). The STAT1 homodimer translocates to the nucleus, binds to transcription factor response elements, such as the Gamma-Activated Sequence (GAS) in target gene promoters, and initiates transcription (Decker *et al.*, 1997). IFN-γ predominantly activates STAT1, which mediates enhanced microbial killing by IFN-γ by increasing MHC class I and II expression and inflammatory cytokine production (Chatterjee-Kishore *et al.*, 2000; Hu *et al.*, 2008). AP-1 transcription factors are rapidly activated by IFN-γ independent of JAK1/2 and STAT-1 (Gough *et al.*, 2007).

IFN-α/β binding to IFNAR 1 and 2 cell surface receptors similarly leads to receptor-associated JAK kinase 1 and 2 activation and tyrosine kinase 2 (Tyk2) phosphorylation, and transphosphorylation of JAKs and receptor subunits. Subsequently, cytoplasmic STAT1 and STAT2 are phosphorylated by JAK and Tyk2 respectively, translocated to the nucleus, bind to transcription factor-binding sequences, such as the IRF7 and ISRE (IFN-stimulated response element) response elements in target gene promoters, and initiate transcription (Fig. 1.6; (Christian, 2000).

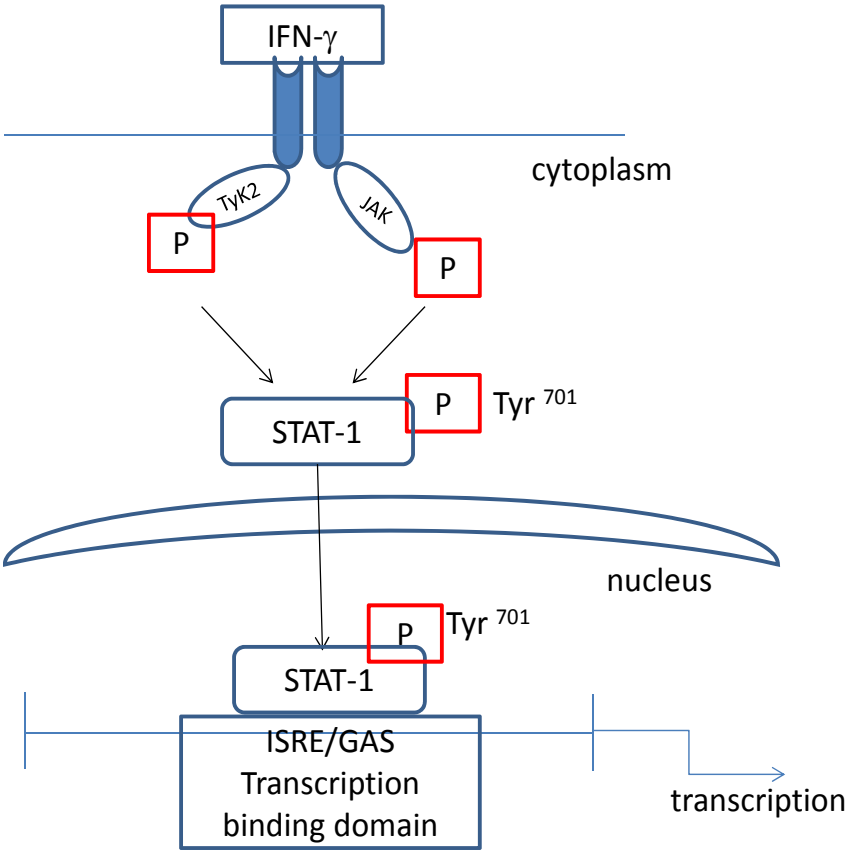

Figure 1.5. The IFN-γ signalling cascade. IFN-γ binds to IFNGR and JAK/TYK2, which are then phosphorylated. Subsequently, STAT-1 becomes phosphorylated at Tyr^{701} and is translocated to the nucleus, where it binds to ISRE and GAS (ISRE/GAS) response elements in target genes, such as MHC class I and β2-microglobulin, resulting in their transcription.

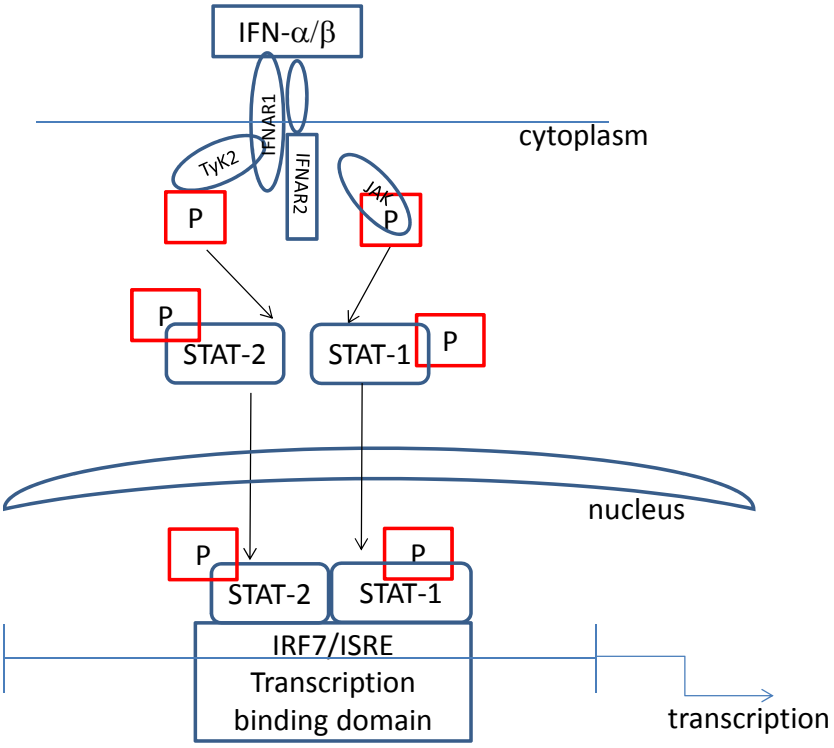

Figure 1.6. IFN-α/β signalling and target gene activation. IFN-α/β bind to IFNAR1/ IGNAR2, leading to JAK/Tyk2 activation and phosphorylation. Subsequently, STAT-1 and STAT2 become phosphorylated, are translocated into the nucleus, bind to the IFN-α/β - stimulated response element (ISRE) and the IRF7 binding sequence in target genes, such as MHC class I, and stimulate their transcription.

1.2.3 Other signalling pathways control downstream pro-inflammatory cytokine production

The pro-inflammatory cytokines, such as IL-1β, IL-6, IL-8 and TNF-α, are important cytokines that induce inflammatory responses and trigger the immune response. As previously mentioned, TNF-α production is not only induced by TLRs but also by other signalling proteins, including members of the MAPK and C/EBP families.

1.2.3.1 Biological functions of the MAPK pathway

The MAPK family consists of both stress-activated and mitogen-activated protein kinases. The MAPK pathway mediates signal transduction from cell surface receptors to downstream transcription factors, leading to cellular responses such as cell proliferation, growth, motility, survival and apoptosis (Robinson and Cobb, 1997). These kinases are activated by conserved upstream protein kinase signalling modules, MEKs, which activate MAPK by dual-site phosphorylation on threonine and tyrosine residues within a Thr-X-Tyr motif located in protein kinase subdomain VIII (Widmann *et al.*, 1999).

The classical MAPK cascade is activated by mitogens and growth factors or by cytokines that control cell growth and differentiation (Robinson and Cobb, 1997; Seger and Krebs, 1995). There are three major classes of MAPKs. The first is the extracellular signal-regulated kinases (ERK1/2) that acts through the Ras–Raf–MAPK kinase pathway to regulate meiosis, mitosis and post-mitotic modification in differentiated cells (Seger and Krebs, 1995). Ras–GTP activates the Raf serine/ threonine kinase, which in turn phosphorylates and activates the MEK1 and MEK2

dual-specificity kinases via a series of intermediate kinases. MEKs 1 and 2 then phosphorylate ERK1 and ERK2, which are then translocated to the nucleus where they regulate the activity of various transcription factors, including cyclin D1, jun, fos and myc. Cyclin D1 is important in cell cycle progression, and jun, fos and myc are proto-oncogenes (Roberts and Der, 2007). ERKs are predominantly activated by growth factors or phorbol esters but can also be induced by TNF-α and IL-1 (Gortz *et al*., 2005; Roberts and Der, 2007). Once activated, ERKs phosphorylate a number of cellular substrates that can trigger diverse signalling cascades, and accumulating evidence suggests an important role for ERKs in the regulation of inducible nitric oxide synthase (iNOS) generation in macrophages via NF-κB dependent pathways (Jaramillo *et al.*, 2004). Moreover, the ERK1/2 pathway regulates Bcl2 family proteins to promote cell survival (Balmanno and Cook, 2008).

The c-jun N-terminal kinases (JNK1, JNK2 and JNK3) are important for controlling programmed cell death (Tournier *et al.*, 2000). The JNK signalling cascade is activated by stress, bacterial infection and pro-inflammatory cytokines, and results in phosphorylation of AP1 transcription factors (Seger and Krebs, 1995). JNK is involved in infection-related inflammation and septic shock, which suggests that JNK activation may prevent acute inflammation (Kaminska, 2005). The last major MAPK class is the p38 kinases (α, β, γ, δ), which are activated by various pro-inflammatory and stress stimuli, similar to JNK activation (Lee *et al.*, 1994). In addition, p38 is a well-studied participant in inflammatory responses, mediating inflammatory cytokines, such as IL-1, IL-6, IL-8 and TNF-α, that lead to immune responses involved in both inflammation and cancer development (Lee *et al.*, 1994; Yong *et al.*, 2009). Therefore, p38 may be a suitable therapeutic target for controlling

these disease processes (Yong *et al.*, 2009).

Table 1.2. Summary of the MAPK members

Family member	ERK	JNK	P38
Synonym	p42/p44	SAPK1	SAPK2
Molecular weight (kDa)	42/44	48–52	41
Isoforms	ERK1/ERK2	JNK1–3	α/β/γ/δ
Location	Cytosolic, nuclear	Cytosolic, nuclear	Cytosolic, nuclear
Upstream activators	MEK1, MEK2	MKK4, MKK7	MKK3, MKK6
Activators	Mitogens, cytokines	Stress, cytokines	Stress, cytokines
Physiological function	Immune function, differentiation and cell survival	Immune function, differentiation and apoptosis	Immune function, differentiation and apoptosis

This table was modified from the Sigma-Aldrich–RBI handbook.

1.2.3.2 The importance of the CCAAT enhancer-binding protein pathway

Regulation of the C/EBP by IFN-γ and TLRs

C/EBPs belong to a large family of bZIP transcription factors (Akira and Kishimoto, 1997). In mammalian systems, C/EBP members participate in a number of physiological activities, including fat storage, tissue differentiation, growth, proliferation, apoptosis, immune responses and anti-bacterial defence (Anastasov *et al.*, 2010; Darlington *et al.*, 1998; Gade *et al.*, 2008; Poli, 1998; Pradervand *et al.*, 2006; Zahnow *et al.*, 2001).

The C/EBP subfamily includes the structurally similar but genetically and functionally distinct proteins, C/EBP-α, C/EBP-β, C/EBP-γ, C/EBP-δ, C/EBP-ε and C/EBP-ζ. Deficiency in C/EBP-α is linked to the pathogenesis of acute myeloid leukaemia (AML) (Pabst and Mueller, 2007). Although the mechanism through which C/EBP-α causes AML is unknown, it is thought that hypo- or hyper-

expression of CEBP-α can lead to the development of different types of cancer (Pabst and Mueller, 2007). C/EBP-β (also known as nuclear factor induced by IL-6; NF-IL-6) has a wider range of transcriptional targets than other C/EBP family members, including LAP1 (liver activating protein-1), LAP2 (liver activating protein-2) and LIP (liver inhibitory protein). The LAPs are transcriptional activators, while LIP may act as an inhibitor of C/EBPβ transcriptional activity (Calkhoven *et al.*, 2000). C/EBP-β regulates IL-6 function and the expression of IL-6-induced cytokines such as IL-1, IL-8, TNF-α and granulocyte colony-stimulating factor (Akira and Kishimoto, 1997; Li *et al.*, 2007), and is induced by IFN-γ in different tissues, including the spleen, liver, heart and thymus (Roy *et al.*, 2000). Moreover, IFN-γ enhances the expression of C/EBPβ through MEK/ERK stimulation (Bonjardim *et al.*, 2009; Hu *et al.*, 2001; Li *et al.*, 2007). Activated C/EBPβ is thought to require IFN-γ stimulation to induce STAT1-dependent ERK1/2 phosphorylation (Hu *et al.*, 2001). The ERK1/2 phosphorylation site on human LAP has been identified as Thr^{235} (Anastasov *et al.*, 2010; Pilipuk *et al.*, 2003). Furthermore, the induction of MyD88 signalling by TLR2 and TLR4 activates not only NF-κB but also C/EBPβ and C/EBPδ (Lu *et al.*, 2009).

In macrophage biology, C/EBPβ signalling is essential for oncogenic transformation following insulin-like growth factor I stimulation (Wessells *et al.*, 2004). In addition, C/EBPβ knockdown in macrophages is thought to decrease their proliferation and survival (Wessells *et al.*, 2004). In contrast, C/EBPβ overexpression leads to macrophage hyperproliferation and increased cell size (Sebastian and Johnson, 2006). In macrophages of C/EBPβ-deficient mice infected with *Listeria*

monocytogenes and *Salmonella typhimurium*, these pathogens escape from the phagosome to the cytoplasm (Li *et al.*, 2007). Although C/EBPβ has been well studied, the relative contribution of different isoforms to C/EBPβ biological function remains unclear (Zahnow, 2009).

1.3 The potential roles of Tribbles in dog and *Drosophila*

The original name of *Tribbles* (*Trib*) was C5FW, and it was originally identified as one of the genes up-regulated in the thyroid of dogs in response to mitogens (Wilkin *et al.*, 1996). Later, the function of the *Drosophila* homologue was discovered and the gene was renamed *Tribbles* (Grosshans and Wieschaus, 2000; Johnston, 2000; Mata *et al.*, 2000). Trib is a regulator of *Drosophila* development (Grosshans and Wieschaus, 2000). Moreover, Trib overexpression causes G_2/M arrest, indicating that the *Trib* gene is a cell cycle regulator (Mata *et al.*, 2000; Seher and Leptin, 2000). Additionally, Trib protein localisation to the nucleus and the cytoplasm may be cell cycle-dependent (Mata *et al.*, 2000).

1.4 The major functions of Trib

Trib encodes a predicted 483 amino acid protein containing a central domain with extensive similarity to serine/threonine kinase domains VIII and IX (Mata *et al.*, 2000) (Seher and Leptin, 2000). However, sequence analysis of other regions of the Trib protein has not provided clues to its function. The function of the Trib kinase-like domain was classified by Bowers *et al.* (2003). Although Trib contains a putative kinase-like domain, a typical core ATP-binding site or protein–protein interaction domain is absent. Therefore, Trib protein is classified as a pseudokinase (Hegedus *et*

al., 2007). Recent evidence has identified functions for the C-terminus (Qi *et al.*, 2006; Yokoyama *et al.*, 2010), which contains two important motifs: a MEK1 binding motif and a constitutive photomorphogenesis-1 (COP-1) binding site (Fig. 1.7).

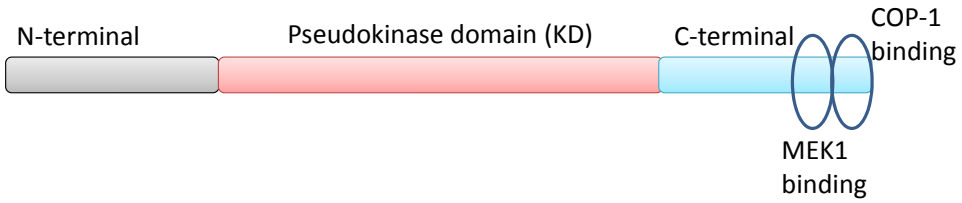

Figure 1.7. Trib protein structure. Trib contains three unique motifs: a central pseudokinase domain and C-terminal MEK1-binding and COP-1-binding sites (adapted from Yokoyama *et al.*, 2011).

There are three Trib gene family members in mammals, namely Trib1, Trib2 and Trib3 (Hegedus *et al.*, 2006). The amino acid sequences between human Trib sequences are: Trib1/Trib2, 71.3%; Trib1/Trib3, 53.3%; and Trib2/Trib3, 53.7% (Yokoyama and Nakamura, 2011). Furthermore, the amino acid sequences of Trib are highly conserved between human and mouse (Trib1, 97.5%; Trib2, 99.2%; Trib3, 81.2%) (Yokoyama and Nakamura, 2011). Trib1 and Trib3 are thought to be nuclear proteins, whereas Trib2 localises to the cytoplasm (Hegedus *et al.*, 2007).

Trib proteins function as adaptors or scaffolds in many signalling pathways (Hegedus *et al.*, 2006), and have been implicated in regulating the activity of MAPK, NF-κB and C/EBP in inflammation and cancer, as well as in glucose, lipid and insulin metabolism (Du *et al.*, 2003; Iynedjian, 2005; Qi *et al.*, 2006). For instance, human Trib proteins associate with several MAP kinase kinases (MAPKK) to modulate MAPK signalling (Kiss-Toth *et al.*, 2004; Yokoyama *et al.*, 2010) (Fig. 1.8). Mouse Trib2 and Trib3 have been reported to be Akt-binding proteins that inhibit Akt

activation in hepatocytes and adipocytes (Du *et al.*, 2003; Naiki *et al.*, 2007). Deficiency in C/EBPα expression is reported to be strongly linked to AML development (section 1.2.3.2) (Pabst and Mueller, 2007), albeit through an undefined mechanism. Interestingly, a conserved C-terminal-binding site for E3 ubiquitin ligases in Trib proteins facilitates the degradation of Trib targets such as C/EBPα in several biological systems (Keeshan *et al.*, 2010; Keeshan *et al.*, 2006; Mata *et al.*, 2000; Qi *et al.*, 2006; Rorth *et al.*, 2000) (Fig. 1.9). Therefore, it is suggested that Trib-mediated C/EBPα degradation may be one of the possible mechanisms which contributes to AML pathogenesis (Dedhia et al., 2010; Pabst and Mueller, 2007) .

The regulation of cell signalling in response to stimulation is known to be cell type dependent (Sung *et al.*, 2006). Therefore, Trib proteins may be multifunctional and their major functions have yet to be determined.

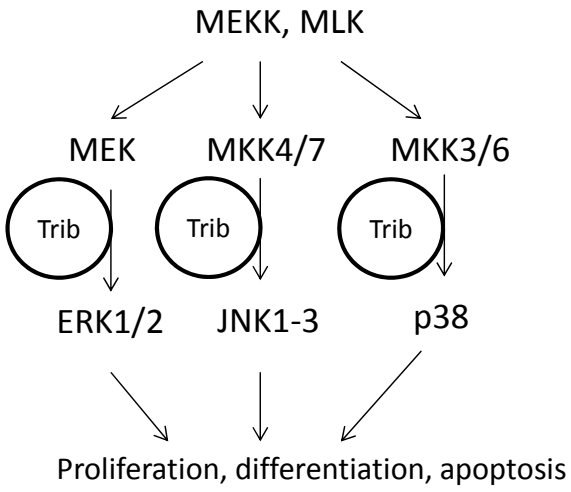

Figure 1.8. MAPK activation is modulated by Trib expressions. This figure indicates the proposed level at which Trib interacts with the MAPK cascade. The downstream biological effects on proliferation, differentiation and apoptosis are mediated by Trib–ERK, Trib–JNK and Trib–p38 interactions (adapted from Sung *et al.*, 2006 and Yokoyama *et al.*, 2010).

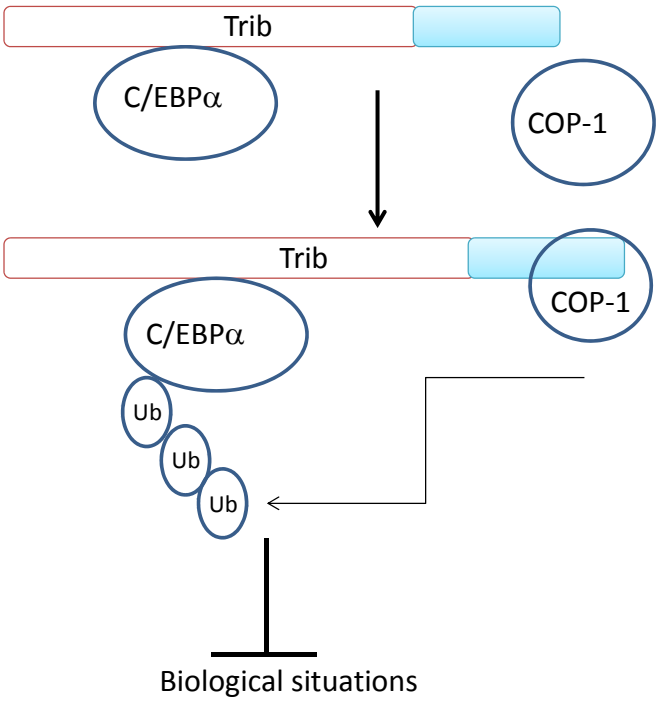

Figure 1.9. Trib interacts with COP1 and regulates C/EBPα. Trib recruitment of COP1 to the COP1-binding site is required for C/EBPα ubiquitination. Following C/EBPα ubiquitination, proteasome-mediated degradation and post-transcriptional suppression of C/EBPα initiates biological processes, such as myeloid differentiation (adapted from Keeshan *et al.,* 2010; and Yokoyama *et al.*, 2011).

1.4.1 Mammalian Trib1

Human *Trib1* was first identified as a *Trib2* homologue based on a partial cDNA sequence (Wilkin *et al.*, 1997). Alternative names for Trib1 include C8FW (Wilkin *et al.*, 1997) and SKIP (Bowers *et al.*, 2003). Trib1 is associated with both innate and adaptive immunity, inflammation and leukocyte differentiation. Moreover, Trib1 protein interacts with the MAPK and C/EBPs pathways to modulate downstream responses, including inflammation.

Trib1 was first evaluated as a regulator of the Toll/IL-1 receptor in innate immune cells and was found to mediate inflammatory gene expression in HeLa cells (Kiss-

Toth *et al.*, 2004; 2005). Trib1-deficient mice were generated by Yamamoto *et al.* (2007), and macrophages from these mice demonstrated that loss of Trib1 up-regulates inflammatory mediators, including prostaglandin E synthase, arginase II and plasminogen activator inhibitor type II. LPS-stimulated C/EBPβ expression was also inhibited in Trib1-deficient macrophages. In the nematode (*Caenorhabditis elegans*) system, a kinase identified by Pujol's group that resembles human Trib1 protects against fungal infection, possibly by activating MAPK signalling upstream of MAPKK (Pujol *et al.*, 2008). Together with Kiss-Toth's work, which found that Trib1 regulates the MAPK pathway in HeLa cells (Kiss-Toth *et al.*, 2004), these studies indicate that Trib1 is associated with the innate immune response against infection.

Trib1 expression was also detected in human $CD4^+$ $CD25^+$ regulatory T (Treg)-cells by microarray analysis (Pfoertner *et al.*, 2006). Trib1 is also expressed in activated APCs and in endothelial cells (Ashton-Chess *et al.*, 2008), where it may play a role in activating the adaptive immune response. Therefore, Trib1 plays a role in both innate and adaptive immunity.

Human Trib1 has been reported to control the proliferation of vascular smooth muscle cells and chemotaxis via inhibition of the MAPK–JNK pathway (Sung *et al.*, 2007). In addition, Trib1 expression is increased in human atherosclerotic arteries relative to non-atherosclerotic controls, implying that Trib1 may be associated with atherosclerosis disease *in vivo*. Recently, Trib1 was reported to control white adipose tissue (WAT) inflammation by direct regulation of the NF-κB pathway in pro-inflammatory signalling (Ostertag *et al.*, 2010). This study confirms that Trib1 has a functional role in the regulation of metabolic (adipocytes) and immune cells in WAT-

induced inflammation.

There is a strong correlation between Trib1 and myeloid leukaemia. Trib1 is a novel myeloid oncogene that enhances ERK phosphorylation, resulting in the inhibition of apoptosis during myeloid leukaemogenesis (Jin *et al.*, 2007). The *Hox* gene has a key role in haematopoiesis and regulates myeloid differentiation, and *HoxA* is important for myeloid leukaemogenesis, along with Meis1 (Argiropoulos and Humphries, 2007). Trib1 expression is up-regulated by retroviral integration in the mouse leukaemogenesis model and cooperates with *Hox*, *Meis1* and *Evil*. Therefore, Trib1 is associated with the induction of AML in mice (Jin *et al.*, 2007), as well as in humans. Trib1 degrades C/EBPα during myeloid leukaemogenesis through interaction with MEK-1 (Yokoyama *et al.*, 2010). These findings suggest that Trib1 both promotes C/EBPα degradation and inhibits C/EBPβ expression.

Retinoic acid (RA) has an important function in development and homeostasis through regulating cell proliferation, differentiation and apoptosis (Mark *et al.*, 2006). Trib1 is also thought to interact with nuclear receptors and may contribute to retinoic acid receptor signalling by inhibiting the function of RA receptors involved in the progression of cancers, including AML (Imajo and Nishida, 2010).

In addition to its pro-inflammatory role, *Trib1* has been reported to function in the differentiation of HC11 mammary epithelial cells (Perotti *et al.*, 2009), which are widely used for studying proliferation, signal transduction and differentiation (Chammas *et al.*, 1994). Perotti's group surveyed more than 15,000 genes and found that approximately 20% of genes to undergo differentiation and *Trib1* is inclusive. Thus, *Trib1* is involved in mammary epithelial cell differentiation (Perotti *et al.*, 2009).

In conclusion, Trib1 is involved in many biological processes, including the innate and adaptive immune responses, inflammation and differentiation.

1.4.2 Mammalian Trib2

Trib2 was first identified by Wilkin *et al.* (1996) as a phosphoprotein expressed in dog thyroid cells. Trib2 mainly contributes to the regulation of haematopoietic diseases, such as AML, as well as chronic inflammatory diseases, such as atherosclerosis.

Bisoffi *et al.* (2004) showed that Trib2 was markedly up-regulated in androgen-independent bone metastatic prostate cancer cells compared with their non-metastatic counterparts. This data indicates that Trib2 may play a role in tumour metastasis. Similar to Trib1, Trib2 cooperates with *HoxA9* to induce AML by inactivating C/EBPα (Keeshan *et al.*, 2006; Keeshan *et al.*, 2008). Accumulated evidence indicates that Trib1 and Trib2 have potential roles in inducing AML via C/EBPα inactivation (Dedhia *et al.*, 2010). Moreover, sequence analysis reveals that the C-terminal region of Trib2 also contains a COP-1 binding site. COP-1 recruitment is essential for Trib2-induced AML; in the absence of COP-1 binding, C/EBPα function is normal and AML doesn't develop (Keeshan *et al.*, 2010). In addition, Trib2/ C/EBPα may contribute to human lung cancer through another E3 ligase, TRIM21 (Grandinetti *et al.*, 2011). Further, Trib2 is reported to be pro-apoptotic in haematopoietic precursor cells (Lin *et al.*, 2007). The Trib2 transcript is down-regulated following treatment of Notch-dependent T cell acute lymphoblastic leukaemia cells with γ-secretase inhibitors, and is Trib is therefore assumed to be a Notch target (Wouters *et al.*, 2007).

Trib2 has been reported to bind Akt and inhibit Akt activation during adipocyte differentiation (Naiki *et al.*, 2007). Recently, Trib2 was shown to negatively regulate forkhead box protein O (FOXO), a downstream transcription factor of the Akt pathway. In addition, Trib2 supports the growth and survival of melanomas by down-regulating FOXO activity (Zanella *et al.*, 2010).

Interestingly, Trib2 was reported to inhibit MEK1 and MKK7 in macrophages and to modulate IL-8 production (Eder *et al.*, 2008), thus connecting Trib2 activity to the immune response. In addition, Trib2 is up-regulated in macrophages within human atherosclerotic regions, suggesting that Trib2 is a marker of atherosclerosis progression (Deng *et al.*, 2009).

Thus, the main functions of Trib2 are to down-regulate C/EBPα, Akt and MAPK for modulating the progression of haematopoietic diseases, cancers and atherosclerosis.

1.4.3 Mammalian Trib3

Trib3 is a well-studied member of the mammalian Trib family (Hegedus *et al.*, 2006) associated with a broad range of biological activities, such as nutrient metabolism, and diseases, including cancers and atherosclerosis. Trib3 plays a role in these processes through regulating signalling pathways, such as Akt and MAPK.

In 1999, Mayumi's group identified Trib3 as a factor induced in neuron cell death (Mayumi-Matsuda *et al.*, 1999). Trib3 is highly expressed in human liver, with lower levels of expression in haematopoietic compartments such as the bone marrow, spleen, thymus and peripheral blood leukocytes (Bowers *et al.*, 2003).

Trib3 function is associated with several biological processes such as glucose and lipid metabolism (Du *et al.*, 2003; Iynedjian, 2005; Koo *et al.*, 2004; Okamoto *et al.*, 2007; Qi *et al.*, 2006). Trib3 has been proposed to block insulin signalling through inhibition of Akt phosphorylation in the liver (Du *et al.*, 2003). However, another study found that Trib3 overexpression does not reduce insulin-induced Akt phosphorylation in the liver (Iynedjian, 2005). Interestingly, Okamoto and his colleagues reported that Trib3 knockout mice have normal insulin signalling and glucose homeostasis in the liver (Okamoto *et al.*, 2007). Therefore, the role of Trib3 in nutrient metabolism remains controversial.

Trib3 negatively regulates a variety of signal transducers through different mechanisms. For instance, Trib3 interacts with the activation transcription factor 4 (ATF4) receptor (Ord D and Ord, 2003) to block Akt phosphorylation (Du *et al.*, 2003). Corcoran and his colleagues (Corcoran *et al.*, 2005) showed that cellular stress can up- or down-regulate Trib3 expression through the p65 NF-κB signalling pathway. Further, Trib3 stimulates the degradation of acetyl CoA carboxylase (ACC), an important enzyme in fatty acid synthesis, by recruiting the E3 ubiquitin ligase, COP1 (Qi *et al.*, 2006). Trib3 is also reported to interact with MEK1 and MKK7, the upstream components of the MAPK pathway (Kiss-Toth *et al.*, 2004), that the consequences of this interaction are unknown

Similar to Trib1 and Trib2, Trib3 is associated with the development of atherosclerosis (see sections 1.4.1 and 1.4.2; (Deng *et al.*, 2009; Shang *et al.*, 2009; Sung *et al.*, 2007). Trib3 is also involved in caspase 3-mediated macrophage apoptosis, and is induced by oxidised low-density lipoprotein (ox-LDL). Moreover, it plays an essential role in the progression of vulnerable atherosclerotic plaques.

Consequently, Trib3 mediates macrophage apoptosis induced by ox-LDL and is also associated with inflammation (Shang *et al.*, 2009).

In summary, Trib1 is involved in immunity, inflammation and differentiation, and is associated with haematopoietic diseases and chronic inflammation. Trib3 plays roles in nutrient starvation and cancer development, as well as in chronic inflammation. A summary of the major signalling pathways involving Trib family members is shown in Table1.3.

Table 1.3. Summary of Trib functional roles in different signalling pathways

Pathway	Trib1	Trib2	Trib3
MAPK	Interaction with MEK1/MKK4 (Kiss-Toth *et al.*, 2004)	Inhibition of MEK1/MKK7 (Eder *et al.*, 2008)	Interaction with MEK1/MKK7 (Kiss-Toth *et al.*, 2004)
Akt	Unknown	Negative regulator (Naiki *et al.*, 2007)	Negative regulator (Du *et al.*, 2003)
C/EBPα	Inhibition through MEK1 in AML (Dedhia *et al.*, 2010; Yokoyama *et al.*, 2010)	Inhibition through COP-1 in AML (Keeshan *et al.*, 2010)	Failed to degrade C/EBPα in AML (Dedhia *et al.*, 2010)
C/EBPβ	Inhibition (Yamamoto *et al.*, 2007)	Unknown	Unclear
Notch	Unknown	Downstream target (Wouters *et al.*, 2007)	Unidentified

1.5 Aims of this PhD project

From previous studies, it is clear that Trib family members are associated with inflammatory processes and disease, including atherosclerosis (Trib1/2/3). Trib1 is involved in LPS stimulation of murine bone marrow derived macrophages through C/EBPβ. Trib family members modulate many signalling pathways, such as the MAPK pathway, and C/EBPs during inflammation and cancer development. However, some findings are contradictory in different mammalian systems. Moreover, no direct evidence links Trib family members to TLRs, cytokine-induced inflammation or stimulation of the innate immune system.

Therefore, the aims of this study are to investigate the biological functions of Trib family members and to determine whether they contribute to innate immunity, for example through regulating macrophage function, within *in vitro* systems. Previous reports have not defined how Trib family members activate the innate immune system. Specifically, it remains unclear how Trib family members contribute to macrophage activation or inactivation following stimulation with TLRs and pro- and anti-inflammatory cytokines. Trib functions were previously examined in *Drosophila*; however, these remain controversial in mammalian systems.

Hypothesis

My overall hypothesis is that Trib family members play a modulatory role during TLR- and pro-inflammatory cytokine-induced inflammation in macrophages.

Specifically, the thesis aims are:

1. to identify which Trib family members are expressed under inflammatory conditions in a myeloid cell line (RAW264.7) and to determine the level and pattern of Trib expression;
2. to identify novel targets of Trib-associated signalling in macrophages;
3. to establish a Trib loss-of-function system using short interfering RNA (siRNA) targeting techniques in order to understand the physiological and biological functions of Trib family members in activated macrophages.

Chapter 2: Materials and methods

2.1 *In vitro* experimental design

2.1.1 Cell culture

Passage 6 murine monocyte/macrophage RAW264.7 cells, generated from BALB/c mice (ATCC number TIB-71), were kindly provided by Professor Tony Nash (Royal Dick School of Veterinary Studies, University of Edinburgh). RAW264.7 cells were cultured in Dulbecco's modified essential medium (DMEM) (GIBCO, Paisley, UK) supplemented with 10 % (v/v) FCS, 100 μg/ml streptomycin and 100 U/ml penicillin (GIBCO, Paisley, UK) in a humidified incubator at 37°C with 5% CO_2.

To passage cells, medium was removed by pipetting, and cells were washed twice in 10 ml PBS (phosphate-buffered saline). Cells were detached by a cell scraper (240 mm, Helena Bioscience, UK) that according to ATCC instructions. Cells were split as required (1:20) and seeded directly into new culture vessels with fresh medium.

2.1.2 Cell stimulation

Cell numbers were adjusted to 2×10^5 cells/well incubated overnight. Culture medium (0.5 ml) was removed from each well and replaced with 0.5 ml fresh medium containing cytokines (recombinant mouse IFN-γ and IL-10, both purchased from eBioscience, UK) and/or TLR ligands (TLR1/2 stimulation, Pam_3CSK_4 was referred to TLR2 ligand in the thesis, and TLR9 ligand, ODN1826 CpG DNA; InvivoGen, San Diego, USA) to the final concentrations shown in Table 2.1. Cells were harvested 0 hr, 0.5 hr, 1 hr, 3 hr, 6 hr, 8 hr and 24 hr post-stimulation for RNA extraction. Culture supernatants from 24 hr and 48 hr time points were stored at -20°C for ELISA analysis.

Table 2.1. Concentrations of the immune modulators used in this study.

Immune modulator	Low concentration	High concentration
untreated	-	-
IL-10	1.0 ng/ml	10 ng/ml
IFN-γ	0.1 ng/ml	1.0 ng/ml
TLR9 ligands (ODN1826 CpG DNA)	1 nM	100 nM
IL-10+TLR9L	TLR9L(1 nM)	IL-10 (10 ng/ml)
IFN-γ TLR9L	TLR9L (1 nM)	IFN-γ (1.0 ng/ml)
TLR2 ligands (Pam_3CSK_4)	1 ng/ml	50 ng/ml
IL-10+TLR2L	TLR2L (1 ng/ml)	IL-10 (10 ng/ml)
IFN-γ TLR2L	TLR2L (1 ng/ml)	IFN-γ (1.0 ng/ml)

2.1.3 Cell storage in liquid nitrogen

RAW264.7 cells were grown to near confluency and frozen at a concentration of approximately 5×10^6 cells in 0.5 ml freezing medium (Appendix B). The cell suspension was centrifuged at 200×*g* for 5 min, resuspended in an appropriate volume of freezing medium, aliquoted into cryovials, transferred to an isopropanol chamber and placed at -80°C. Using an isopropanol freezing vessel provides a steady freezing rate of 1°C/min, which ensures the successful cryopreservation of cells and reduces cell death. After at least 3 hr, cryovials were transferred to liquid nitrogen for long-term storage.

2.2 Molecular techniques

2.2.1 Total RNA extraction

Total RNA was extracted from RAW264.7 cells using an RNeasy Mini Kit (Qiagen, Crawley, UK, 74104) according to the manufacturer's instructions. Culture medium was removed and cells were washed in PBS. RLT buffer (350 µl) containing 3.5 µl β-mercaptoethanol (β-ME) was added to the cells, lysates were obtained by pipetting and transferred to a QIAshredder (Qiagen, Crawley, UK, 79654) spin

column, followed by centrifugation at 8,000× *g* (Eppendorf, MiniSpinPlus) for 2 min. An equal volume of 70% (v/v) ethanol was added to the lysate, mixed by pipetting. The mixture was transferred to an RNeasy spin column and centrifuged for 15 s at 8,000×*g*. Buffer RW1 (700 µl) was added to the column, and the column was centrifuged for 15 s, washed twice with 500 µl RPE/ethanol buffer, and centrifugation for another 1 min. Finally, 30 µl nuclease-free water was added to elute the RNA.

2.2.2 DNA removal

To ensure no DNA contaminated the RNA samples, 3 µl of 10× TURBO DNase buffer and 1.5 µl TURBO DNase (TURBO DNA-free kit, AppliedBiosystems AM1907, Foster City, CA, USA) were added to the eluted RNA, mixed gently and incubated at 37°C for 30 min. DNase Inactivation Reagent (typically one-tenth volume) was added, mixed well and incubated for 5 min at room temperature. Tubes were centrifuged at 10,000×*g* (Eppendorf, Centrifuge 5415R) for 1.5 min and RNA was transferred to a new tube. RNA concentration was measured using a NanoDrop ND1000 (Thermo Fisher Scientific, Leicestershire, UK) according to the manufacturer's manual at absorbances of 230 nm, 260 nm and 280 nm (A_{230}, A_{260}, and A_{280}, respectively). RNA purity of was determined by calculating the A_{260}/A_{280} ratio. Only good quality RNA with a ratio of 1.9–2.1 was used for experiments.

2.2.3 cDNA synthesis

All DNA oligonucleotides were purchased from Eurofins MWG Operon (eurofinsdna.com). Primers were designed using the Primer 3 programme (http://fokker.wi.mit.edu/primer3/primer3_code.html) and with a T_m setting of ≤60°C.

2.2.3.1 Reverse transcription

cDNA was synthesised from RNA using a Reverse Transcription System (Promega, Hampshire, UK). RNA (0.4 μg) was added to a master mix solution containing 4 μl of 25 mM $MgCl_2$, 2 μl of 10× reverse transcription buffer, 2 μl of 10 mM dNTP mixture, 0.5 μl RNasin ribonuclease inhibitor, 15U of avian myeloblastoma virus reverse transcriptase (AMV-RT) and 2.5 μl random hexamers adjusted to a final volume of 20 μl with RNase-free water. Samples were incubated for 10 min at room temperature, then at 42°C for 1 hr to synthesise cDNA, before heating to 95°C for 5 min and then incubating at 0°C for 10 min to inactivate the AMV-RT. cDNA samples were stored at -20°C.

2.2.3.2 DNA amplification by the polymerase chain reaction (PCR)

cDNA samples were used as templates to amplify Tribs 1–3 and GAPDH. PCR reactions comprised 100 pmol forward primer, 100 pmol reverse primer, 2 μl of 10× PCR master mix buffer, 0.5 μl BIOTAQ Red DNA polymerase (Bioline, UK) and 2 μl cDNA, adjusted to a final volume of 20 μl with RNase-free water. PCR cycling conditions were 1 cycle of 94°C for 2 min; 30 cycles of 94°C for 1 min, 55°C for 1 min, 72°C for 1 min; and a final step of 72°C for 10 min. PTC-100 hot lid thermal cyclers were used (MJ Research Inc., Watertown, Mass, USA). To assess the consistency of sample loading and PCR conditions between individual experiments, cDNA amplification of the abundantly expressed housekeeping gene glyceraldehyde 3-phosphate dehydrogenase (GAPDH) was included as the internal control. Primer pairs used in this study are listed in Table 2.2.

Table 2.2. List of primers used in this study

Primer name	Sequences (5′ to 3′)	Expected amplicon size (bp)
Murine Trib1 forward	ACTAATTGCTTTGGGAAGTG	294
Murine Trib1reverse	TTTGCAGATAGAGCTTGGAT	
Murine Trib2 forward	GGAAAAACATTTTGCCACTC	221
Murine Trib2 reverse	TCTGTCCCAATACGCACCTT	
Murine Trib3 forward	GGCTGTTTCTTCCTCCAGAA	246
Murine Trib3 reverse	CCCTGGTTGAGAGAGGATCA	
Murine GAPDH forward	AACTTTGGCATTGTGGAAGG	472
Murine GAPDH reverse	CCCTGTTGCTGTAGCCGTAT	

2.2.3.3 Agarose gel electrophoresis

Agarose (2.0% (w/v); Bioline, London, UK) gels made with 1× TAE buffer (Appendix B) were used for the standard analysis of DNA fragments by electrophoresis (Flowgen, Ashby de la Zouch, UK).

Samples of PCR products were loaded and run on gels in 1× TAE buffer at 100 V for 60 min, stained with Biotium GelRed (Cambridge Bioscience, Cambridge, UK) and DNA bands were visualised using the Bio-Rad gel documentation system (Bio-Rad Molecular Imager FX, Hercules, CA). DNA ladder (1µg of 1kb plus, Invitrogen, Renfrew, UK) was used as a size marker. Kodak Digital Science 1D Image Analysis software (PerkinElmer) was used for measuring DNA band intensities.

2.2.3.4 Purification of PCR products

PCR products were purified for sequencing using the Wizard PCR Preps DNA Purification System (Promega, Hampshire, UK). PCR products (100 µl) were mixed with 1 ml DNA–binding resin and vortexed vigorously three times for 1 min. The DNA–resin mixture was added to a Wizard PCR Preps DNA Purification System mini column, the resin was washed with 2 ml of 80% (v/v) isopropanol, and then 40 µl nuclease-free water was used to elute purified DNA from the resin.

2.2.3.5 DNA sequencing

In order to confirm primer specificity and that no mutations had been introduced during DNA amplification, DNA samples were sequenced by DBS Genomics at Durham University, UK, using an Applied-Biosystems 3730 DNA Analyser (AppliedBiosystems, Warrington, UK). Sequencing samples (5 µl PCR products diluted in nuclease-free water, together with 1 µl primer) were sequenced in both directions using the BigDye Terminator v3.1 (Applied Biosystems, UK) sequencing reaction, followed by capillary analysis using an ABI3730 DNA analyser (AppliedBiosystems, UK).

2.2.4 Quantification of gene expression using real-time PCR

All real-time PCR reactions were performed on a Roche LightCycler 480 Instrument using LightCycler 480 Multiwell Plate 96 following the manufacturer's recommendations. To compare relative mRNA levels in treated and control samples, duplicate samples were analysed as three technical replicates. Two negative controls were included in all assays; a 'no template' control (in which the cDNA template was replaced with nuclease-free water) and an RNA control (in which reverse transcriptase has been omitted from the cDNA synthesis reaction, and which checks for genomic DNA contamination of RNA samples).

2.2.4.1 Reverse transcription

cDNA synthesis was performed using the Transcriptor High Fidelity cDNA Synthesis Kit (Roche, West Sussex, UK). Total RNA (0.4 µg) and 2 µl of random hexamer primers were mixed and the volume was made up to 11.4 µl with nuclease-free water. PCR tubes were placed in the thermocycler (iCycler, Bio-Rad, Hemel Hempstead, UK) and incubated at 65°C for 10 min to allow primer annealing. This

reaction was then added to a solution containing 20 U of Protector RNase Inhibitor, 1 mM of each dNTP, 5 mM of DTT and 10 U of rRT in manufacturer's buffer was aliquoted into the template-primer mixes and incubated at 50°C for 30 minutes. The enzyme was inactivated by an incubation step at 85°C for 5 minutes. Nuclease-free water (80 µl) was added and the single-stranded cDNA was stored at -20°C.

2.2.4.2 Quantitative real-time PCR (qPCR)

qPCR reactions were performed using a LightCycler 480 Real-Time PCR System (Roche, West Sussex, UK) according to the manufacturer's protocol. Diluted cDNA samples (5 µl) were added to a PCR mixture containing 10 µl of 2× Universal PCR Master Mix (Roche), 1 pair of primers (FP and RP) containing 1µl FAM-probe and a second pair of primers containing 1 µl VIC-probe, and made up to 20 µl final volume with nuclease-free water. Trib 1–3 primers and probes were obtained from ABI (Trib1 Mm00454875_m1, Trib2 Mm00454876_m1 and Trib3 Mm00454879_m1, AppliedBiosystems, Warrington, UK). Negative controls contained water or RNA samples, as described above. qPCR reaction steps were: pre-incubation at 95°C for 10 min; 45 cycles of denaturation at 95°C for 10 s, annealing at 60°C for 30 s, extension at 72°C for 1 s; cooling at 40°C for 10 s. Each sample was normalised to mGAPDH expression (Mm03302249_g1).

2.2.4.3 Relative gene expression analysis

Relative gene expression analysis was performed using the comparative delta–delta method (Pfaffl, 2001).

The analyses of real-time PCR described in Chapter 3 were performed under different conditions from those in Chapters 4 and 5. For the experiments described in Chapter 3, the reference gene and target gene primers were added to the same well

(multiplexing Trib1 and mGAPDH). The delta Ct value (dCt = mean Ct of target gene − mean Ct of reference gene) was calculated for each sample, and the time zero control samples (t0) were then averaged and the time zero control dCt0 value was calculated. The delta–delta Ct value (ddCt) represents the difference between the dCt value for the treated (untreated) sample and the time zero control sample. The relative expression of the target gene was then calculated from the formula shown below.

Relative expression (RE) = 2^{-ddCt}

The 2^{-ddCt} equation was used to measure the expression efficiency of target genes.

In Chapters 4 and 5, real-time PCR reactions were performed in duplicate on transfected samples and untransfected controls, and the reference gene and target gene primers were added to the same well (multiplexing Trib1 and mGAPDH). The delta Ct value (dCt = mean Ct target gene − mean Ct reference gene) was calculated for each sample, and the untransfected controls were averaged to produce the untransfected control dCt_{unt} value. The delta–delta Ct value (ddCt) was the defined as the difference between the dCt values for transfected cells and untransfected controls. The relative expression level of the target gene was then calculated using the formula shown above.

2.2.5 Bacterial transformation

The pCMV-Trib1 expression plasmid was purchased from Source BioScience (Nottingham, UK). An *AmpR* gene was incorporated into the pCMV-Trib1 vector to allow the selection of transformed colonies by antibiotic-resistant. The *Trib1* insert size was 2,600 bp approximately when it was cut by the two restriction enzymes; SalI (5′) and NotI (3′).

Plasmid DNA (500 ng) was added to 200 µl competent *Escherichia coli* DH5α cells (Invitrogen, Paisley, UK). DNA and incubated on ice for 30 min. Next, the DNA and bacteria mixture was heat-shocked at 42°C for 1 min and then cooled on ice for 2 min. Super Optimal broth and Catabolite repression medium (SOC) (1 ml; 2% Bacto-tryptone, 0.5% Bacto-yeast extract, 8.5 mM NaCl, 2.5 mM KCl and 20 mM glucose, pH7.0) was added and incubated at 37°C, with shaking at 250 rpm for 1 hr. Transformants were plated onto LB agar containing 50 µg/ml ampicillin.

2.2.6 Preparation of plasmid DNA

2.2.6.1 Mini preps.

Individual *E. coli* DH5α transformed colonies were picked and propagated overnight in 5 ml Luria-Bertani (Appendix B) medium containing 50 µg/ml ampicillin at 37°C with shaking at 250 rpm. Plasmid DNA was recovered using a Pure Yield Plasmid MiniPrep System (Promega, Hampshire, UK). Bacterial culture (3 ml) was pelleted by centrifugation at 10,000×*g* for 5 min and the supernatant was removed. Pelleted cells (200 µl) were mixed with 200 µl cell lysis solution, and then 200 µl cell neutralisation solution was added and mixed, and the mixture was centrifuged to remove cell debris. The clarified supernatant was added to 1ml DNA-binding resin and applied to a mini column. Endotoxin removal wash (200 µl) was added to the mini column and it was centrifuged at maximum speed for 15 s. Column wash solution (2 ml) was then added to the mini column and removed by centrifugation. Nuclease-free water (50 µl) was added to the column and centrifuged to elute purified plasmid DNA.

2.2.6.2 Maxi preps.

A single transformed bacterial colony was inoculated into 3 ml LB containing 50 µg/ml ampicillin and incubated for 6 hr at 37°C with shaking to produce a starter culture. The starter culture was diluted 1:500 into 150 ml LB containing 50 µg/ml ampicillin and incubated overnight at 37°C with shaking at 250 rpm. Large-scale plasmid DNA extraction was carried out using the GenElute HP Endotoxin-Free Plasmid Maxiprep Kit (Sigma-Aldrich, Dorset, UK). Briefly, 150 ml bacterial culture was pelleted by centrifugation at 5,000×*g* for 10 min at 4°C, and the supernatant was discarded. During this time, a binding column was prepared by allowing 12 ml column preparation solution to flow through the column matrix. The bacterial pellet was resuspended in 12 ml resuspension/RNaseA solution, 12 ml lysis solution was added, mixed and then incubated at room temperature for 5 min. Chilled neutralisation solution (12 ml) was added, gently inverted to mix, and then incubated at room temperature for 5 min. Insoluble proteins were removed by passing through an endotoxin-free Maxi cartridge. Binding buffer (9 ml) was added to the filtered lysate and mixed, and the mixture was added to a binding column and allowed to pass through by gravity. The column was washed sequentially with 12 ml each of wash solution 1 and was solution 2 and the column was then air-dried for at least 30 min. Nuclease-free water (5 ml) was then added to the matrix and the column was centrifuged at 8,000×*g* to elute the DNA. The concentration of plasmid DNA was measured using a NanoDrop ND1000.

2.3 Transient transfection of mammalian cells

RAW264.7 cells were transfected by electroporation. All transfection protocols were optimised to obtain the maximum gene knockdown while maintaining high cell viability and transfection efficiency.

2.3.1 Transfection by electroporation

For small interfering RNA (siRNA) knockdown experiments, 2×10^6 RAW264.7 cells were transfected with siRNA using the Amaxa Cell Line Nucleofector Kit V (cat.no. VCA-1003) and programme D-32 (Nucleofector II). Confluent RAW264.7 cells were split at a ratio of 1:4 into new 75cm^2 flasks24 hr before transfection. The following day, cells were harvested and washed twice with PBS. Subsequently, 2×10^6 cells were resuspended in 90 µl solution V and mixed with 10 µl siRNA in a 1.5 ml microcentrifuge tube. Cells were transfected with either a scrambled siRNA as a negative control or the pmaxGFP green fluorescent protein (GFP) expression vector (Amaxa, provided with the kit) as a positive control. After transfection, 500 µl warmed culture medium was added to the microcentrifuge tube and transfected cells were transferred into pre-warmed 6-well plates for overnight incubation. The transfection efficiency was analysed by counting GFP-positive cells by FACS and knockdown efficiency was analysed at the mRNA level by qPCR. Trib1 specific siRNAs and negative control *Silencer* Select siRNAs were purchased from Ambion, AppliedBiosystems (see Table 2.3 for sequences).

Table 2.3. Trib1 specific siRNA sequences used in this study

siRNA identification code	Sequences (5′ to 3′)
s102503 sense	CGCUUUUGGUCGGACGAUAtt
s102503 antisense	UAUCGUCCGACCAAAAGCGta
s102505 sense	GAUGAUGCGCUGUCAGAUAtt
s102505 antisense	UAUCUGACAGCGCAUCAUCtt
s202130 sense	GGGCUAUGUUGACUCAGAAtt
s202130 antisense	UUCUGAGUCAACAUAGCCCgg

2.3.2 Microscopic analysis

For experiments described in Chapter 3, the morphology of treated and control RAW264.7 cells were examined using a Leitz Laborlux S microscope (Leica Microsystems GmbH, Wetzlar, Germany) at 25× magnification. Digital images were captured using an Exwave HAD 3CCD video camera.

For experiments described in Chapters 4 and 5, the morphology of transfected cells was examined by inverted microscope (Axiovert 40CFL, Carl Zeiss, MicroImaging GmbH, Jena, Germany) after overnight incubation. Cytocentrifuge smears were prepared from non-adherent cells as follows. Double cytofunnel cuvettes (Cytospin3, Shandon, Thermo Fisher Scientific Inc., Waltham, MA, USA) were mounted onto Superfrost microscope slides in metal holders. Cell suspension (100 µl) was place into each cuvette and cuvettes centrifuged at 350 rpm for 3 min in a Cytospin3 centrifuge (Cytospin3, Shandon, Thermo Fisher Scientific Inc., Waltham, MA, USA). Slides were carefully extracted and air-dried and then cells were examined using an inverted microscope. Photographs were taken using an AxioCam camera mounted on the inverted microscope.

2.4 Protein analysis

2.4.1 Preparation of RAW264.7 whole cell protein extracts

Culture medium was removed and cells were rinsed with cold PBS containing 1× β-phosphatase inhibitors. Cells were detached using a scraper, transferred to 1.5 ml microcentrifuge tubes and washed with cold PBS. Cold NP-40 lysis buffer (20 µl; 1% (v/v) NP-40, 150 mM KCl, 25 mM HEPES, 5 mM DTT, 50 mM NaF and 1× Roche Protease Inhibitor Cocktail Tablets) was added to each cell pellet. Cells were lysed by thorough pipetting in lysis buffer and incubated on ice for 15 min. Lysates were centrifuged at 10,000×*g* (Eppendorf, Centrifuge 5415R) for 15 min at 4°C and supernatants containing whole cell soluble protein extracts were stored at -70°C.

2.4.2 Determination of protein concentration by the Bradford method

A Quick Start Bradford Protein Assay (Bio-Rad, Hemel Hempstead, UK) was performed according to the manufacturer's protocol to determine the protein concentration of the cell lysates. Samples were diluted 1:10 and 5 µl of each protein standard or sample was pipetted into individual wells of a 96-well plate containing 250 µl 1× dye reagent (Bio-Rad, Hemel Hempstead, UK). Samples were incubated room temperature for 10 min to allow colour development and the absorbance at 595 nm was measured using a 1420 VICTOR3 plate reader (PerkinElmer). Protein concentrations were calculated by reference to a bovine serum albumin standard curve.

2.4.3 Sodium dodecyl sulphate polyacrylamide gel electrophoresis (SDS-PAGE)

Protein electrophoresis was carried out using a Bio-Rad Mini Protean III system (Bio-Rad, Hemel Hempstead, UK) and standard 12% Laemmli SDS-polyacrylamide gels (Appendix B). The resolving gel (Appendix B) was poured first, overlaid with

distilled water to prevent air bubbles forming, allowed to set at room temperature and then the distilled water was removed. The stacking gel (Appendix B) was poured, ten-well combs were inserted and the gel was allowed to set at room temperature.

Protein samples (40–50 µg) were prepared in 2× SDS sample buffer (Appendix B) and boiled in a heat block for 5 min at 95°C to denature the proteins. The gel was immersed in running buffer (Appendix B), and samples were loaded into wells and subjected to electrophoresis at 150 V until the dye front had run off the bottom of the resolving gel. Gel plates were disassembled and the gels placed in 1× transfer buffer (Appendix B) for 10 min. Pre-stained Full Range Rainbow Markers (5 µl; Amersham Pharmacia Biotech) were included to allow size estimation of protein bands.

2.4.4 Protein transfer to nitrocellulose membranes

Gels containing separated proteins were assembled in the transfer cassette with nitrocellulose membrane (GE healthcare, Chalfont St Giles, UK, RPN203D) and Whatman filter papers, according to the manufacturer's instructions. The transfer cassette (Mini Trans-Blot Cell, Bio-Rad Hemel Hempstead, UK) was placed in a transfer tank containing 1× transfer buffer and protein transfer was performed at 100 V for 1 hr at room temperature with an ice pack.

2.4.5 Immunoblotting

Nitrocellulose membranes were rinsed with water and reversibly stained with 0.1% (w/v) Ponceau-S solution in 5% acetic acid (Sigma-Aldrich, Dorset, UK) to check the efficiency of protein transfer, and then washed in TBST (Appendix B) buffer. Membranes were blocked with 5% (w/v in TBST) skimmed milk powder (OXOID, Cambridge, UK) solution for 1 hr at room temperature, and then incubated with the appropriate antibody dilution (in 3% (w/v) skimmed milk in TBST; see

Table 2.4) overnight at 4°C. The membranes were then washed three times in TBST for 5 min each time to remove excess antibody. Membranes were then incubated with horseradish peroxidase-linked (HRP) secondary antibody (diluted in 3% (w/v) skimmed milk in TBST; see Table 2.4) for 1 hr at room temperature, washed five times in TBST for 5 min each time, and protein signals were detected using the ECL reagent (1:1 mixture of solutions 1 and 2; Appendix B) and exposure to Lumi-Film chemiluminescent detection film (Amersham Biosciences). Protein sizes were determined by comparison with pre-stained markers.

Table 2.4. List of the primary and secondary antibodies

Primary antibody	**Host animal**	**Source (catalogue number)**	**Dilution**
Anti-α/β tubulin	Rabbit	Cell Signaling (2148)	1:1000
Anti-total ERK1/2	Mouse	Cell Signaling (9272)	1:2000
Anti-Phospho-ERK1/2 (E10)	Mouse	Cell Signaling (9106)	1:2000
Anti-C/EBPβ (C-19)	Rabbit	Santa Cruz (sc-150)	1:100
Anti-human Trib1	Goat	Prosci (46912)	1:100
Anti-human Trib1	Rabbit	Millipore (09-126)	1:2500
Secondary antibodies	**Host animal**	**Source (Catalogue number)**	**Dilution**
Anti-mouse Ig-HRP	Rabbit	Dako (P0260)	1:2000
Anti-rabbit Ig-HRP	Swine	Dako (P0217)	1:2000
Anti-goat Ig-HRP	Rabbit	Dako (P0449)	1:1500

2.4.6 Stripping proteins from nitrocellulose membranes

Nitrocellulose membranes were incubated in stripping solution (Restore Plus Western Blot Stripping Buffer, Thermo Fisher Scientific, Rockford, USA) for 8 min at room temperature. Stripped membranes were washed four times with TBST before re-use.

2.5 TNF-α and IL-6 ELISA

TNF-α and IL-6 secretion into culture medium was quantitated using ELISA kits (R&D Systems, UK) according to the manufacturer's instructions. Recombinant standard solutions and 1:4 dilutions of samples were prepared, and 50 µl/well standard or sample was added to a 96-well plate and incubated at room temperature for 2 hr. The plate was washed four times with wash buffer, 100 µl/well HRP-conjugated secondary antibody was added and the plate was incubated at room temperature for 2 hr. The plate was washed five times with wash buffer, 100 µl/ well substrate solution was added, and the plate was incubated for up to 30 min at room temperature. After this time, 100 µl stop solution was added. The optical density at 450 nm was measured within 30 min using a microplate reader (Model 550, Bio-Rad, Hemel Hempstead, UK), with the correction wavelength set to 570 nm.

2.6 Cell migration assay

Cell migration was measured using a transwell assay with 24-well transwell chambers (Corning, NY) described previously (Kanellis *et al.*, 2004). Culture medium (600 µl) medium with or without 200 ng/ml recombinant murine MCP-1 (PeproTech, USA) was placed in the lower wells of chambers and 100 µl cell suspension was added to upper wells (Fig. 2.1A). Upper and lower wells were separated by polyvinylpyrrolidone-free polycarbonate filters (5 µm pore size, 6.5 mm insert diameter). Transwell chambers were incubated at 37°C in 5% CO_2 for 90 min. The upper surfaces of the membranes were then washed three times with cold PBS to remove cells that had settled on the separated upper surface of the separated. Cells trapped in the filter pores or adhering to the underside of the membrane were fixed in

cold methanol, stained with haematoxylin solution (Fluka) and counted (Fig. 2.1B). The total number of cells trapped in the pores was counted for each well.

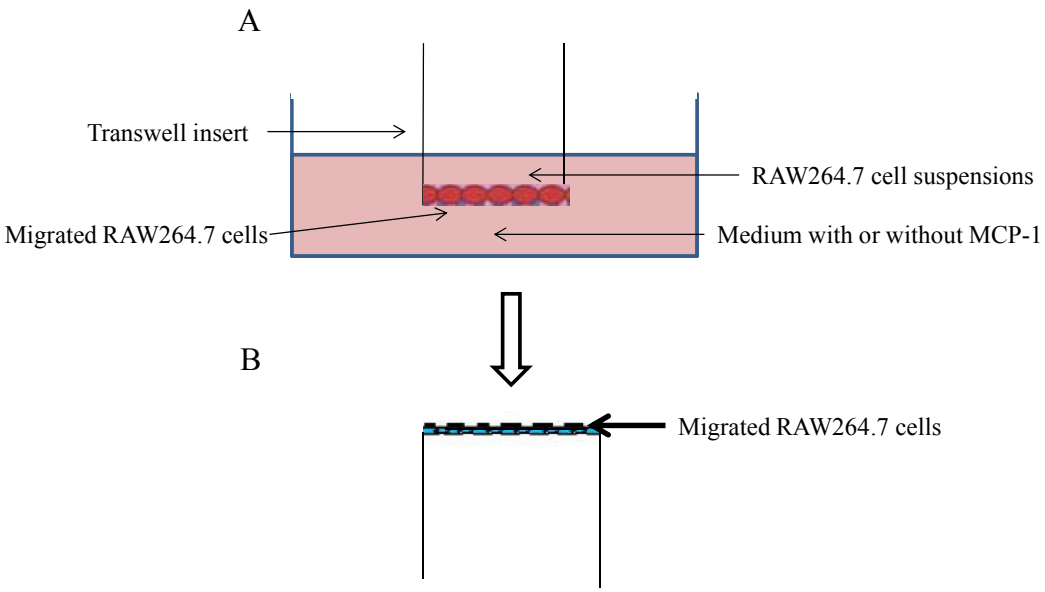

Figure 2.1. Diagram of the cell migration assay. (A) A transwell insert showing cell migration through a permeable membrane of 5 μm pore size. (B) After incubation, the transwell was placed upside down, and cells were fixed with cold methanol and stained with haematoxylin solution.

2.7 Flow cytometry analysis

Flow cytometry was performed following transfections with Trib1 or scrambled control siRNA or with pmaxGFP plasmid (Chapter 2.3) to determine transfection efficiency and cell viability.

2.7.1 Cell viability and transfection efficiency

Briefly, cells were washed with PBS, detached from the well surface and centrifuged at 300×*g*, 4°C for 5 min. Cell pellets were resuspended in 1 ml PBS, transferred to flow cytometer tubes and stored on ice until analysed. Flow cytometer analysis was performed using a BD FACSCalibur Flow Cytometer (BD Biosciences, San Jose, California, USA) using FITC and PE propidium iodide (PI) channels. For each sample 10,000 events were counted, and then 0.2 mg/ml PI was added to the

cell suspension to a final concentration of 50 μg/ml in order to stain dead cells. A further 10,000 events were then counted. Data were analysed using FACSDiva software version 5.02 (Becton Dickinson-Biosciences, USA) and transfection efficiency and cell viability were determined for each sample.

2.7.2 Cell cycle analysis

Trib1-silenced and untransfected RAW264.7 cells were harvested by centrifugation at 300×*g* rpm for 5 min and resuspended in 1 ml cold PBS. Ice-cold 100% ethanol (3ml) was added to the cells, providing a final concentration of approximately 70% (v/v) ethanol, and mixed by vortexing. Samples were incubated on ice for at least 30 min, and then cells were washed twice with PBS. After centrifugation at 500×*g,* the supernatant was carefully decanted. RNase (50 μl of a 100 μg/ml solution) was added, and samples were flicked gently to mix and then incubated at 37°C for 15 min. Lastly, 200 μl PI was added to a final concentration of 40 μg/ml. For the analysis, only signals from single cells were considered and 10,000 cells were assayed for each sample.

2.7.3 Detection of Annexin V-FITC and PI staining

Apoptosis and necrosis of RAW264.7 cells was determined by Annexin V-FITC and PI staining using a BD Annexin V-FITC apoptosis kit. After transfection (72 hr), 1×10^5 cells were incubated with 5 μl Annexin V (20 μg/ml in 1× binding buffer) and 5 μl PI (50 μg/ml in 1× binding buffer) for 15 min in the dark at room temperature. Next, 400 μl of 1× binding buffer was added to each tube and the samples were analysed by flow cytometry within 1 hr.

2.8 Statistical analyses

Linear mixed effect (LME) models were used to analyse the data presented in this thesis. According to the classification of Paterson (2003), datasets containing repeated measurement in a single experiment fit this model (Paterson S and Lello J, 2003). The reason for choosing this model is that datasets were not independent in the experimental design, which involved repeated measurements of duplicate cell samples within a single experiment. The mixed model contains both fixed effects and random effects. A fixed effect compares measurement, for example of TNF-α stimulation by different immune modulators, in a single group and the random effect is important for correcting errors within a group (experiment) or between wells (some experiments are done using multiwell plates). For some datasets, for example all qPCR results and the optimisation of TNF-α production, Log2/Log10 transformation was necessary to normalise the residuals before analysis.

Standard *post-hoc* (*Tukey*) tests were used for pair-wise comparisons of all treatments.

In addition to LME models, generalised LME models were used to analyse data in this thesis, in particular the count data in Chapter 5. The migrated cell counts were fitted using the Poisson process. Fixed effects were groups (untransfected cells, or cells transfected with scrambled or Trib1 siRNA) and random effects were introduced by different wells within an experiment. For the cell cycle analysis, the percentage of cells through FACS sorting was G_1/S/G_2M phase and we used Binomial process. For Tables 5.1, 5.2 and 5.3, the percentage apoptosis analysis used Pearson's Chi-squared test and $p < 0.05$ compared to the vehicle controls (vector or scrambled siRNA group) was considered to indicate a statistically significant

difference.

Data was analysed using the free statistical software environment R (The R Foundation, Software version 2.14.1, Copyright (C) 2011, Vienna, Austria). In all cases, a *p*-value of <0.05 was considered to be statistically significant. All graphs and diagrams were generated using Microsoft Office 2010 software (Microsoft Corporation).

Chapter 3: Expression profiles of Trib family members during inflammatory responses in RAW264.7 cells

Abstract

Macrophages comprise one of the major effector cell populations of the innate immune system. TLRs recognise a variety of microbial components and mediate downstream signalling pathways such as NF-κB and MAPK. IL-10 is an anti-inflammatory cytokine that suppresses macrophage function; in contrast, IFN-γ is a potent macrophage activator. Trib family members have been implicated in regulating inflammatory responses. To clarify the function of Trib family members in TLR-induced inflammation in the presence of pro- or anti-inflammatory cytokines, RAW264.7 cells were treated with TLR2/9 ligands in the presence or absence of IL-10 or IFN-γ. High basal levels of Trib1 expression were observed in RAW264.7 cell. TNF-α production was used as an indicator of RAW264.7 cells activation. Real-time PCR experiments showed that *Trib1* expression was increased following treatment with TLR2/9 ligands, whereas IL-10-induced *Trib*1 expression was low.

In this chapter, I demonstrate that Trib1 is expressed in RAW264.7 cells and might contribute to TLR-induced pro- and anti-inflammatory responses.

3.1 Introduction

Macrophages are key components of inflammatory responses and much is known of the signalling pathways that are activated in macrophages in response to pro-inflammatory and inhibitory stimuli, such as microbial infections. Moreover, macrophages and other components of the innate immune system have an important additional role in activating adaptive immunity (Gordon, 2003). After myeloid cells differentiate to form macrophages, they express different surface markers. For instance, CD11b is specifically expressed on both murine and human macrophages, whereas CD11c is specifically expressed on human macrophages (Gordon and Taylor, 2005). Classical activated macrophages respond to two signals: IFN-γ and PAMPs (Farrar and Schreiber, 1993; McCoy and O'Neill, 2008; Medzhitov, 2001). Macrophage stimulation with IFN-γ induces direct killing microbial responses, as well as up-regulating antigen processing and presentation pathways (Pestka *et al.*, 1997; Schroder *et al.*, 2006). PAMPs stimulate macrophage activation through TLRs, which induce the innate immune response (Medzhitov, 2001). In contrast, the macrophage response to IL-4, IL-13 or IL-10 is known as alternative activation or M2 macrophage activation (Mantovani *et al.*, 2002; Mills *et al.*, 2000). For example, TAMs that originate from blood monocytes and have been stimulated by factors such as IL-10 and TGF-β are recognised to be M2 type macrophages. These stimulated TAMs secrete autocrine IL-10 and chemokines to suppress T cell-induced adaptive immunity (Mantovani *et al.*, 2002; Pollard, 2004; Solinas *et al.*, 2009).

IL-10 performs a unique role in negatively regulating immunity and inflammation, primarily through a mechanism involving the selective inhibition of the expression of pro-inflammatory genes encoding cytokines, chemokines and cell surface molecules,

such as B7 and ICAM-1. IL-10 also inhibits potent pro-inflammatory cytokines, such as TNF-α (Moore *et al.*, 2001), and inhibits constitutive and inducible expression of MHC class II on monocytes (Haddad *et al.*, 2003). In addition, IL-10 inhibits the antigen presentation process in macrophages (Bailey *et al.*, 2006; Haddad *et al.*, 2003; Murray, 2006) (Fig. 3.1).

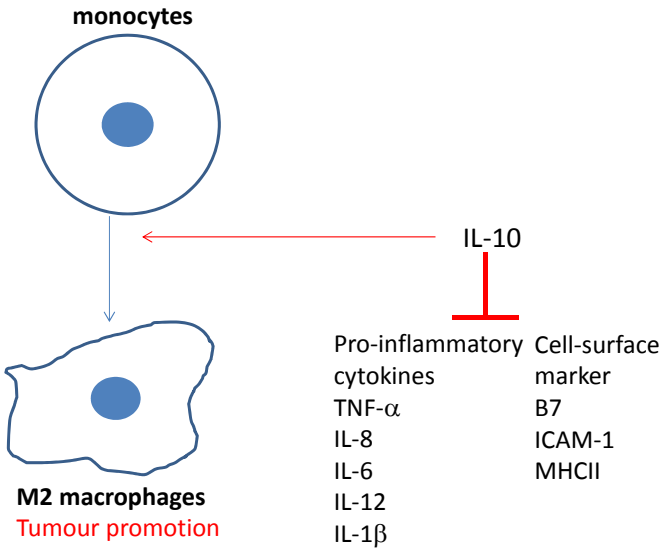

Figure 3.1. Polarisation of monocytes into M2 macrophages following IL-10 stimulation. Monocytes stimulated by IL-10 differentiate into M2 macrophages. Moreover, IL-10 inhibits pro-inflammatory cytokines and cell surface markers to promote tumour progression.

TLR9 is involved in the recognition of unmethlyated CpG motifs in bacterial DNA. TLR9 is expressed in the endosome. However, several studies have reported that CpG DNA is detected in the endosome following internalisation of bacterial DNA, thus allowing it to be bound by the TLR9 receptor (Hallman M, 2001; Kaisho and Akira, 2001; Takeuchi and Akira, 2010). Interestingly, $TLR9^{-/-}$ mice are deficient in several CpG DNA responses, including cytokine production by macrophages, B cell proliferation and DC maturation (Akira *et al.*, 2001; Takeuchi and Akira, 2010). Furthermore, CpG DNA stimulates the production the Th1-polarizing cytokine IL-12 in macrophages, leading to the development of Th1 immune responses (Takeda *et al.*,

2003). TLR9 is also a sensor of DNA viruses that contain genomes rich in the CpG DNA motif. Therefore, TLR9 stimulation results in activation of inflammatory cytokines such as IL-12 and type I IFN secretion (Pasare and Medzhitov, 2004).

Three Trib gene family members have been identified in mammalian systems: *Trib1*, *Trib2* and *Trib3* (Hegedus *et al.*, 2006). These mammalian Trib family members have been implicated in regulating in inflammation, cancer development and nutrient metabolism (Du *et al.*, 2003; Iynedjian, 2005; Qi *et al.*, 2006). Importantly, Trib1 exerts a pro-inflammatory role in human HeLa cells (Kiss-Toth *et al.*, 2006). Consistent with this, Trib1 has been implicated in macrophage activation and negatively regulate C/EBPβ expression under conditions of LPS-induced inflammation (Yamamoto *et al.*, 2007). However, how Trib family members regulate innate immunity and inflammation remain unclear.

Aim

The questions addressed in this chapter are which Trib family members are expressed in macrophages; and Trib expression relates to TLR-induced responses in the presence of pro- or anti-inflammatory cytokines.

Conventional PCR was used to determine the expression profile of Trib family members in order to select the most highly expressed Trib gene for further study. TNF-α production was used to measure macrophages activation levels. Finally, real-time PCR was used to understand how the gene expression of Trib family members is affected by TLR-induced pro- or anti-inflammatory conditions.

3.2 Experimental design

Cell culture and stimulation scheme

Cells were grouped as described in Table 2.1 and Fig. 3.2.

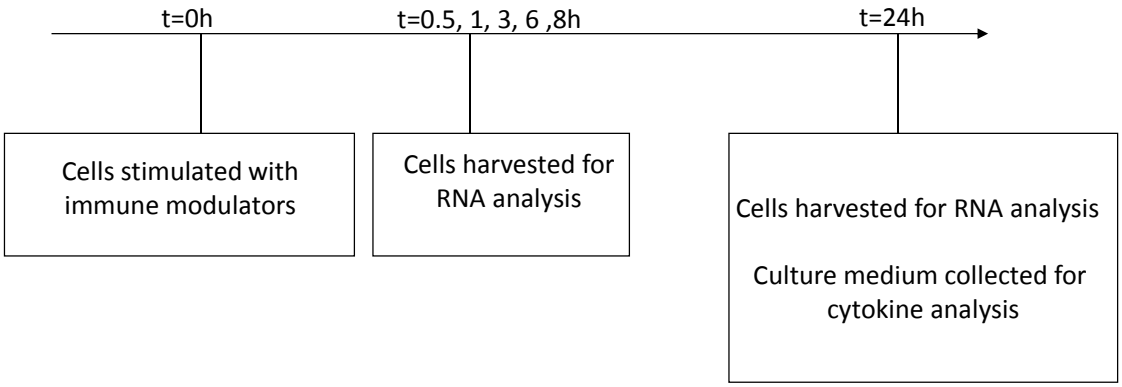

Figure 3.2. Experimental design of the macrophage activation experiment.

3.3 Results

3.3.1 Expression profile of Trib family members in RAW264.7 cells

RAW264.7 is a murine monocyte/macrophage cell line. The morphology of normal RAW264.7 cells includes a monocyte-like round appearance and macrophage-like features, such as cytoskeletal extensions (Fig. 3.3A). The expression patterns of Trib1, 2 and 3 in RAW264.7 cells were previously unreported. My PCR results indicated that RAW264.7 cells express *Trib1* and *Trib3* transcripts, but no detectable *Trib2* (Fig. 3.3B, lane 1 and 3 vs. lane 2). Murine splenocytes were used to check that the primers were functional (Appendix A)(Ashton-Chess *et al.*, 2008). Following this, qPCR was used to examine the expression levels of Trib family members in RAW264.7 cells (Fig. 3.3C). The result indicated that *Trib2* is not expressed in the RAW264.7 cells, consistent with the previous result (Fig. 3.3B). Furthermore, *Trib1* expression was significantly higher than *Trib3* expression in macrophages ($p = 0.002$; Fig. 3.3C). Therefore, further studies in this thesis focussed on *Trib1* expression.


A
50 μm

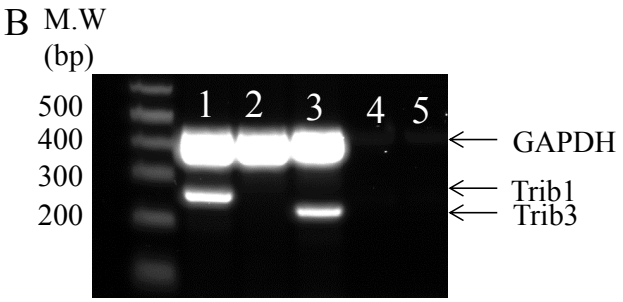
B
M.W
(bp)
500
400
300
200
1
2
3
4
5
GAPDH
Trib1
Trib3

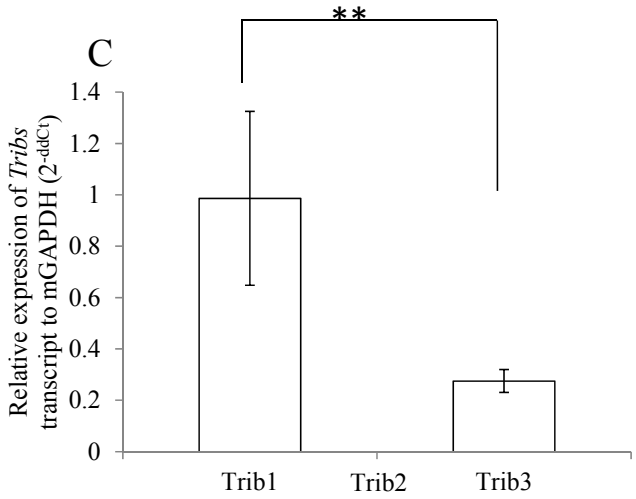
C
**
Relative expression of Tribs transcript to mGAPDH (2-ddCt)
1.4
1.2
1
0.8
0.6
0.4
0.2
0
Trib1
Trib2
Trib3

Figure 3.3. Morphology, Trib expression profile of Trib family members in RAW264.7 cells. (A) Morphology of normal RAW264.7 cells examined using an inverted microscope. The arrow indicated the monocyte-like cells and the arrowhead indicates a cell with a macrophage-like morphology. The scale bar represents 50 μm. (B) The expression profile of *Trib1* (lane 1; 294 bp), *Trib2* (lane 2; 221 bp) and *Trib3* (lane 3; 246 bp) transcripts. Lanes 4 and 5 contained RNA and water negative control samples. A housekeeping gene (GAPDH, 472 bp) was used as an internal control for the PCR. (C) Expression profile of *Trib1*, *2* and *3* in RAW264.7 cells. Total RNAs were subjected to qPCR. The values represent the mean ± SD calculated from triplicate wells and two independent experiments. The relative ddCt formula is provided in Chapter 2. The LME model was used for statistical analysis. This data required Log2 transformation to normalise the residuals before analysis. $p<0.05$ were indicated as significant difference. For further details, refer to sections 2.8. $^{**}p = 0.002$, comparing *Trib1* and *Trib3* transcript levels.

3.3.2 Optimisation of IL-10, IFN-γ, TLR2 and TLR9 ligand concentrations required to stimulate RAW264.7 cells

Trib1 was more highly expressed than Trib3 in macrophages. Therefore, changes in Trib1 expression were measured in an inflammatory environment. This required using a macrophage activation marker as a control. It was previously reported that RAW264.7 cells up-regulated TNF-α in response to treatment with IFN-γ or LPS, indicated an TNF-α is marker of RAW264.7 activation (Vila-del Sol, 2008). Consequently, TNF-α production was used as an indicator of RAW264.7 cell activation in this thesis.

In order to determine the optimal concentrations of IL-10, IFN-γ, TLR2 and TLR9 ligands for RAW264.7 cell stimulation, a dose response curve was established for each of these reagents and TNF-α production was measured to determine macrophage activation (Figs. 3.4).

The effect of IL-10 treatment is shown in Fig 3.4A, in which an increasing dosage of IL-10 resulted in a small but significant increase in TNF-α production (basal levels were 390 pg/ml). Based on this result, a high concentration (10 ng/ml) was used for subsequent IL-10 treatments. IFN-γ treatment of RAW264.7 cells led to a large increase in TNF-α production, even at the lowest concentration of 0.1 ng/ml IFN-γ (p <0.001, compared to basal levels). All concentrations of IFN-γ resulted in a significant increase in TNF-α production. Maximal TNF-α production (1660 pg/ml) was induced following stimulation with 1.0 ng/ml IFN-γ (Fig 3.4B); therefore, this

dose was selected for all subsequent IFN-γ cell treatments throughout the thesis.

In contrast, TLR2L and TLR9L treatments induced dramatic and statistically significant increases in TNF-α production over basal levels even at low concentrations, for example 1 ng/ml TLR2L (7500 pg/ml TNF-α) and 1 nM of TLR9L (4500 pg/ml TNF-α; Figs 3.4C, D). Therefore, these low concentrations of TLR2L and TLR9L were chosen for all subsequent cell treatments.

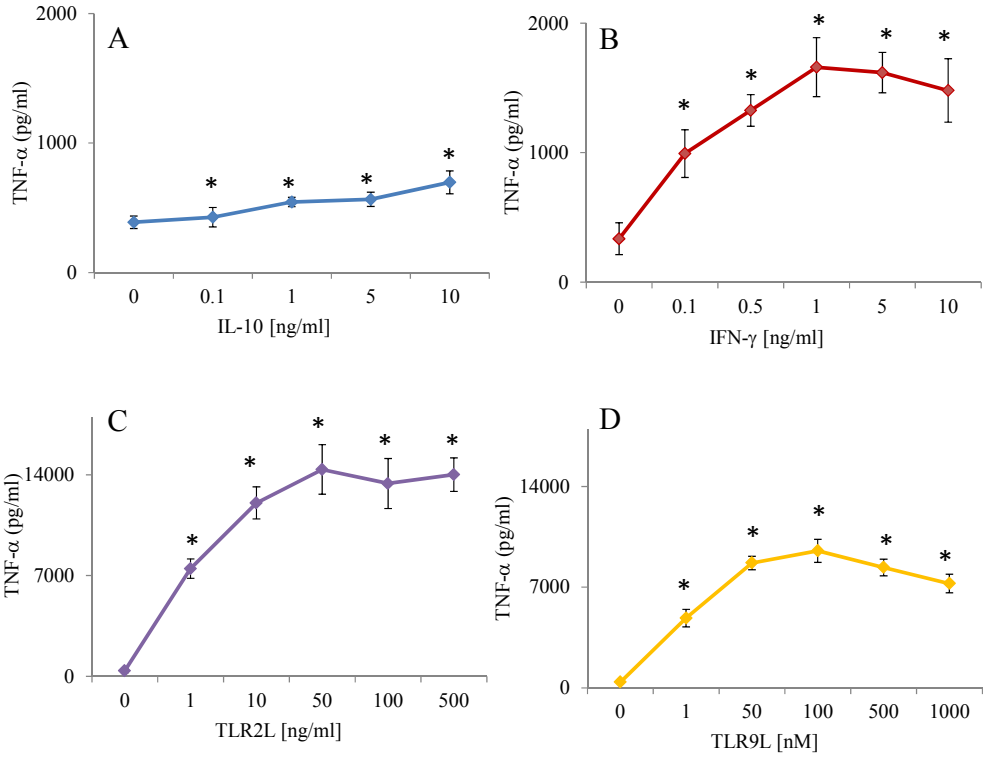

Figure 3.4. TNF-α production in the mouse macrophage RAW264.7 cells induced by anti- and pro-inflammatory signals. RAW264.7 cells (2×10^5 cells/ml) were cultured in DMEM medium supplemented with 10% FCS overnight and then stimulated with different concentrations of IL-10 (A), IFN-γ, (B), TLR2 (C) and TLR9 (D) ligands, as indicated. After 24 hr, cell supernatants were collected and TNF-α production was determined by ELISA. Values represent the mean ± SD calculated from two independent experiments, each consisting of triplicate samples in two culture plates. For details of the statistical analysis, see sections 2.8. The analysis examined TNF-α production and random effects were plates within experiment. The statistical analysis for TLR2L and TLR9L treatments required Log10 transformation to normalise the residuals pre-analysis. *p <0.001 compared to the untreated control.

In the following experiments, cell numbers were optimised to $2x10^5$ cells/well and prior to stimulation, cells were plated at this density, incubated overnight and then 1 ml culture medium from each well was replace by 1 ml fresh medium containing cytokines or TLR ligands at the concentrations shown in Table 3.1.

Table 3.1. Optimised concentrations of the immune modulators used in this study

Immune modulator	Concentration
untreated	-
IL-10	10 ng/ml
IFN-γ	1.0 ng/ml
TLR9 ligand (ODN1826 CpG DNA)	1 nM
IL-10 + TLR9L	IL-10 (10 ng/ml) / TLR9L(1 nM)
IFN-γ + TLR9L	IFN-γ (1.0 ng/ml) / TLR9L (1 nM)
TLR2 ligand (Pam_3CSK_4)	1 ng/ml
IL-10 + TLR2L	IL-10 (10 ng/ml) / TLR2L (1 ng/ml)
IFN-γ + TLR2L	IFN-γ (1.0 ng/ml) / TLR2L (1 ng/ml)

3.3.3 TNF-α production is a marker of RAW264.7 cell activation

Using TNF-α production as an indicator of activation, RAW264.7 cells were treated with immune modulators at the optimal concentrations indicated in the previous result. Treatment with IL-10 (10 ng/ml), IFN-γ (1.0 ng/ml), TLR2L (1.0 ng/ml) and TLR9L (1nM) resulted in a significant increase in TNF-α production compared with untreated cells. Cell culture supernatants were collected at 24 hr and 48 hr after treatment (Fig 3.5).

After 24 hr, TNF-α production in all treated cells was significantly increased compared to untreated controls. Combined treatments, such as IFN-γ with TLR2L, did not show a synergistic effect (for TLR2L single treatment compared with combined treatment, $p = 0.981$). Conversely, combined IFN-γ and TLR9L treatment led to a decrease in TNF-α production (TLR9L single treatment compared with combined treatment, $p < 0.001$). Additionally, in groups treated with combined IL-10 and TLR2L or TLR9L, there was a significantly increased TNF-α production compared with IL-10 single treatment ($p < 0.001$). This result was consistent with the previous result (Fig. 3.4) and confirms TNF-α production to be an activation marker for RAW264.7 cells.

However, after 48 hr, TNF-α production was significantly increased in all treatment groups relative to untreated cells, except for combined IL-10/IFN-γ and TLR9L treatment ($p = 0.651$ and $p = 0.649$, respectively). More interestingly, comparing 24 hr and 48 hr treatment times revealed that TNF-α production was

significantly increased by IL-10 (p <0.001), TLR2L (p <0.001), IL-10 combined with TLR2L (p <0.001), IFN-γ combined with TLR2L (p <0.001) treatment. A significant reduction in TNF-α production resulted from treatment with IFN-γ (p <0.001), TLR9L (p <0.001), IL-10 combined with TLR9L (p <0.001) and IFN-γ combined with TLR9L (p <0.001).

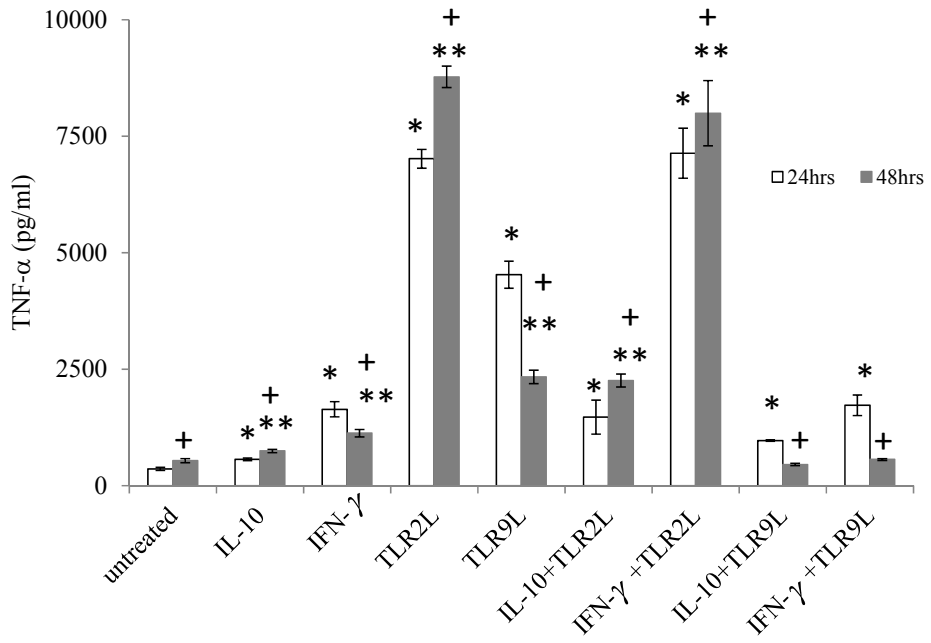

Figure 3.5. Kinetics of TNF-α production by RAW264.7 cells following stimulation with pro- and anti-inflammatory cytokines. TNF-α production in RAW 264.7 cells was measured at 24 hr and 48 hr post-stimulation. RAW264.7 cells produced low basal levels of TNF-α. Values represent the mean ± SD of three independent experiments each consisting of triplicate samples in two culture plates. Log10 transformation was required. A standard *post-hoc* (*Tukey*) test was used to carry out pair-wise comparisons of all treatments. *, p <0.001 comparing each treatment to untreated controls after 24 hr; **, p <0.001 comparing each treatment to untreated controls after 48 hr; +, p <0.001 comparing 24 hr treatment to that of 48 hr. For details of the statistical analysis, see sections 2.8.

3.3.4 Changes in RAW264.7 cell morphology following stimulation by IL-10 or IFN-γ combined with TLR2/9 ligands

RAW264.7 cells were plated at $2x10^5$ cells/ml in 24-well plates, incubated overnight and then stimulated by immune modulators (see Table 3.1).

Microscopic analysis of RAW264.7 cell morphology revealed differences between control (Fig. 3.6A) and stimulated cells, and also between cells treated with single treatment (Fig. 3.6) and combined treatments (Fig. 3.7).

Following IL-10 and TLR9L single treatments (Fig. 3.6B, E), most cells presented a smaller, more rounded phenotype with few cytoplasmic extensions as the similar phenotype as control (Fig. 3.6A). In contrast, following single treatment with IFN-γ (Fig. 3.6C) and TLR2L (Fig. 3.6D), RAW264.7 cells were larger and exhibited numerous cytoskeletal extensions.

RAW264.7 cells subjected to combined IL-10/TLR2L or IL-10/TLR9L treatments displayed the same phenotype as cells treated with IL-10 alone (Fig. 3.7A, C). However, RAW264.7 cells treated with IFN-γ combined with TLR2L showed strong spreading, cytoskeletal projections and membrane ruffling (Fig. 3.7B, arrow). This phenotype was observed in cells treated with combined IFN-γ and TLR9L (Fig. 3.7D)

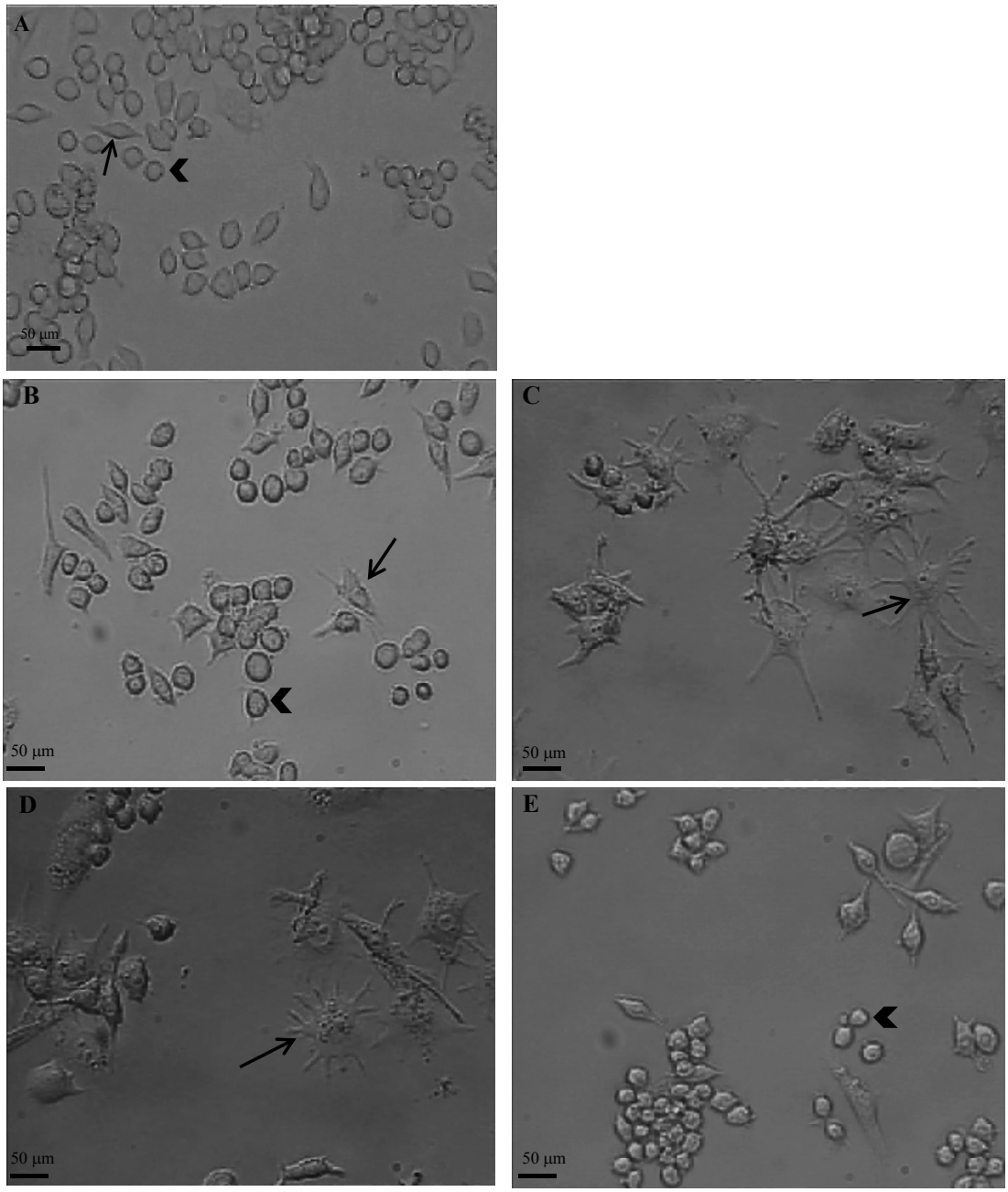

Figure 3.6. Morphology of RAW264.7 cells after stimulation with different immune modulators . RAW264.7 cells were untreated (A) and treated with (B) IL-10, (C) IFN-γ, (D) TLR2 ligands and (E) TLR9 ligands for 24 hr, and then digital images were captured using an Exwave HAD 3CCD colour video camera mounted on an inverted microscope. Concentrations of immune modulators are shown in Table 3.1. The scale bar represents 50 µm. Arrowheads indicates cells with monocyte-like morphology and arrows show cells with macrophage-like morphology.

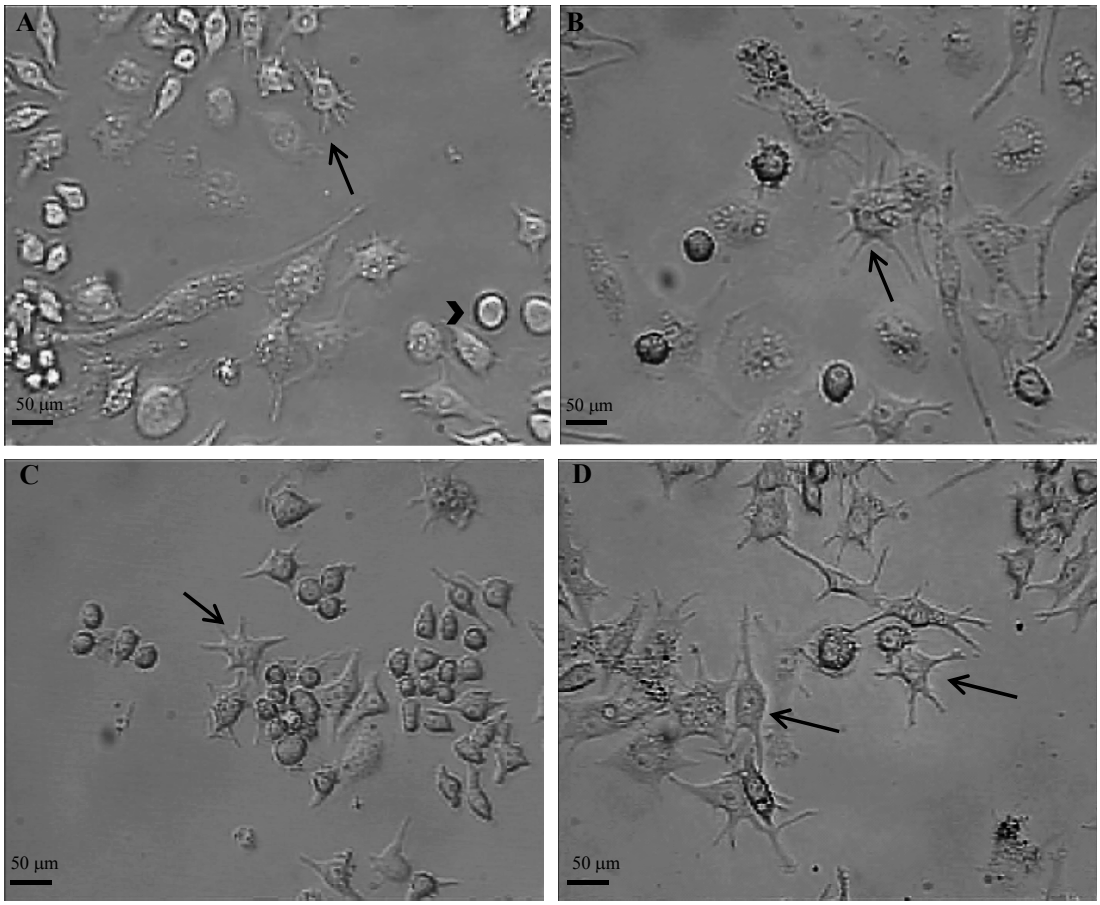

Figure 3.7. Morphology of RAW264.7 cells after stimulation with different treatment combinations. RAW264.7 cells were treated for 24 hr with (A) IL-10 plus TLR2 ligands, (B) IFN-γ plus TLR2 ligands, (C) IL-10 plus TLR9 ligands and (D) IFN-γ plus TLR9 ligands, and then digital images were captured using an Exwave HAD 3CCD colour video camera mounted on an inverted microscope. Concentrations of the immune modulators are shown in Table 3.1. The scale bar represents 50 µm. Arrowheads indicate monocyte-like macrophages, and arrows indicate cells with increased spreading, more cytoskeletal characteristics and a macrophage-like morphology.

3.3.5.1 IL-10 and TLR9 ligands transiently up-regulate *Trib1* expression in RAW264.7 cells

Real-time PCR was used to study the time course of *Trib1* expression in RAW264.7 cells following combined IL-10/TLR9L and IL-10/TLR2L treatment.

Optimised concentrations of immune modulators were added to RAW264.7 cells and total RNAs were extracted after 0.5, 1, 3, 6, 8 and 24 hr. Untreated controls were used to establish baseline *Trib1* expression, which did not vary over the time course.

In general, IL-10 and TLR9L did not induce a high level of *Trib1* expression over the course of the experiment. Only at the 1 and 3 hr time points did IL-10 treatment induce a significant increase in *Trib1* expression over the baseline (Table 3.2; $p = 0.002$ and $p = 0.04$, respectively). In contrast, IL-10 down-regulated of *Trib1* expression after 30 min ($p < 0.001$), 6 hr ($p = 0.001$), 8 hr ($p = 0.001$) and 24 hr ($p < 0.001$).

TLR9L single treatment rapidly up-regulated *Trib1* expression after 1 hr compared to untreated cells ($p = 0.002$), but did not significantly down-regulate *Trib1* expression at 0.5, 6, 8 and 24 hr time points compared to untreated cells ($p > 0.10$). Surprisingly, following combined treatment with IL-10 and TLR9L, *Trib1* expression was not significantly different from untreated cells (Fig. 3.8A; $p > 0.10$).

Thus, in the presence of both IL-10 and TLR9L, *Trib1* expression was low, but *Trib1* expression was transiently up-regulated following single IL-10 and single TLR9L treatments.

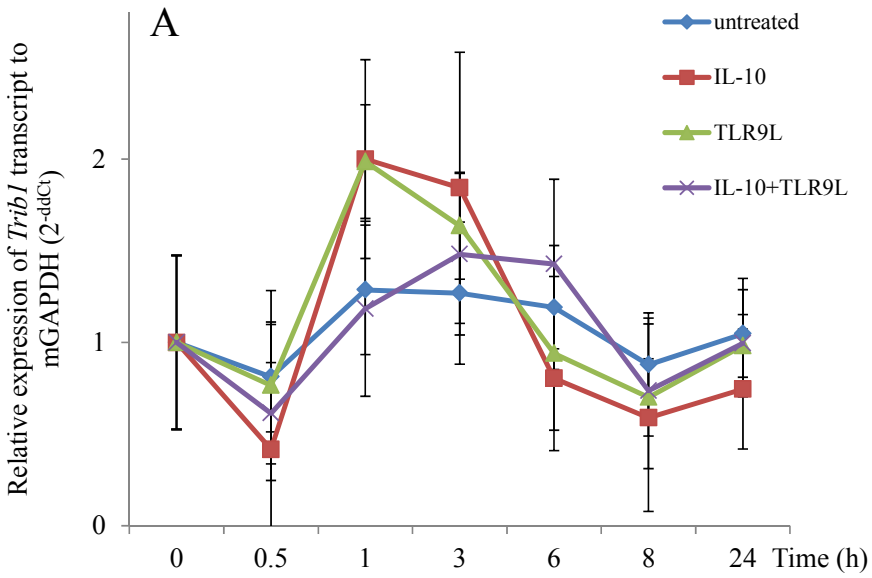

Figure 3.8 (A). Timecourse of *Trib1* expression in treated RAW264.7 cells. RAW264.7 cells were stimulated with IL-10 in the presence or absence of TLR9 ligands for different times. Total RNA was extracted from cells of each treatment group and *Trib1* expression was measured by qPCR. Values comprise the mean ± SD of three independent experiments done in triplicate. *Trib1* expression was normalised to mGAPDH expression and the relative ddCt formula is described in Chapter 2. Relative Trib1 mRNA expression was compared to a calibrator, the zero time point. Statistical analysis is described in sections 2.8. LME was used to examine *Trib1* ddCt relative to treatment, and random effects were experiment. All data required Log2 transformation to normalise the residuals pre-analysis. A standard *post-hoc* (*Tukey*) test was used to carry out pair-wise comparisons of all treatments. In all cases, $p < 0.05$ relative to the untreated group was considered to indicate statistical significance. Details of *p*-values are shown in Tables 3.2.

Table 3.2. Statistical analysis of *Trib1* expression following treated single or dual treatment with IL-10 and TLR9L

Comparison	0.5 hr	1 hr	3 hr	6 hr	8 hr	24 hr
Untreated vs. IL-10	***p* <0.001**	***p* <0.01**	***p* <0.05**	***p* <0.01**	***p* <0.01**	***p* <0.001**
Untreated vs. TLR9L	$p = 0.982$	***p* <0.01**	$p = 0.274$	$p = 0.130$	$p = 0.168$	$p = 0.891$
Untreated vs. dual	$p = 0.288$	$p = 0.909$	$p = 0.693$	$p = 0.338$	$p = 0.379$	$p = 0.943$
IL-10 vs. TLR9L	***p* <0.001**	$p = 0.909$	$p = 0.834$	$p = 0.476$	$p = 0.396$	***p* <0.05**
IL-10 vs. dual	$p = 0.07$	***p* <0.001**	$p = 0.409$	***p* <0.001**	$p = 0.17$	***p* <0.01**
TLR9L vs. dual	$p = 0.502$	***p* <0.001**	$p = 0.896$	***p* <0.001**	$p = 0.968$	$p = 0.998$

3.3.5.2 TLR2 ligands induce high levels of *Trib1* expression in RAW264.7 cells

Conversely, when RAW264.7 cells were treated with TLR2L, *Trib1* expression was potently induced, reaching maximal expression peak after 30min (Fig. 3.8B), and then decreasing between 1hr and 24 hr. From 30 min to 6 hr after treatment, *Trib1* expression was significantly higher than in untreated controls (Table 3.3; $p < 0.002$). After 24 hr, *Trib1* expression was lower than baseline ($p < 0.001$).

Combined TLR2L and IL-10 treatment up-regulated *Trib1* transcripts from 30 min onwards, reaching a peak after 3 hr (Trib1 expression at 30min, 1hr and 3hr time points were above basal levels, $p < 0.001$) and followed by a gradual decrease after 6 hr and a return to basal levels (Fig. 3.8B; $p < 0.01$). After 24 hr, Trib1 expression was lower than in untreated cells, but not significantly ($p = 0.06$).

In contrast to TLR9L, TLR2L treatment induced a rapid, high level of *Trib1* expression from 30 min to 6 hr. Further, combined IL-10 and TLR2L treatment reduced *Trib1* expression from 30min to 3 hr.

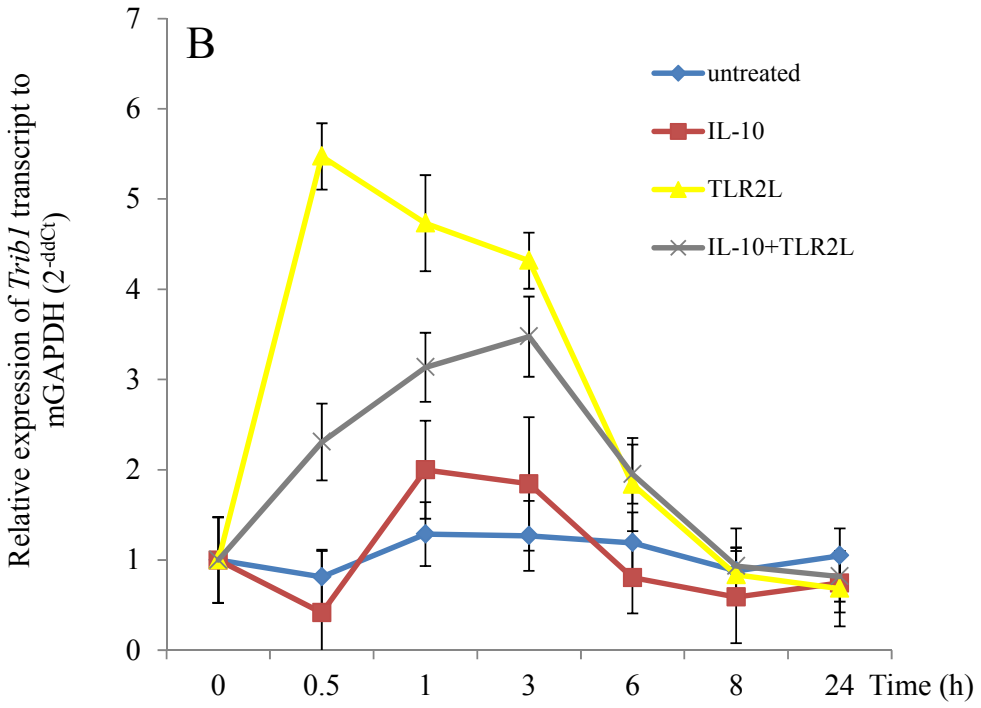

Figure 3.8 (B). Timecourse of *Trib1* expression in treated RAW264.7 cells. RAW264.7 cells were stimulated with IL-10 in the presence or absence of TLR2 ligands for different times. Total RNA was extracted from cells of each treatment group and *Trib1* expression was measured by qPCR. Values comprise the mean ± SD of three independent experiments done in triplicate. *Trib1* expression was normalised to mGAPDH expression and the relative ddCt formula is described in Chapter 2. Relative Trib1 mRNA expression was compared to a calibrator, the zero time point. Statistical analysis is described in sections 2.8. LME was used to examine Trib1 ddCt relative to treatment, and random effects were experiment. All data required Log2 transformation to normalise the residuals pre-analysis. A standard *post-hoc* (*Tukey*) test was used to carry out pair-wise comparisons of all treatments. In all cases, $p < 0.05$ relative to the untreated group was considered to indicate statistical significance. Details of *p*-values are shown in Tables 3.3.

Table 3.3. Statistical analysis of *Trib1* expression following single or dual treatment with IL-10 and TLR2L

Comparison	0.5 hr	1 hr	3 hr	6 hr	8 hr	24 hr
Untreated vs. IL-10	***p* <0.001**	***p* <0.01**	***p* <0.05**	***p* <0.01**	***p* <0.01**	***p* <0.001**
Untreated vs. TLR2L	***p* <0.001**	***p* <0.001**	***p* <0.001**	***p* <0.01**	$p = 0.969$	***p* <0.001**
Untreated vs. dual	***p* <0.001**	***p* <0.001**	***p* <0.001**	***p* <0.01**	$p = 0.949$	$p = 0.063$
IL-10 vs. TLR2L	***p* <0.001**	***p* <0.001**	***p* <0.001**	***p* <0.001**	***p* <0.05**	$p = 0.819$
IL-10 vs. dual	***p* <0.001**	***p* <0.01**	***p* <0.001**	***p* <0.001**	***p* <0.001**	$p = 0.794$
TLR2L vs. dual	***p* <0.001**	***p* <0.01**	$p = 0.492$	$p = 0.956$	$p = 0.754$	$p = 0.277$

3.3.6.1 IFN-γ strongly induces *Trib1* expression in RAW264.7 cells

Stimulation of RAW264.7 cells with IFN-γ induced a high level of *Trib1* expression. *Trib1* transcript expression was up-regulated from 1 hr onwards, with a peak of expression at 3 hr, followed by a decrease to baseline after 8 hr (Fig. 3.9A). Between 1 hr to 6 hr, IFN-γ-induced *Trib1* expression was significantly higher in untreated cells (p <0.001, p <0.001 and p <0.001 for 1hr, 3hr and 6hr samples, respectively, Table 3.4).

Treatment with TLR9L alone induced a rapid up-regulation of *Trib1*expression after 1 hr (p = 0.002), tailing off from 3 hr to 8 hr. However, *Trib1* expression was not significantly down-regulated after 6 hr, 8 hr or 24 hr compared to untreated cells (Fig. 3.9A; p >0.10).

Interestingly, dual IFN-γ/TLR9L treatment restored the expression profile to that seen following IFN-γ treatment alone. After 6 hr, IFN-γ-induced *Trib1* expression was significantly higher than in the dual treatment group (p = 0.04). Therefore, compared with IL-10-induced *Trib1* expression (Fig. 3.8), IFN-γ up-regulated *Trib1* expression was from 1 hr to 6 hr.

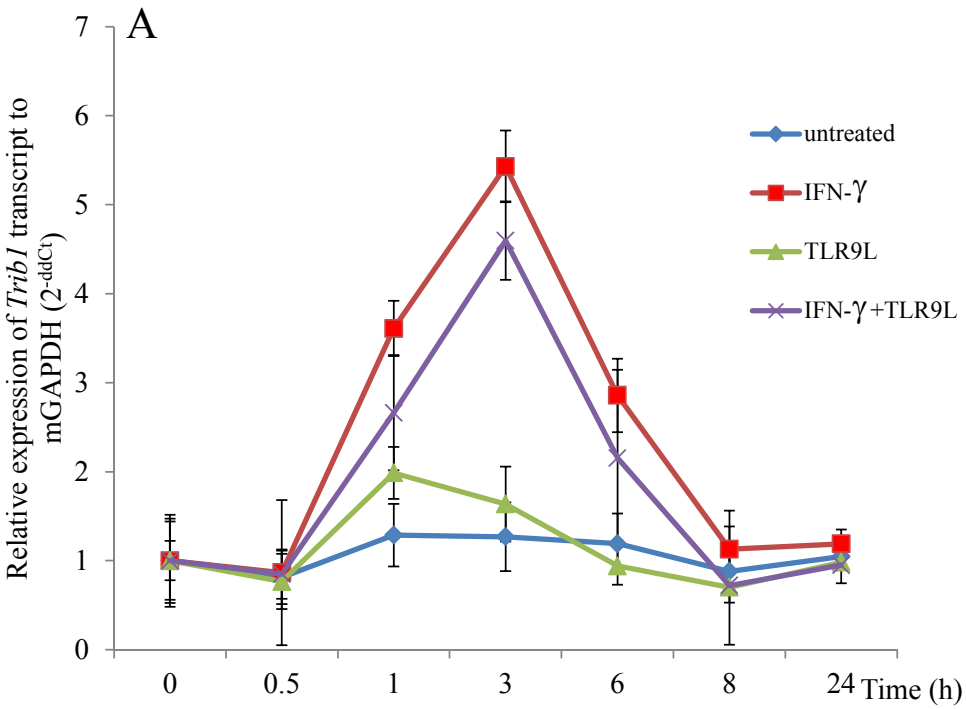

Figure 3.9 (A). Timecourse of *Trib1* expression in treated RAW264.7 cells. RAW264.7 cells were stimulated with IFN-γ in the presence or absence of TLR9 ligands for different times. Total RNA was extracted from cells of each treatment group and *Trib1* expression was measured by qPCR. Values comprise the mean ± SD of three independent experiments done in triplicate. Trib1 expression was normalised to mGAPDH expression and the relative ddCt formula is described in Chapter 2. Relative Trib1 mRNA expression was compared to a calibrator, the zero time point. Statistical analysis is described in sections 2.8. LME was used to examine Trib1 ddCt relative to treatment, and random effects were experiment. All data required Log2 transformation to normalise the residuals pre-analysis. A standard *post-hoc* (*Tukey*) test was used to carry out pair-wise comparisons of all treatments. In all cases, p <0.05 relative to the untreated group was considered to indicate statistical significance. Details of p-values are shown in Tables 3.4.

Table 3.4. Statistical analysis of *Trib1* expression following single or dual treatment with IFN-γ and TLR9L

Comparison	0.5 hr	1 hr	3 hr	6 hr	8 hr	24 hr
Untreated vs. IFN-γ	$p = 0.937$	$\mathbf{p < 0.001}$	$\mathbf{p < 0.001}$	$\mathbf{p < 0.001}$	$p = 0.117$	$p = 0.775$
Untreated vs. TLR9L	$p = 0.982$	$\mathbf{p < 0.01}$	$p = 0.274$	$p = 0.130$	$p = 0.168$	$p = 0.891$
Untreated vs. dual	$p = 0.986$	$\mathbf{p < 0.001}$	$\mathbf{p < 0.001}$	$\mathbf{p < 0.001}$	$p = 0.998$	$p = 0.90$
IFN-γ vs TLR9L	$p = 0.774$	$\mathbf{p < 0.001}$	$\mathbf{p < 0.001}$	$\mathbf{p < 0.001}$	$\mathbf{p < 0.05}$	$p = 0.52$
IFN-γ vs. dual	$p = 0.998$	$p = 0.171$	$p = 0.617$	$\mathbf{p < 0.05}$	$p = 0.281$	$p = 0.378$
TLR9L vs. dual	$p = 0.851$	$p = 0.201$	$\mathbf{p < 0.001}$	$\mathbf{p < 0.001}$	$p = 0.554$	$p = 0.996$

3.3.6.2 IFN-γ combined with TLR2 ligands enhance *Trib1* expression in RAW264.7 cells

According to the previous result (Fig.3.8B), *Trib1* expression is strongly increased in RAW264.7 cells following TLR2L treatment, peaking after 30 min (Fig. 3.9B).

Combined IFN-γ and TLR2L treatment induced a similar expression pattern to that with IFN-γ alone, with increased expression along with an earlier peak of expression (Fig. 3.9B; from 3 hr to 1 hr). From 30 min to 6 hr, *Trib1* expression induced by combined treatment was significantly higher than in untreated controls (Table 3.5; $p < 0.001$), but decreased to baseline at the 8 hr and 24 hr time points ($p > 0.10$ for both relative to basal levels). After 24 hr, *Trib1* expression had returned to basal levels for all three treatments.

From another perspective, the TLR2L-induced peak of *Trib1* expression occurred after 30 min and was significantly higher than the basal and IFN-γ-induced expression, as well as Trib1 expression following combined treatment (p <0.001 for all). At this time point, the *Trib1* expression following combined treatment was higher than in cells treated with IFN-γ alone (p <0.001). For dual treatment-induced *Trib1* expression, the time point for maximal expression was 1 hr and expression levels were higher than in cells treated with IFN-γ alone (p = 0.004), but was not significantly different from TLR2L-treated cells (p = 0.298). After 3 hr, IFN-γ-induced *Trib1* expression was higher than in cells subjected to combined treatment (p <0.001), but was not significantly different from in expression in TLR2L-treated cells (p = 0.111).

Thus, following stimulation with IFN-γ and TLR2L, *Trib1* expression is strongly increased between 30 min and 3 hr (Fig. 3.9B).

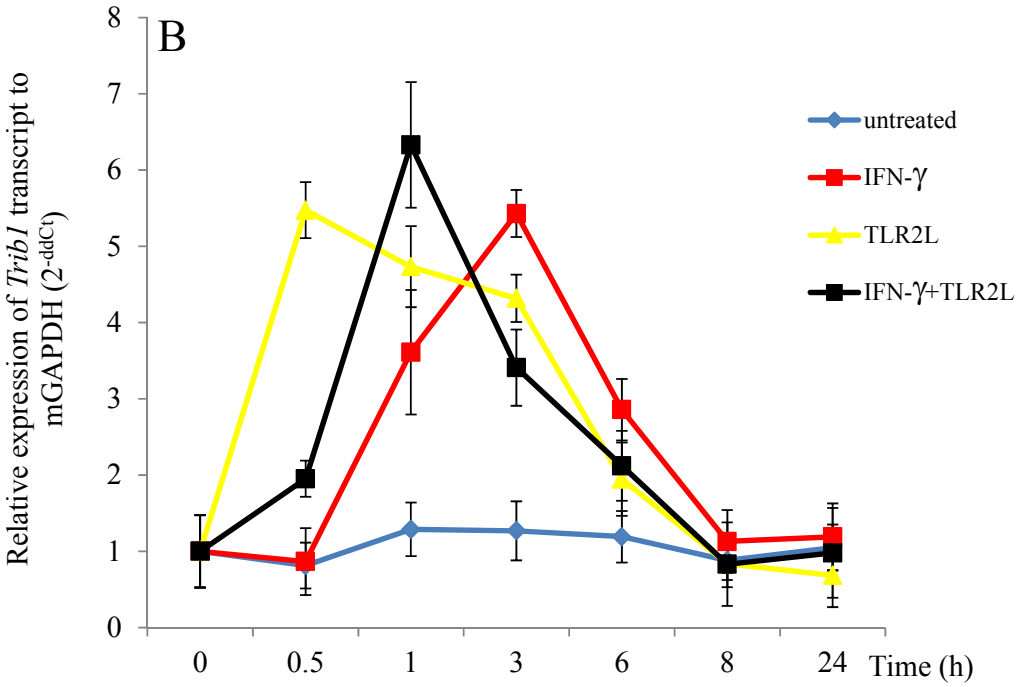

Figure 3.9 (B). Timecourse of *Trib1* expression in treated RAW264.7 cells. RAW264.7 cells were stimulated with IFN-γ in the presence or absence of TLR2 ligands for different times. Total RNA was extracted from cells of each treatment group and *Trib1* expression was measured by qPCR. Values comprise the mean ± SD of three independent experiments done in triplicate. Trib1 expression was normalised to mGAPDH expression and the relative ddCt formula is described in Chapter 2. Relative Trib1 mRNA expression was compared to a calibrator, the zero time point. Statistical analysis is described in sections 2.8. LME was used to examine Trib1 ddCt relative to treatment, and random effects were experiment. All data required Log2 transformation to normalise the residuals pre-analysis. A standard *post-hoc* (*Tukey*) test was used to carry out pair-wise comparisons of all treatments. In all cases, $p < 0.05$ relative to the untreated group was considered to indicate statistical significance. Details of *p*-values are shown in Tables 3.5.

Table 3.5. Statistical analysis of *Trib1* expression following single or dual treatment with IFN-γ and TLR2L.

Comparison	0.5 hr	1 hr	3 hr	6 hr	8 hr	24 hr
Untreated vs. IFN-γ	$p = 0.937$	***p* <0.001**	***p* <0.001**	***p* <0.001**	$p = 0.117$	$p = 0.775$
Untreated vs. TLR2L	***p* <0.001**	***p* <0.001**	***p* <0.001**	***p* <0.01**	$p = 0.969$	***p* <0.001**
Untreated vs. dual	***p* <0.001**	***p* <0.001**	***p* <0.001**	***p* <0.001**	$p = 0.957$	$p = 0.955$
IFN-γ vs. TLR2L	***p* <0.001**	$p = 0.364$	$p = 0.128$	***p* <0.001**	***p* <0.05**	***p* <0.001**
IFN-γ vs. dual	***p* <0.001**	***p* <0.01**	***p* <0.001**	***p* <0.05**	***p* <0.05**	$p = 0.455$
TLR2L vs. dual	***p* <0.001**	$p = 0.298$	$p = 0.111$	$p = 0.60$	$p = 0.998$	***p* <0.05**

3.4 Discussion

In this chapter, I sought to measure the expression profiles of *Trib* family members and to determine how *Trib1* expression changes in response to stimuli in macrophages. For this, I used reverse-transcription PCR (RT-PCR) to show that *Trib1* and *Trib3* were expressed in RAW264.7 myeloid cells, but that *Trib2* was not. Moreover, qPCR demonstrated that *Trib1* expression was higher than *Trib3*; therefore, *Trib1* expression was assessed in subsequent experiments. Moreover, IFN-γ and TLR2 ligands induced high levels of *Trib1* expression from 30 min to 6 hr, whereas IL-10 and TLR9 ligands induced weaker *Trib1* expression.

Trib1 and *Trib3* were expressed in RAW264.7 cells (Fig. 3.3B), in agreement with a previous report that *Trib1* and *Trib3* are expressed in monocytes (Ashton-Chess *et al.*, 2008). Moreover, the discovery that *Trib2* is not expressed in RAW264.7 cells (Fig. 3.3B) suggests that *Trib2* is not expressed in immortalised cell line. The expression profiles of Trib family members showed that each Trib family member exhibits cell-type specificity, also consistent with previously studies (Ashton-Chess *et al.*, 2008; Sung *et al.*, 2006).

The second aim of this chapter was to identify a good macrophage activation marker following TLR2/9 ligands and IL-10/IFN-γ stimuli. Moreover, the effective concentrations of these immune modulators were established for further experiments. I identified TNF-α production to be an effective indicator for these stimulators. TNF-α is a pro-inflammatory cytokine that is mainly up-regulated by activation of the NF-κB pathway (Jongeneel, 1994). Dose response curves showed a statistically

significant induction of TNF-α following IFN-γ treatment (Fig. 3.4B and Fig. 3.5). Most IFN-γ signalling occurs through activation of the STAT1 pathway, and not the NF-κB pathway (Lang, 2005). Hence, the increase in TNF-α production is probably not a direct result of IFN-γ stimulation, but instead may occur through activation of NF-κB by IFN-responsive genes (Lang, 2005). A greater increase in TNF-α production was seen following treatment with TLR2L and TLR9L, especially TLR2L. TLR2 receptor signalling leads to MAPK activation, which directly activates the NF-κB signalling pathway (Krishnan *et al.*, 2007). Although TLR9 receptor signalling preferentially activates the Interferon Regulatory Factor 7 (IRF7) pathway, the NF-κB pathway is also activated to a lesser degree (Sabroe *et al.*, 2008). The induction of NF-κB-induced TNF-α production by TLR signalling pathways was shown in Figs 3.4 and 3.5. Moreover, TLR2L-induced TNF-α production was constitutive, since TNF-α production remained high 48 hr after single or combined treatments. Conversely, combined IFN-γ and TLR2L treatment resulted in decreased TNF-α production compared with TLR2L treatment alone. IFN-γ has been reported to inhibit TLR2L activation of the MAPK pathway in macrophages (Hu *et al.*, 2006), which may explain my observations (Fig. 3.5). However, the same result was seen following combined treatment with TLR9L and IFN-γ, although crosstalk between IFN-γ and TLR9 has not been reported.

IL-10, an anti-inflammatory cytokine, cannot activate NF-κB signalling and this is borne out by the reduced induction of TNF-α production even in combined treatments. IL-10 inhibits the expression of MHC class II and the co-stimulatory

CD80/CD86 molecules in macrophages, and suppresses the production of pro-inflammatory cytokines, such as IL-6, IL-12 and TNF-α via the STAT-3 pathway (Haddad *et al.*, 2003). In macrophages, low TNF-α production is associated with IL-10 inhibition of the *TNF* gene through inhibition of transcriptional elongation (Smallie *et al.*, 2010), which may in part explain my observation of low TNF-α production in IL-10-treated cells (Fig. 3.4A and Fig. 3.5). I went on to investigate Trib1-associated signalling pathways in the next chapter.

My observations of RAW264.7 cell morphology indicated different stimulators induce various characteristics in macrophages. IL-10 treated macrophages (Fig 3.6B) are more monocyte-like than macrophage-like in appearance, indicating that IL-10 cannot activate macrophages. In contrast, IFN-γ- and TLR2L- treated macrophages (Fig. 3.6 C, D) showed a strong activation, consistent with previous findings (Gordon, 2003). The presence of pseudopodia and cytoplasmic extensions shows that there are more lysozymes and macrophages present and that cells are competent to undergo phagocytosis. Macrophage phagocytosis of microorganisms is important for host immunity, and activated macrophages kill ingested pathogens by the production of reactive oxygen and nitrogen metabolites (Gordon and Taylor, 2005). However, TLR9L-treated macrophages (Fig. 3.6E) retained a monocyte-like morphology, indicating that the concentrations of TLR9L used might not be sufficient to induce the macrophage activation. Interestingly, this morphological observation is consistent with TNF-α production, which demonstrated that TLR2 ligands cooperate with IFN-γ to induce macrophage activation.

The main aim of this chapter was to explore *Trib1* expression levels following stimulation with TLR2/TLR9 ligands and IL-10/IFN-γ. The qPCR results demonstrated that macrophage *Trib1* expression is transiently up-regulated by IL-10 after 1 hr and 3 hr, but is down-regulated at 0.5 hr, 6 hr, 8 hr and 24 hr time points (Figs. 3.8). IL-10 supresses macrophage activation (Haddad *et al.*, 2003), and I observed that IL-10-induced *Trib1* expression is very weak (Fig. 3.8). It is reasonable to speculate that *Trib1* is associated with IL-10 which inhibits macrophage activation. Moreover, IL-10 is an autocrine cytokine in macrophages (Lang *et al.*, 2002), and IL-10 treatment of differentiated macrophages results in decreased inflammation by induction of the inhibitory C/EBPβ protein (Csoka *et al.*, 2007). Furthermore, C/EBPβ function is inhibited by Trib1 (Yamamoto *et al.*, 2007). Therefore, it is important to determine whether IL-10 down-regulates Trib1 in macrophages, and whether Trib1 inhibits IL-10 production through C/EBPβ. It is possible that a negative feedback loop is involved in the suppression of Trib1 by IL-10, leading to macrophage deactivation (Gordon, 2003). Trib2 can suppress IL-10 synthesis in human monocyte-derived macrophages (Deng *et al.*, 2009), which suggests that Trib1 also may suppress IL-10 in macrophages. Therefore, the precise mechanism whereby IL-10 suppresses Trib1 in macrophage remains to be determined.

The failure of TLR9L to induce *Trib1* expression may be due to the concentration being too low or the time used for stimulating TLR9 being suboptimal. I chose 1nM TLR9L, as this was the optimal concentration for TNF-α production (Fig. 3.4D). TLR9 is expressed in the endosome, and can therefore recognise endosomal CpG DNA following internalisation of bacterial DNA. The time required for

internalisation is greater than the time required for TLR2 response (Hallman M, 2001; Kaisho and Akira, 2001; Takeuchi and Akira, 2010). Therefore, it is important to measure different TLRs-mediated inflammation at the correct time point.

For microorganism infection, the first line of response is rapid and potent. When TLR2 ligands engage with TLR2 receptors, MyD88 is rapidly activated and TRAF6, MAPK and NF-κB mediate the downstream production of pro-inflammatory cytokines and activate macrophages (Kaisho and Akira, 2001). I observed that macrophage Trib1 was up-regulated quickly (30 min) following treatment with TLR2 ligands. Interestingly, combined IL-10 and TLR2L treatment resulted in rapid (within 30 min) and extended *Trib1* expression (up to 3 hr), followed by a decrease to baseline. This expression pattern was similar to the TLR2L single treatment, but with a lower degree of expression. IL-10 inhibition of TLR2L-induced inflammation has been reported in *Yersinia pestis* infections (Hu *et al.*, 2006; Sing *et al.*, 2002). Induction of IL-10 by TLR2L is proposed to play a role in suppression of host immune responses and it is possible that Trib1 might be involved in this process.

In addition, compared to TLR2L plus cytokine treatment, the *Trib1* expression peak following IFN-γ treatment occurred after 3 hr. IFN-γ is a strong macrophage activator. This specific *Trib1* up-regulation in macrophages treated with IFN-γ and TLR2L indicates that Trib1 contributes to innate immunity processes, such as macrophage activation, and also to microbial infection. Here, IFN-γ induced *Trib1* expression at a high level in macrophages, compared IL-10-induced *Trib1* expression. This reinforces the possibility that Trib1 is associated with macrophage activation.

Therefore, induction of Trib1 expression is a consequence of pro-inflammatory activation of macrophages.

Immunoblots showed that the anti-Trib1 antibody was not specific (data not shown) and therefore I could not examine Trib1 protein expression in these cells. Therefore, in this study, only *Trib1* mRNA results are presented.

Compared to IL-10- and IFN-γ-induced *Trib1* expression, *Trib1* expression was very low following combined with TLR9L treatments. Conversely, IFN-γ-induced *Trib1* expression followed by TLR2L was strong. Hence, further experiments will only focus on the IFN-γ and TLR2L treatments. Moreover, as TLR2L and IFN-γ induced TNF-α production through the MAPK pathway, they are more likely to link with Trib1. Therefore, in the following chapters, IFN-γ- and TLR2L induced Trib1 expression will be evaluated.

To summarise this data, Trib1 is a macrophage marker and functions by triggering macrophages to be activated or deactivated by different signalling pathways in response to infection. Moreover, this data also highlighted a negative feedback loop between Trib1 and IL-10 in macrophages via TNF-α production, which deactivates macrophage function.

The results of this chapter demonstrate that Trib1 is expressed in RAW264.7 cells. Moreover, the Trib1 responses in macrophages to pro- or anti-inflammatory cytokines in the presence of TLR2/9 ligand-induced inflammation are distinct. IL-10

induces weak *Trib1* expression, indicating that IL-10 deactivation of macrophages may occur via Trib1 modulation.

In conclusion, *Trib1* expression is influenced by pro-/anti-inflammatory cytokines and/or TLR ligand stimulation of RAW264.7 cells (Fig. 3.10). More details of this pathway interaction will be addressed in the next chapter.

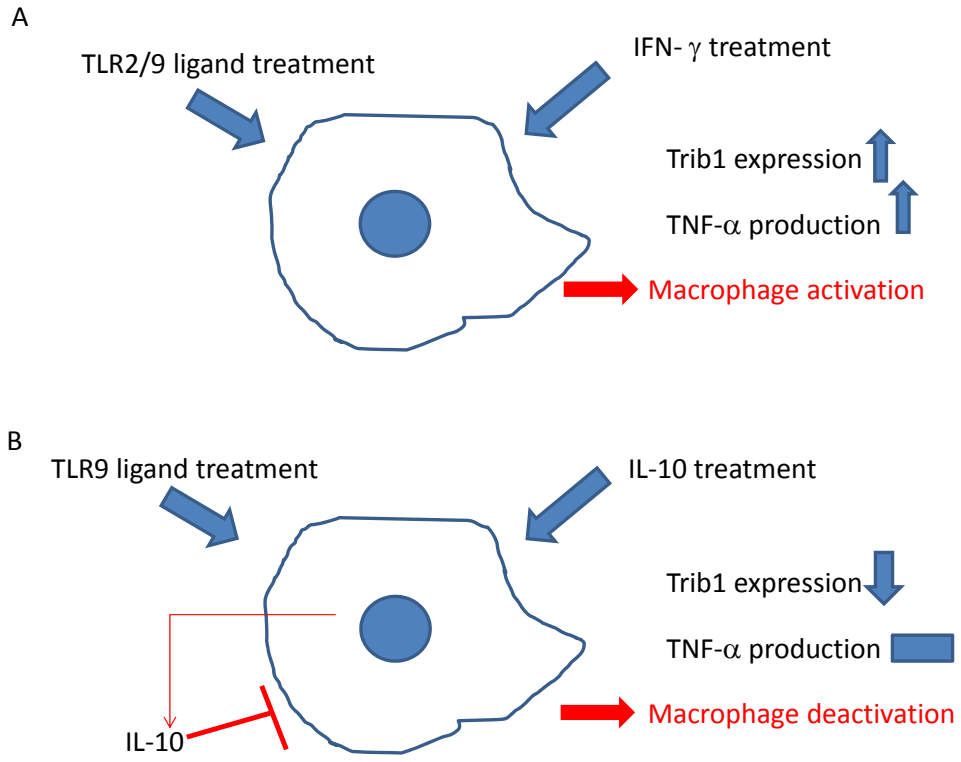

Figure 3.10. Summary of Trib1 expression in macrophages treated with TLR ligands, and cytokine-induced responses. (A) When macrophages are treated with IFN-γ and TLR2/9 ligands, Trib1 expression is induced and TNF-α production is increased, leading to macrophages activation. (B) Conversely, when macrophages are treated with IL-10 and TLR9 ligands, Trib1 expression is weak and TNF-α production is low. Under these conditions, macrophages may become deactivated.

Chapter 4: Silencing of Trib1 to investigate its biological function

Abstract

Trib was first described in dog thyroid cells and its functions were identified in *Drosophila* in 2000. In mammalian systems, three members of the Trib family have been identified. They function as scaffold proteins to control the activity of signalling pathways, e.g., Trib1 regulates MAPK, NF-κB and C/EBPβ. To investigate the role of Trib1 in the TLR-induced inflammatory response to pro-inflammatory cytokines, RAW264.7 cells were stimulated with TLR2 ligands in the presence or absence of IFN-γ. SiRNA-mediated *Trib1* knockdown resulted in inhibition of C/EBPβ expression at the translational level in both stimulated and resting macrophage populations. TNF-α production increased in *Trib1*-knockdown cells after treatment with IFN-γ and/or TLR2L, while IL-6 secretion remained unchanged. Finally, expression of ERK1/2 was reduced in Trib1 siRNA-treated cells.

In conclusion, these results suggest that Trib1 contributes to the pro-inflammatory response of macrophages by acting as a regulator of ERK1/2 and C/EBPβ during TLR2 ligand-mediated macrophage activation.

4.1 Introduction

Trib1 is a regulator of Toll/IL-1-induced downstream signalling and works as a scaffold protein to modulate MAPK signalling pathways (Hegedus *et al.*, 2007; Kiss-Toth *et al.*, 2004). In *Caenorhabditis elegans* nematodes, the NIPI-3 kinase-like protein acts upstream of MAPK and has homology to human Trib1 (Pujol *et al.*, 2008). Up-regulation of Trib1 in vascular smooth muscle cells treated with IL-1β or LPS induces proliferation and chemotaxis via inhibition of the JNK pathway (Sung *et al.*, 2007). Moreover, using Trib1-deficient macrophages it has been demonstrated that Trib1 negatively regulates C/EBPβ expression in TLR-mediated signalling. However, macrophages in which Trib1 has been deleted have the same levels of phosphorylated MAPKs (p38, JNK and ERK) and IκB as normal macrophages (Yamamoto *et al.*, 2007). Trib1 is also involved in C/EBPα degradation during myeloid leukaemogenesis through a Trib1–MEK1 interaction (Yokoyama *et al.*, 2010).

The innate immune system responds to infection by producing pro-inflammatory mediators such as TNF-α and IL-6 (Matsusaka *et al.*, 1993). Conserved pathogen-associated molecular patterns on microorganisms are recognised by TLRs, which mediate signals to activate immune cells via association with different intracellular adaptor proteins. Activation of TLR2 occurs after binding to the relevant ligands, such as bacterial lipoarabinomannan (LAM), bacterial lipoprotein (BLP) and peptidoglycans (PGN), as well as the yeast cell wall particle, zymosan (Takeda *et al.*, 2003). TNF-α is a prototypical pro-inflammatory cytokine for which induction by TLRs is dependent on NF-κB and MAPKs, and as well as on C/EBPβ and C/EBPδ (Akira, 2003; Lu *et al.*, 2009) (Fig. 4.1).

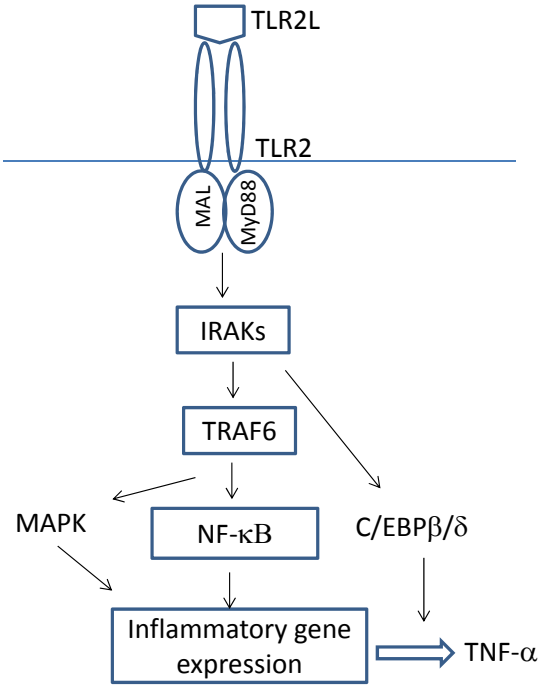

Figure 4.1. Regulation of TLR2 signalling pathway is mediated by C/EBPβ and δ, and MAPK. In addition to the well-known TLR2 signalling cascade (MyD88/TRAF/NF-κB), the C/EBPβ and C/EBPδ transcription factors are also trigger pro-inflammatory cytokine production. MyD88 is recruited activated TLRs, then binds to IRAK4, which activates C/EBPβ and C/EBPδ, leading to inflammatory gene expression.

IFN-γ influences LPS-dependent signalling by promoting ligand–receptor interactions, as well as by activating downstream signalling machinery. Many effects of LPS are mediated by the NF-κB transcription factor. In the RAW264.7 macrophage-like cell line, IFN-γ pre-treatment promotes rapid NF-κB activation and degradation of the NF-κB inhibitor, IκB, upon LPS exposure (Adib-Conquy and Cavaillon, 2002; Tamai *et al.*, 2003). Compared with TLRs, IFN-γ is a weak activator of MAPK, but can trigger activation of the MEK1/ERK1/2 pathway in a range of cell lines and primary cells (Hu *et al.*, 2001; Hu *et al.*, 2007b).

When IFN-γ stimulates this pathway, two waves of ERK activation occur. An early wave (after approximately 30 min) leads to AP-1 activation independent of the JAK–STAT1 pathway (Gough *et al.*, 2007). A second pathway, necessary for STAT1 Ser^{727} phosphorylation, is activated after longer (2 hr) exposure to IFN-γ (Hu *et al.*, 2001) (Fig. 4.2). However, the ability of IFN-γ to activate the p38 and JNK pathways remains undetermined. Additionally, C/EBPβ-dependent gene transcription responds to IFN-γ through ERK1/2 (Hu *et al.*, 2001).

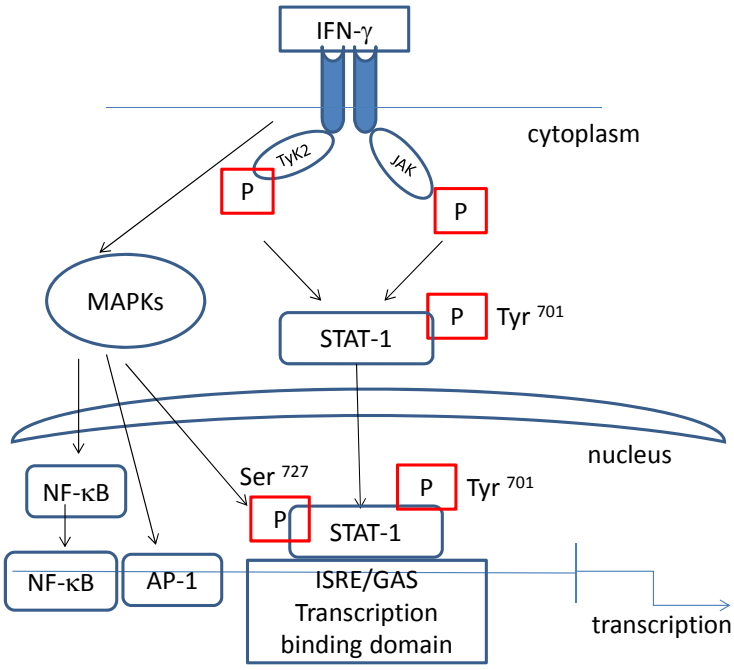

Figure 4.2. IFN-γ activates a signalling through STAT-1 and MAPK. IFN-ɣ binds to IFNGR and JAK/TYK2, which are then phosphorylated. Most IFN-γ signalling occurs through STAT-1, which becomes phosphorylated at Tyr^{701} and is translocated into the nucleus, where it binds to the ISRE and GAS (ISRE/GAS) binding domain on the target genes such as MHC class I and II, leading to transcription. IFN-γ alternatively triggers the MAPK cascade, resulting in STAT-1 phosphorylation at Ser^{727}. Finally, IFN-γ activates ERK1/2 mediated by AP-1. Upon LPS exposure, IFN-γ triggers NF-κB activation, resulting in TNF-α production.

RNA interference (RNAi) was first described in the nematode *Caenorhabditis elegans* in 1998 (Fire *et al.*). Three years later, RNAi was described in mammalian cells by Tuschl and colleagues (Elbashir *et al.*, 2001). RNAi induces post-transcriptional gene silencing by targeting mRNA for degradation and thus inhibiting protein translation (Pai *et al.*, 2005). Therefore, in recent years, RNAi-mediated gene knockdown techniques have been extensively used to investigate gene function. It is a powerful tool for assaying gene function in mammalian cell lines, particularly for identifying potential regulators of signalling pathways (Martin and Caplen, 2007).

Although the experiments described in Chapter 3 did not provide direct evidence that Trib1 regulates the MAPK pathway, as reported previously (Kiss-Toth *et al.*, 2004), the results suggested that Trib1 may be involved in regulating the MAPK pathway following IFN-γ and TLR2L treatment to modulate the expression, of genes, such as TNF-α. Based on the literature, the biological functions of Trib1 are not clear, in particular the identity of signalling pathway triggered by Trib1 in macrophages in response to these stimuli.

Aim

In this chapter, I sought to investigate the biological roles of Trib1 in activated macrophages. As the siRNA-mediated gene knockdown technique is a powerful tool for investigating gene function, the first part of this chapter describes experiments to identify the most efficient Trib1 siRNA sequence and concentration for obtaining optimal inhibition. Subsequent experiments used Trib1 gene knockdown to determine the biological functions of Trib1 in RAW264.7 cells and its interface with signalling pathways involved in the regulation of inflammation.

4.2 Materials, methods and experimental design

The experimental design is summarised in Figure 4.3

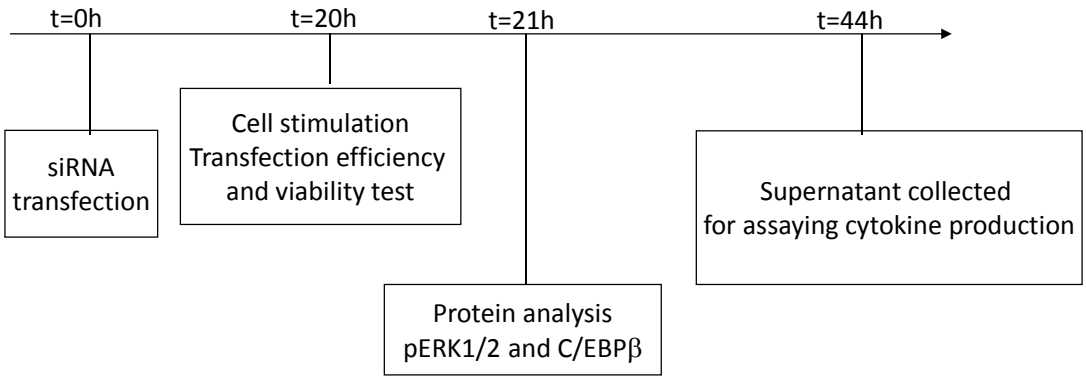

Figure 4.3. The experimental design in this chapter.

4.2.1 Electroporation protocol

The RAW264.7 cell line was optimised for siRNA transfection efficiency, as determined by fluorescence microscopy and flow cytometry, and described in section 2.3.1. Transfections were performed in duplicate in six well plates using three different siRNA sequences at three different concentrations (100 nM, 250 nM and 500 nM) and the electroporation protocol described in section 2.3.1. In short, RAW264.7 cells were harvest and counted, and then 2×10^6 cells were placed in a 1.5 ml microcentrifuge tube with appropriate concentrations of siRNA. The positive control plasmid, pmaxGFP, was co-transfected with siRNA in parallel by electroporation as described in section 2.3.1. Transfection efficiency was analysed by counting GFP-positive cells using FACS, and knockdown efficiency was analysed at the mRNA level by qPCR.

4.3 Results

4.3.1 Optimisation of siRNA concentrations for Trib1 knockdown

Firstly, in order to determine which commercial Trib1 siRNA was the most efficient, RAW264.7 cells were transfected with three different Trib1 siRNA sequences (Table 2.3) using the electroporation method (see sections 2.3.1, 4.2.1).

As suggested in the manufacturer's instruction, 250 nM of siRNA was used for optimisation experiments. After 24 hr, all groups were treated with TLR2L for 1 hr (Fig. 4.3). RNA extracted from treated cells and the efficiency of gene knockdown was examined by qPCR. *Trib1* gene expression in untransfected cells was normalised to a value of one (100%). The results showed that in RAW264.7 cells transfected with scrambled siRNA, relative *Trib1* expression was 95% (Fig. 4.4A). Following transfection with three different Trib1 siRNA sequences combined with TLR2L treatment, *Trib1* expression decreased to 72%, 35% and 50% respectively (Fig. 4.4A). The percentage knockdown using sequences 503 or 505 was significantly lower than the scrambled group (p <0.001) and the efficiency of gene knockdown by sequence 503 was significantly higher than of sequence 505 (p <0.001). Compared with scrambled siRNA controls, sequence 503 suppressed up to 55% of *Trib1* expression (Fig. 4.4A).

Secondly, RAW264.7 cells were co-transfected with commercial Trib1 siRNA and a GFP expression vector and then examined by FACS after 24 hr. The percentage of live cells following co-transfection with the three Trib1 siRNAs were 80%, 87% and 80% (for 130, 503 and 505, respectively; Fig. 4.4B). The transfection efficiency was

not affected by different siRNA sequences (p >0.1). Based on these two sets of experiments, sequence 503 was chosen for all further Trib1 siRNA experiments.

Moreover, in order to identify the Trib1 siRNA concentration providing optimal gene knockdown, a dose response curve was determined for sequence 503 using the concentration range 100–500 nM. The results indicated that 250 nM and 500 nM exhibit the same degree of inhibition (34% and 38%, respectively, p = 0.059) (Fig.4.4C). Therefore, 250 nM of sequence 503 was found to provide optimal inhibition of *Trib1* mRNA expression and these conditions were used in all subsequent experiments.

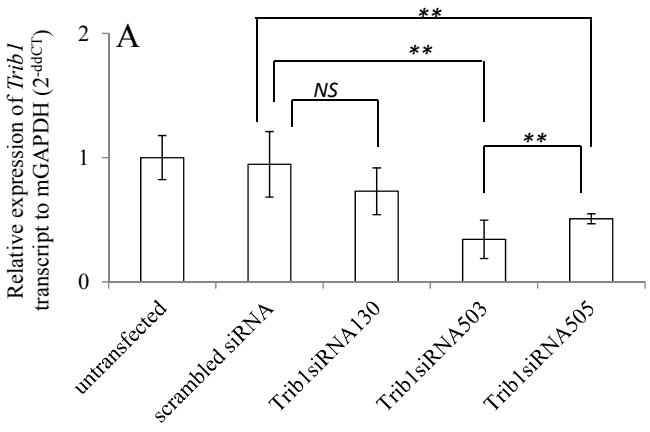
A
Relative expression of Trib1 transcript to mGAPDH (2-ddCT)
2
1
0
**
**
NS
**
untransfected
scrambled siRNA
Trib1siRNA130
Trib1siRNA503
Trib1siRNA505

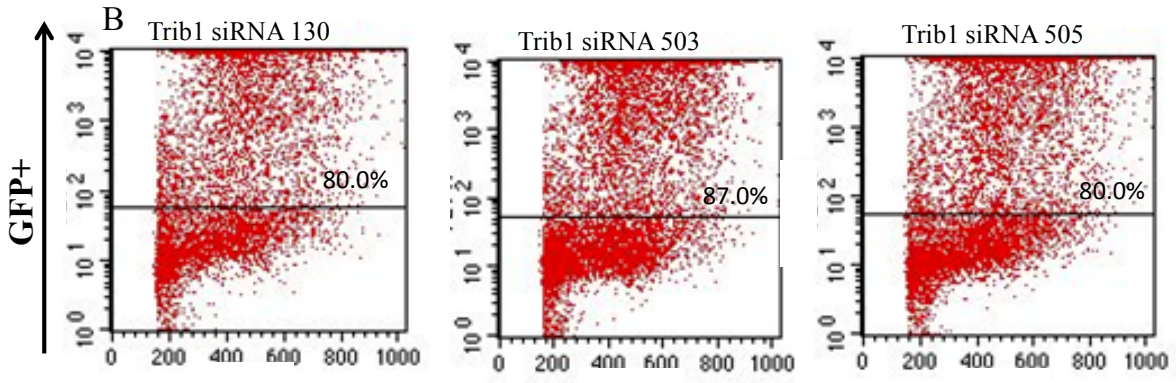
B
GFP+
Trib1 siRNA 130
80.0%
Trib1 siRNA 503
87.0%
Trib1 siRNA 505
80.0%
0
200
400
600
800
1000

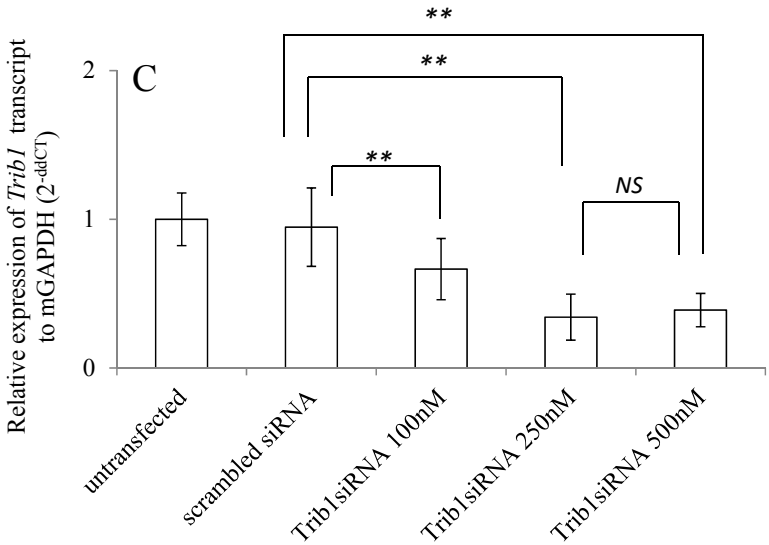
C
Relative expression of Trib1 transcript to mGAPDH (2-ddCT)
2
1
0
**
**
**
NS
untransfected
scrambled siRNA
Trib1siRNA 100nM
Trib1siRNA 250nM
Trib1siRNA 500nM

Figure 4.4. Optimisation of *Trib1* siRNA-mediated gene knockdown. (A) Expression of *Trib1*mRNA in RAW264.7 cells was measured for three commercial Trib1 siRNAs at a concentration of 250 nM, and relative suppression was determined by qPCR. (B) The transfection efficiency of three Trib1 siRNAs co-transfected with GFP was examined by FACS. (C) The optimal concentration of sequence 503 for down-regulating *Trib1* mRNA was determined by qPCR. This experiment was done on two separate occasions with similar results. For details of the statistical analysis, see sections 2.8. Fixed effects were scrambled siRNA in comparison with three siRNA sequences and concentrations and random effects were wells within experiment. This data required Log2 transformation to normalise the residuals before analysis. A standard *post-hoc* (*Tukey*) test was used to carry out pair-wise comparisons of all groups. In all cases, $p < 0.05$ was considered to indicate a statistically significant difference between experimental groups.*, $p < 0.05$ compared with scrambled siRNA; ** $p < 0.001$; NS, not significant.

Untransfected cells had normal RAW264.7 morphology as described in Chapter 3, consisting of a round monocyte-like (arrowhead, Fig. 4.5A) or a macrophage-like shape (arrow, Fig. 4.5A).

RAW264.7 cells transfected with scrambled siRNA had a similar morphology to untransfected controls (Figs.4.5A and B).

Interestingly, after Trib1 silencing by siRNA, RAW264.7 cells developed a more monocyte-like morphology, becoming more rounded with reduced adhesion (Fig. 4.5C), and were easily detached from the culture plate. Therefore, detached RAW264.7 cells were used in the cytocentrifuge smear analysis described in section 2.3.2. Notably, in this smear picture RAW264.7 cells exhibit a monocyte-like, rounded morphology (Fig. 4.5D vs. Fig. 4.5C).

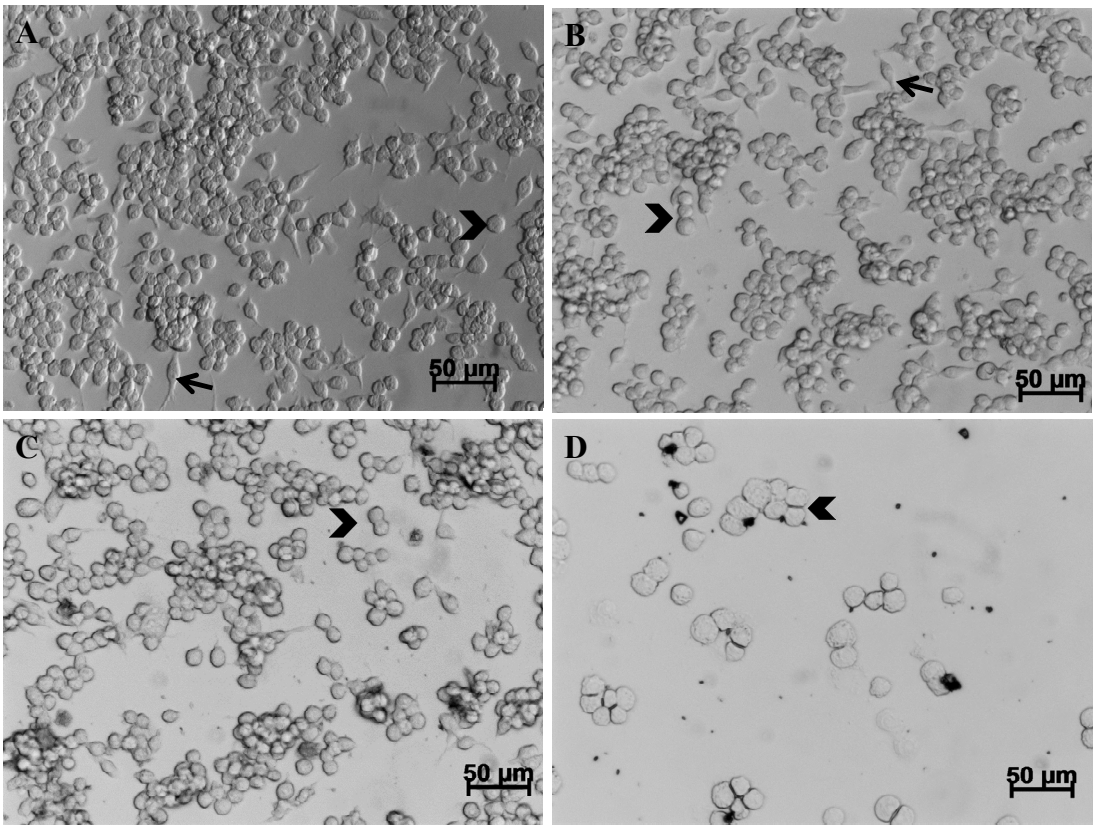

Figure 4.5. RAW264.7 cell morphology following siRNA transfection. (A) Untransfected controls, cells transfected with (B) scrambled siRNA or (C) Trib1 siRNA, and (D) floating cells Trib1 siRNA-treated cells prepared as cytocentrifuge smears. All photomicrographs show cells 24 hr post-transfection. Arrowheads indicate monocyte-like cells, whereas arrows show cells with macrophage-like morphology.

In order to determine whether Trib1 is an essential gene, cell viability was assessed after transfection. After 24 hr, the percentage of live cells in the untransfected group was 88.7% (Fig.4.6B). In the scrambled siRNA group was 81.1%, and was 79.1% in the Trib1 siRNA group (including detached cells) (Figs. 4.6 C and D; Table 4.1). Transfection efficiency of scrambled and Trib1 siRNA was comparable, indicating that cell uptake of these molecules is equivalent (Fig. 4.7 and Table 4.1).

Table. 4.1. Transfection efficiency and viability of siRNA-treated cells

	Scrambled siRNA	**Trib1 siRNA**	**Pearson's Chi-squared test**
Transfection efficiency (%)	84.8 ± 3.81	86.5 ± 5.09	*p= 0.988*
Viability (%)	79.7 ± 1.23	78.4 ± 1.12	*p= 0.991*

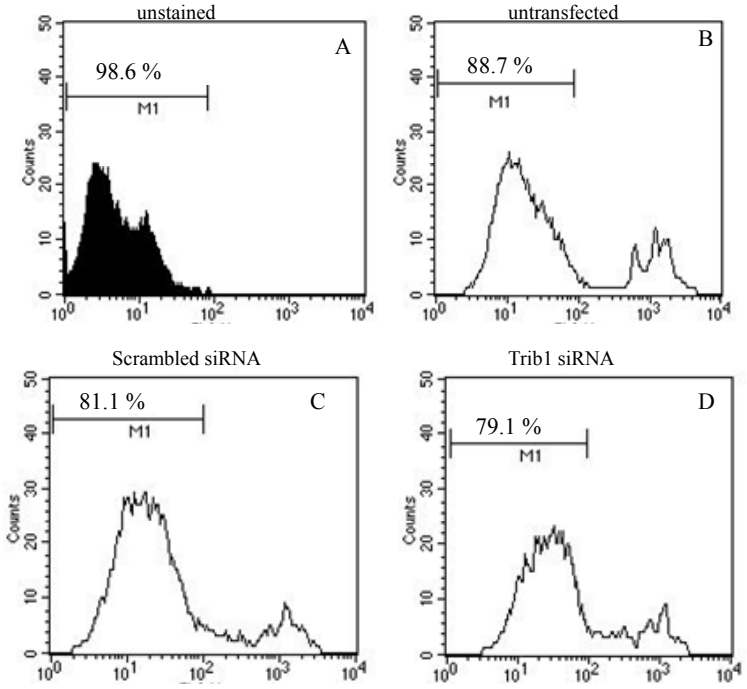

Figure 4.6. PI staining to assess viability of transfected RAW264.7 cells. (A) Untransfected cells without PI staining, and PI-stained (B) untransfected, (C) scrambled siRNA-transfected cells and (D) Trib1 siRNA-transfected cells24 hr post-transfection. Cells were stained with PI and viability was assessed by FACS. The M1 population represents live cells.

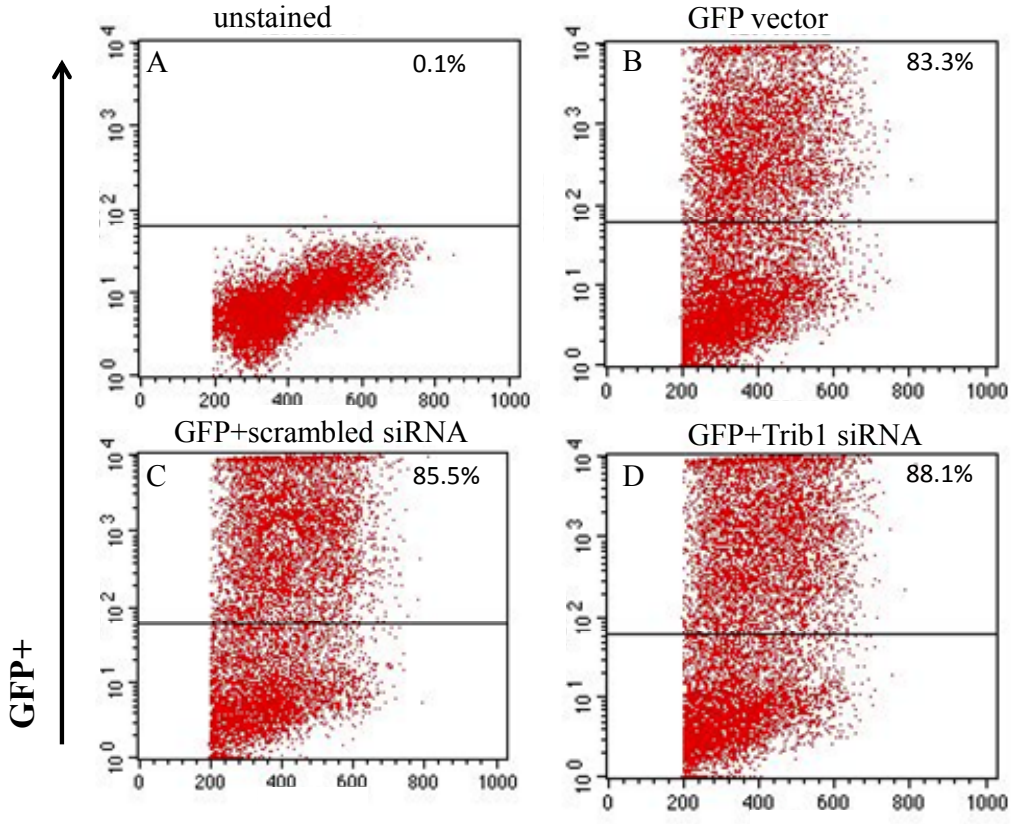

Figure 4.7. FACS determination of transfection efficiency. RAW264.7 cells were co-transfected with scrambled or Trib1 siRNA, together with the GFP expression vector. (A) Untransfected cells, (B) cells expressing GFP, (C) cells co-transfected with scrambled siRNA and the GFP expression vector, and (D) cells co-transfected with Trib1 siRNA and the GFP expression vector.

The last stage of Trib1 siRNA screening was to confirm that Trib1 siRNA specifically inhibits *Trib1* gene expression. Expression of *Trib1* and *Trib3* were measured following transfection with Trib1 siRNA. As shown previously (Fig. 3.3B and C), *Trib2* was not expressed in the RAW264.7 cells. Only *Trib1* expression was inhibited by Trib1 siRNA (p <0.001). *Trib3* expression of was not affected by Trib1 siRNA (*Trib1* vs. *Trib3* expression following Trib1 siRNA treatment, p = 0.075).

Further, there was no difference in *Trib3* expression in scrambled siRNA-treated and Trib1 siRNA-treated cells (Fig. 4.8, $p = 0.081$).

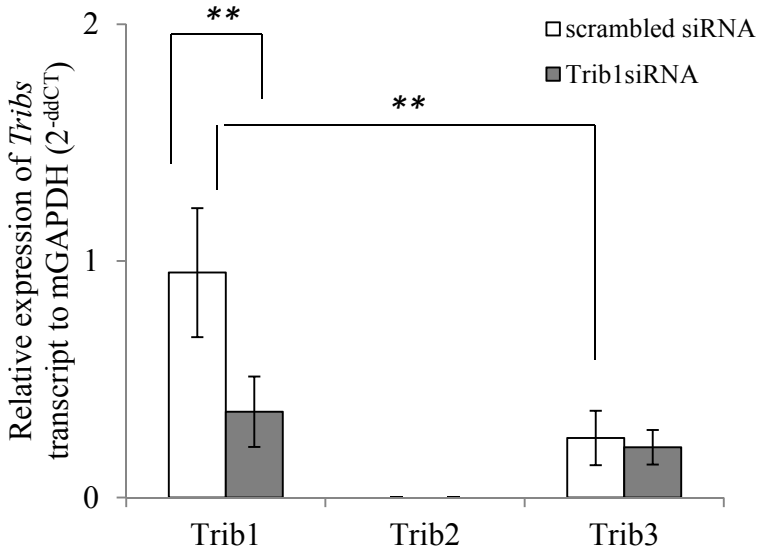

Figure 4.8. The specificity of Trib1 siRNA was assessed for three Trib transcripts by qPCR. After 24 hr transfection, the RAW264.7 cells were stimulated with TLR2L for 1 h. Two separate experiments were done and similar results were obtained for both. Values represent the mean ± SD calculated from data performed in two plates using triplicate wells. Statistical analysis was described in sections 2.8. $p < 0.05$ indicates a statistically significant difference; **, $p < 0.001$.

Previous results established the best commercial Trib1 siRNA sequence and inhibitory concentration, and the specificity of inhibition. Under the optimised conditions, Trib1 siRNA suppressed 55% of *Trib1* gene expression (Fig. 4.4A).

The first part of this chapter was designed to establish the concentration of Trib1 siRNA for investigating novel functions of Trib1 and identifying possible signalling pathway in which Trib1 plays a role.

4.3.2 Trib1 inhibition mediates increased TNF-α production

In Chapter 3, TNF-α was used as a marker for RAW264.7 cell activation. The baseline TNF-α production in untransfected cells and those transfected with scrambled siRNA were similar (287.5 pg/ml and 300.5 pg/ml, respectively).

After RAW264.7 cells were treated with different immune modulators, both scrambled and Trib1 siRNA treatment groups showed abundant TNF-α production (p <0.001). Conversely, after Trib1 silencing, TNF-α production was significantly higher than in the scrambled siRNA-untreated group (320.0 pg/ml vs. 300.5 pg/ml, p = 0.03; Fig. 4.9).

After exposure to different stimulatory signals, TNF-α production increased in both scrambled and Trib1 siRNA groups.

TLR2L induced abundant TNF-α production after Trib1 knockdown, as did combined treatment with TLR2L and IFN-γ (6967.9 pg/ml vs. 3314.9 pg/ml and 8462.8 pg/ml vs. 3590.8 pg/ml, respectively, p <0.001).

Treatment with IFN-γ alone resulted in a small but significant increase in TNF-α production in the Trib1 knockdown group, compared with the scrambled group, (2175.0 pg/ml vs. 896.9 pg/ml, p <0.001). This result demonstrates that Trib1 is associated with the TNF-α production.

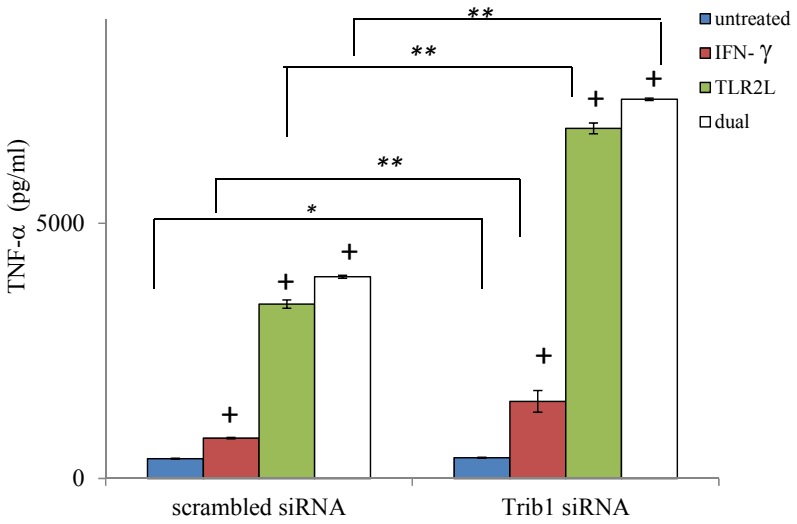

Figure 4.9. Knockdown of Trib1 modulates TNF-α production in RAW264.7 cells. TNF-α production in transfected cells was measured 24 hr post-stimulation. Values represent the mean ± SD in triplicate wells. Statistical analysis was described in sections 2.8. The analysis examined TNF-α production by group (control vs.Trib1 knockdown), the random effect was the experiment and the subsets were different treatments. Log10 transformation was required, and p <0.05 was considered to indicate a statistically significant difference between experimental groups.*, p <0.05 indicates a statistically significant difference relative to the scrambled group. **, p *<0.001*; +, p <0.001 comparing the same group and different treatments with untreated controls.

4.3.3 Trib1 modulates ERK1/2 phosphorylation

From the literature, human Trib1 is known to associate with MAPK. For example, Trib1 inhibits smooth muscle cell proliferation through JNK (Kiss-Toth *et al.*, 2004; Sung *et al.*, 2007). However, Yamamoto and his colleagues reported that Trib1 does not regulate the MAPK pathway in mouse primary macrophages (Yamamoto *et al.*, 2007). To investigate a possible role for Trib1 in MAPK signalling, RAW264.7 cells were transfected with Trib1 or scrambled siRNA overnight and then stimulated with IFN-γ or TLR2L for 1 hr (Fig. 4.3), and then protein expression was analysed by western blotting.

In the scrambled siRNA group, untreated cells expressed high levels of phosphorylated ERK1 (pERK1) and low levels of pERK2 (p42) (Fig. 4.10A). After stimulation with IFN-γ or TLR2L, expression of pERK1 and pERK2 increased. In particular, pERK2 expression was higher in RAW264.7 cells stimulated with IFN-γ or TLR2L. However, ERK2 was phosphorylated to a lesser extent than was ERK1.

Following IFN-γ and TLR2L treatment, pERK1 expression was increased in the Trib1 knockdown group, although levels were lower than in the scrambled control group (Fig. 4.10A and B, $p = 0.03$, $p = 0.01$, $p = 0.03$, respectively). Moreover, pERK2 levels were lower in the Trib1-silenced group compared with the scrambled control group (Fig. 4.10A). Both IFN-γ and TLR2 activated ERK1/2 phosphorylation in scrambled and Trib1 silenced groups ($p < 0.001$; Fig. 4.10B).

Using protein band relatively intensity to compare both groups of transfected cells,

the level of phosphorylated ERK1 was lower after Trib1 silencing than in the scrambled control group (Figs. 4.10B).

Therefore, I concluded that macrophage Trib1 positively regulates ERK1/2 phosphorylation in response to treatment with immune modulators.

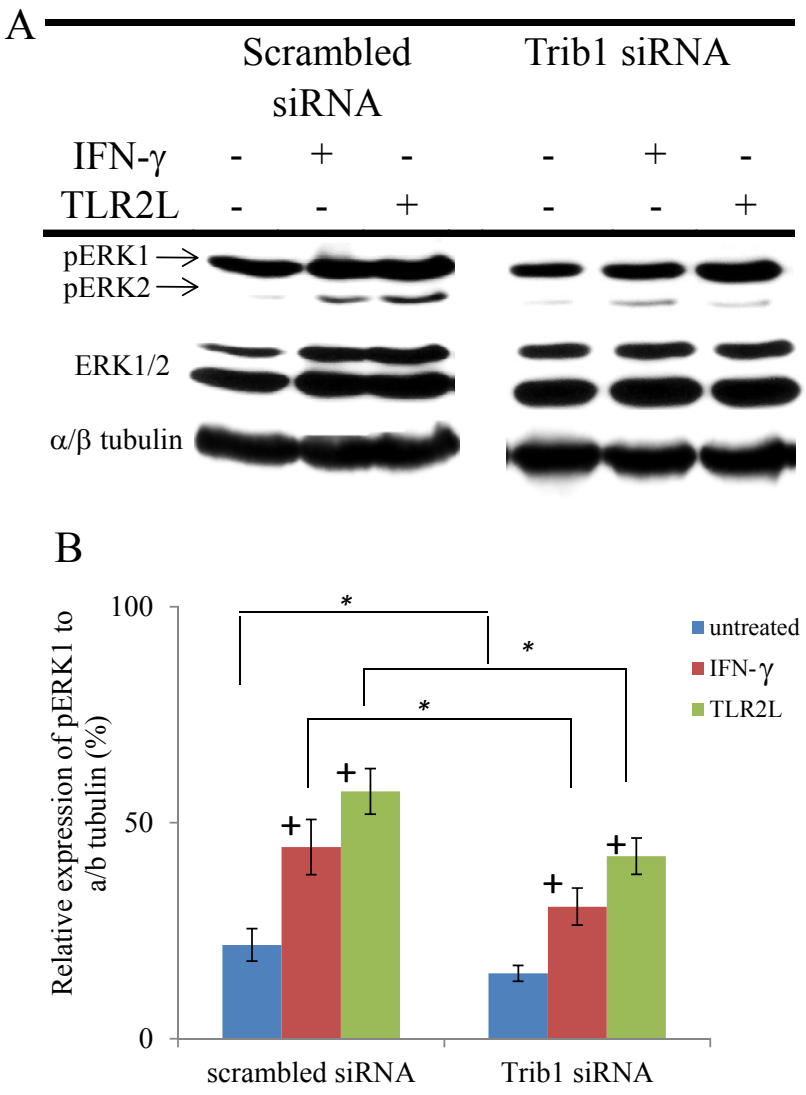

Figure 4.10. Trib1 silencing reduces ERK1/2 phosphorylation. (A) Expression of phosphorylated ERK1/2 (upper band, p44/ERK1; lower band, p42/ERK2) in RAW264.7 cells after stimulation, as determined by western blotting 60 min after treatment. Protein samples (55 μg) were used, as indicated in Chapter 2. Membranes were immunoblotted with primary antibodies specific for phosphorylated mouse ERK1/2 and total ERK1/2, and α/β tubulin was a as loading control. (B) Phosphorylated ERK1 was normalised to α/β tubulin. Two independent experiments were carried out and the values represent the mean ± SD calculated from the relatively intensity normalised to α/β tubulin. Statistical analysis was described in sections 2.8. The analysis examined relative expression by group (scrambled vs.Trib1 knockdown), the random effect was the experiment and the subsets were the different treatments. p <0.05 was considered to indicate a statistically significant difference between experimental groups. *, p <0.05 compared with the scrambled group was considered to indicate statistical significance; +, p <0.001 comparing the same cell group and different treatments with untreated controls.

4.3.4 Trib1 knockdown up-regulates C/EBPβ expression in the presence of IFN-γ, but does not affect IL-6 production

Trib1 silencing leads to C/EBPβ up-regulation after LPS treatment in murine primary macrophages (Yamamoto *et al.*, 2007). However, how Trib1 functions *in vitro* remains unclear.

In the scrambled siRNA group, untreated cells expressed low levels of C/EBPβ (Fig. 4.11A), which increased after stimulation with IFN-γ or TLR2L. Both IFN-γ and TLR2L induced C/EBPβ, especially IFN-γ. In the Trib1 knockdown group, untreated cells expressed low levels of C/EBPβ, but enhanced C/EBPβ expression was seen following treatment with IFN-γ or TLR2L. Interestingly, in comparison to the scrambled group, Trib1 knockdown increased C/EBPβ expression (Fig. 4.11A).

C/EBPβ is a nuclear factor which binds to IL-l responsive elements in the IL-6 gene (Akira *et al.*, 1990). Therefore, I also examined IL-6 production by ELISA. After in scrambled siRNA-treated RAW264.7 cells were stimulated with IFN-γ or TLR2L, IL-6 production increased compared with untreated cells (p <0.001). A similar result was seen in the Trib1-knockdown group (p <0.001). However, there was no difference between the scrambled group and the Trib1 silencing group following treatment (Fig. 4.11B; p >0.1), suggesting that C/EBPβ is not the only factor to regulate IL-6 production.

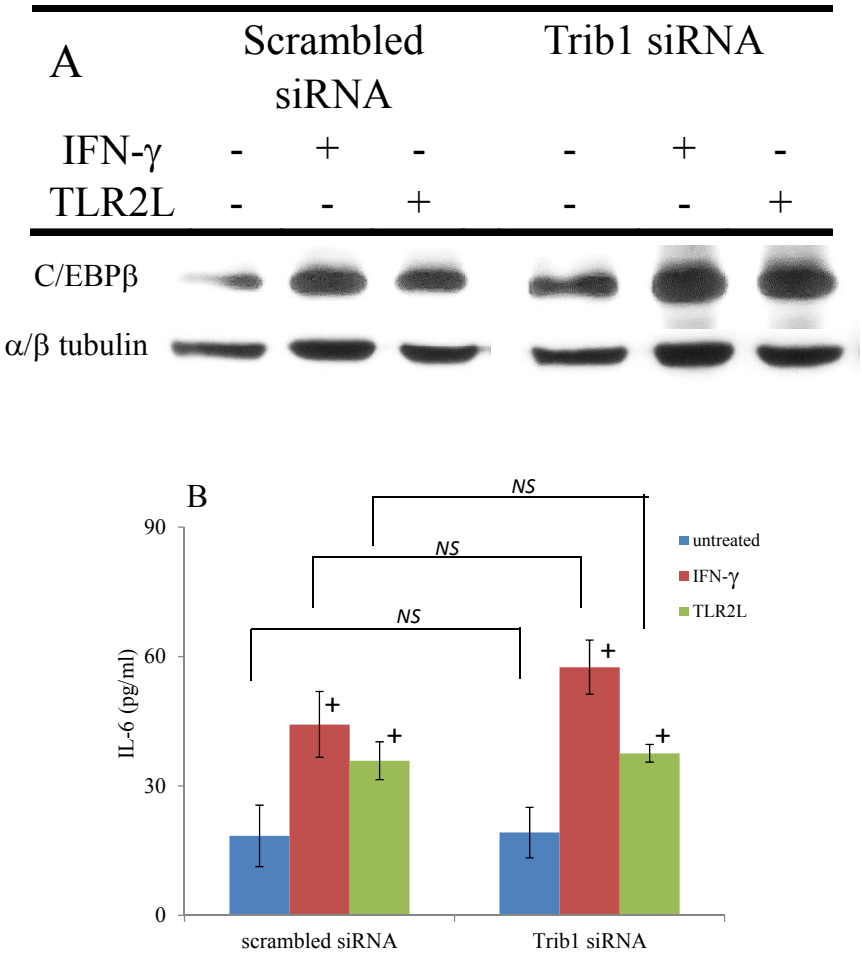

Figure 4.11. C/EBPβ expression and IL-6 production in treated RAW264.7 cells. (A) C/EBPβ protein expression was determined by western blotting 60 min after different treatments. (B) RAW264.7 cells were treated with siRNA following stimulation with IFN-γ or TLR2L for 24 hr, and IL-6 secretion into culture medium was measured by ELISA. Values represent the mean ± SD in triplicate. Similar results were obtained from two separate experiments. Statistical analysis was described in sections Chapter 2.8. The same analysis method was used as described for Fig. 4.9.*, p <0.05 compared with the scrambled group was considered to indicate statistical significance; +, p <0.001 compared the same group/different treatments with untreated controls; NS, not significant.

4.4 Discussion

This chapter demonstrated that commercial Trib1 siRNA could efficiently knockdown Trib1 mRNA and aimed to validate the functional role of Trib1 in macrophages. The results demonstrated that Trib1 silencing results in high TNF-α production, modulation of ERK1/2 phosphorylation and up-regulation of C/EBPβ expression.

The first objective of this chapter was to identify the Trib1 siRNA sequence providing the maximal efficiency of knockdown (Figs.4.4–4.8) to establish an optimal transfection protocol for RAW264.7 cells. Co-transfection with a GFP expression plasmid demonstrated efficient siRNA uptake into cells (Figs. 4.4B and 4.7). The concentration of siRNA used is particularly important. A dose-dependent increase in transfection efficiency was observed with increasing siRNA at low concentrations, but the decreased at higher concentrations (Fig. 4.4C). The highest concentration of 500 nM siRNA was not selected for several reasons. Higher siRNA concentrations can lead to off-target effects and increased toxicity (Scherer and Rossi, 2003). In addition, siRNAs are expensive so finding the lowest effective concentration is necessary.

Demonstrating the specificity of Trib1 siRNA is important, as related human genes contain up to 53.3% sequence homology (Trib1/Trib3), and the amino acid sequences between human and mouse Trib1 and Trib3 are 97.5% and 81.2%, respectively (Yokoyama and Nakamura, 2011). Therefore, I demonstrated that Trib1 siRNA specifically down-regulates *Trib1* mRNA (Fig 4.8). The reduction in target gene

expression obtained by siRNA treatment in this study was 55%. However, due to the poor quality of the only available Trib1 antibody (discussed in Chapter 3), only mRNA knockdown data is presented.

The second part of this chapter aimed to demonstrate the biological function of Trib1 in RAW264.7 cells, and its interface with signalling pathways involved in the regulation of inflammation.

In Chapter 3, I showed that RAW264.7 cells treated with IFN-γ alone or in combination with TLR2 ligation up-regulate Trib1 transcript levels from 30 min to 6 hr (Fig. 3.9). The MAPK signalling pathway is activated by either TLRs or IFN-γ (Gough *et al.*, 2007; Krishnan *et al.*, 2007), which suggests that Trib1 may regulate MAPK signalling in macrophages.

The majority of TNF-α production is modulated by NF-κB (Matsusaka *et al.*, 1993). Furthermore, C/EBPβ-mediated TNF-α production in response to TLR2-induced inflammation has been reported (Lu *et al.*, 2009). Trib1 knockdown resulted in an increase of both TNF-α production (Fig. 4.9) and C/EBPβ expression (Fig. 4.11), consistent with a previous report indicating that C/EBPβ modulates TNF-α production (Lu *et al.*, 2009). However, there is no direct evidence to show that this mechanism is directly mediated by NF-κB activation.

That Trib1 knockdown resulted in increased TNF-α production in this study requires explanation. Firstly, TNF-α is mainly produced by macrophages, and is a

potent pro-inflammatory mediator that regulates macrophage function. It is proposed to be a key inducer in inflammatory cell activation and in inflammatory diseases. Secondly, TNF-α also plays a role in macrophage proliferation, differentiation and apoptosis. In bacterially infected tissue, macrophages become activated to secrete TNF-α and increase endothelial adhesion to allow macrophage migration (Parameswaran and Patial, 2010). These observations, together with the abundant TNF-α production caused by Trib1 knockdown, suggest that Trib1 is involved in macrophage function during inflammation.

Further, the results presented here contrast with those of Yamamoto *et al.* (2007), who reported that macrophages from Trib1-deficient mice have the same levels of IκB and TNF-α production as wild type mice. A possible explanation for this difference is that Yamamoto's group analysed primary cells (peritoneal macrophages), whereas I have used an immortalised cell line (RAW264.7 cells, established from a tumour induced by Abelson murine leukaemia virus; (Raschke *et al.*, 1978). Similarly, while I have demonstrated that the levels of phosphorylated ERK1 and 2 are reduced in Trib1 siRNA-treated cells, Yamamoto *et al.* showed that Trib1-deficient macrophages had the same levels of phosphorylated MAPKs (p38, JNK and ERK) as normal macrophages (Yamamoto *et al.*, 2007). However, a previous study of Trib1-induced murine AML suggested that cell transformation resulted from increased MAPK signalling (Jin *et al.*, 2007). Consistent with the present study, Trib1 knockdown led to decreased ERK1/2 phosphorylation (Fig. 4.10). Trib1 has been reported to interact with MEK1 and MKK4 (Kiss-Toth *et al.*, 2004). IFN-γ triggers activation of the MEK1/2 to ERK1/2 pathway (Gough *et al.*, 2007; Hu *et al.*, 2001) and I demonstrated down-regulation of ERK1/2

phosphorylation by Trib1 in IFN-γ treated macrophages. Therefore, the MAPK pathway appears to be regulated by Trib1.

TLR2L activates the MAPK pathway via JNK and p38 (Akira, 2003; Krishnan *et al.*, 2007); however, JNK was not detected in RAW264.7 cells. Reports from other groups indicate that peptidoglycan (PGN) or LPS treatment induces JNK phosphorylation in RAW 264.7 cells at an early time point (15 min) and that this decreases to baseline after 60 min (Hu *et al.*, 2007a; Lin *et al.*, 2010). Therefore, the JNK pathway may become activated early in microbial infection. I focused on the 60 min time point, which was, in retrospect, not the best time to measure the JNK pathway activity. However, my results agree with Sung *et al.*, (2006), who concluded that role of Trib1 in regulating signalling pathway was cell-type specific. Thus, RAW264.7 cells do not activate the JNK pathway following TLR2 ligand treatment and Trib1 is not involved in TLR2L-induced ERK1/2 phosphorylation (Fig. 4.10). Nonetheless, the mode of action of Trib1 in response to TLR2L-induced signalling remains undefined.

However, there was a small decrease in the level of ERK1 phosphorylation in RAW264.7 cells following treatment with TLR2L in Trib1 and scrambled siRNA transfected group (Fig. 4.10). Therefore, comparing the effects of IFN-γ and TLR2L stimulation reveals that IFN-γ induces the MAPK pathway, especially the ERK1/2, might be one of the Trib1 target pathways in macrophages.

I showed that Trib1 knockdown increases C/EBPβ protein (Fig. 4.11). This finding,

together with Yamamoto's results, indicate that Trib1 inhibits C/EBPβ expression (Yamamoto *et al.*, 2007). Slbo is a *Drosophila* orthologue of mammalian C/EBP (Rorth *et al.*, 2000) and *Drosophila* Trib protein has been reported to negatively regulate Slbo. Thus, these combined data support the hypothesis that mammalian Trib1 functions to inhibit C/EBPβ expression in a similar way to Slbo inactivation by *Drosophila* Trib. Trib1 has been reported to regulate both C/EBPβ and C/EBPα. C/EBPα degradation in myeloid leukaemogenesis through Trib1/ MEK1 interaction (Yokoyama *et al.*, 2010). MEK1 is the upstream regulator of ERK1/2; therefore, taken together with my data, it is reasonable to assume that Trib1 is also involved in C/EBPβ degradation via ERK1/2 pathway in the *in vitro* system.

C/EBPβ is a nuclear factor that specifically binds to an IL-1 responsive element in the IL-6 gene (the original name of C/EBPβ was NF-IL6; (Ray *et al.*, 1989). However, my results showed that not only IL-6 production is regulated by C/EBPβ (Fig.4.11B) A previous report indicated that IL-6 can be synergistically activated by the transcription factors C/EBPβ and NF-κB (Matsusaka *et al.*, 1993). Nevertheless, there is no direct evidence for NF-κB involvement in the present study. However, Trib1 silencing increased C/EBPβ expression and resulted in TNF-α production. This may also suggest that C/EBPβ does not directly regulate IL-6 production in macrophages.

Following monocyte–macrophage differentiation, macrophages become strongly adherent and flattened (Gordon and Taylor, 2005). However, after Trib1 knockdown changes in morphology involved an increased number of rounded and detached cells

with monocyte-like features (Fig. 4.5D). This tempted me to speculate that that Trib1 may have a role in the control of cell morphology. In *Drosophila*, the Trib orthologue controls timing of mitosis during mesoderm morphogenesis and changes in cell shape (Seher and Leptin, 2000), the latter process being regulated by Snail, a downstream target of Trib (Grosshans and Wieschaus, 2000; Lp and Gridley, 2002). Snail expression is regulated by complex signalling networks including MAPK and NF-κB (Wu and Zhou, 2010). However, it is unclear how the Snail pathway regulates Trib activity to coordinate cell division and movement.

In conclusion (Fig. 4.12), in this chapter I have demonstrated that Trib1 plays a role in regulating the ERK1/2 and C/EBPβ pathways and TNF-α production. Furthermore, Trib1 involvement in macrophage migration and other biological processes is addressed in Chapter 5.

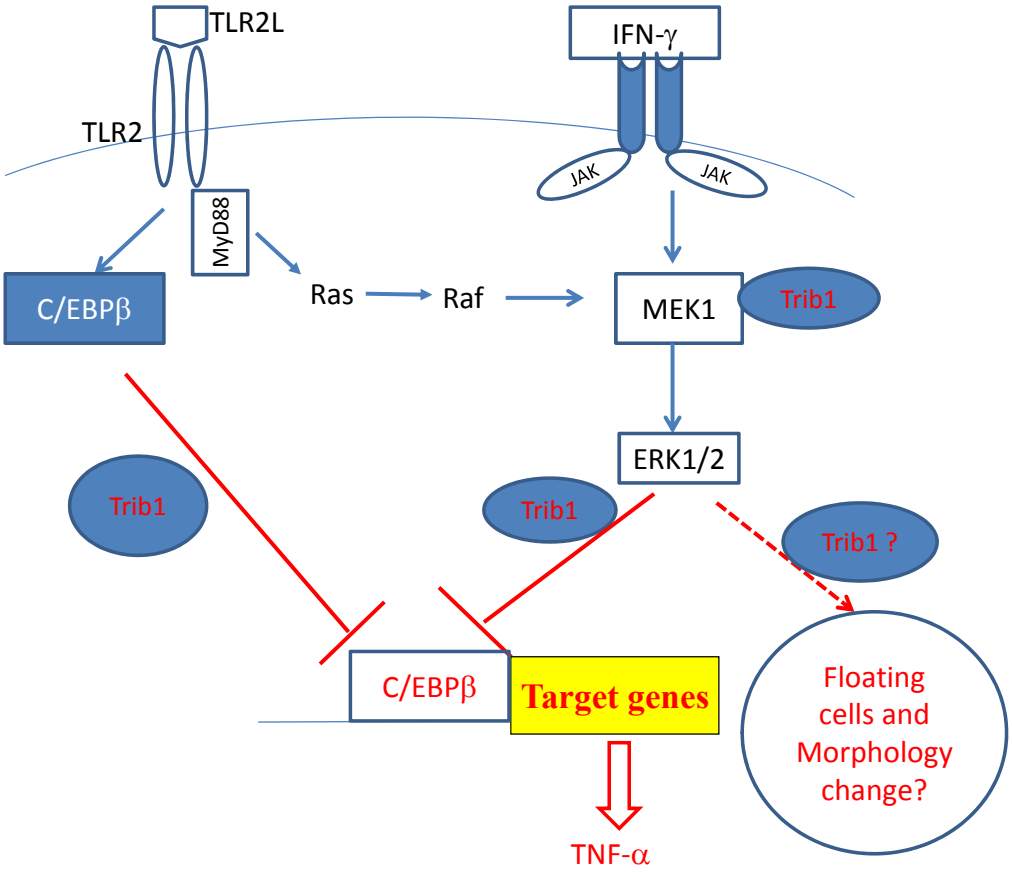

Figure 4.12. Schematic illustration of the possible involvement of Trib1 in signalling pathways induced by IFN-γ and the TLR2 ligands in RAW264.7 cells. Trib1 functions as a scaffold protein linking the MEK1/ERK1/2 pathway and C/EBPβ. Moreover, Trib1 interacts with MEK1 and enhances ERK1/2 phosphorylation. Conversely, ERK1/2 inhibits C/EBPβ expression and regulates TNF-α production. Up-regulated TNF-α may be involved in following unknown biological functions.

Chapter 5: Investigation of novel Trib1 functions in activated macrophages

Abstract

In *Drosophila*, a single Trib gene has been identified that is involved in morphogenesis, cell cycle progression and cell migration. Immune homeostasis is an important factor in immune system regulation. In particular, apoptosis is a normal cellular response and an important part of immune homeostasis. In gene knockdown experiments using Trib1 siRNA, I observed that C/EBPβ expression was inhibited and that this occurred in both stimulated (by IFN-γ and TLR2L) and resting murine macrophage populations. Moreover, expression of pERK1/2 was reduced in Trib1 knockdown cells. The results presented in this chapter indicate that macrophages in which Trib1 expression is down-regulated by siRNA have altered migratory behaviour in response to MCP-1. Experiments examining Trib1 loss or gain of function show that Trib1 functions as a modulator of cell cycle transition and an inhibitor of apoptosis.

In conclusion, my data suggest that Trib1 makes a previously unrecognised contribution to these biological functions in activated macrophages.

5.1 Introduction

Trib, the only member of the Trib homologue family in *Drosophila*, regulates *String/CDC25* activity and affects cell cycle progression, cell proliferation, and morphogenesis (Mata *et al.*, 2000; Seher and Leptin, 2000). Moreover, the *Trib* gene is an important inhibitor of mitosis. Its biological function is to control timing during development and gastrulation in order to allow cell morphology changes to be completed (Seher and Leptin, 2000).

Moreover, *Drosophila* Trib protein negatively regulates the level of *Drosophila* Slbo, which controls border cell migration and is a fly orthologue of the mammalian C/EBP transcription factor (Rorth *et al.*, 2000). In order to investigate its function, Slbo protein was overexpressed or the *Slbo* gene was deleted, leading to an absence of Slbo protein. These experiments showed Slbo overexpression in border cells delayed their migration. Thus, border cells fail to migrate properly if the level of Slbo protein is either too low or too high. Alternatively, Trib may form part of an ubiquitin E3 complex for Slbo (Bowers *et al.*, 2003; Rorth *et al.*, 2000). E3 complexes are defined by their enzymatic activity, which is to stimulate transfer of ubiquitin from specific ubiquitin-charged E2 complexes to substrates, and can be unrelated in sequence (Varshavsky, 1997). Therefore, Slbo protein is degraded via Trib- mediated ubiquitination.

Cell migration is an important process related to many biological functions such as cell movement, shape changes and differentiation (Friedl, 2004). Cell migration can be classified into single cell migration (amoeboid cells) and collective migration modes (cell sheets, tubes and clusters). For instance, macrophage migration is classified as single cell migration (Friedl, 2004).

Apoptosis plays a major role in the development and maintenance of all multicellular organisms. Moreover, apoptosis is a normal cellular response and an important part of immune homeostasis (Crouch *et al.*, 1996). Macrophages play a central role in immune homeostasis (Henson *et al.*, 2001). Expression of the TNF-α receptor during Fas-induced macrophage apoptosis indicates that TNF-α plays a role in macrophage apoptosis (Parameswaran and Patial, 2010). Trib3 is associated with macrophage apoptosis via the caspase-3 pathway in atherosclerosis (Shang *et al.*, 2009). However, the function of Trib1 in macrophage is unclear.

The results in Chapter 4 demonstrated that Trib1 silencing increased C/EBPβ protein expression, indicating that Trib1 inhibits C/EBPβ, consistent with *Drosophila* studies, and that Trib1 function may be related to cell migration via C/EBPβ. However, these potential novel functions of Trib1 remain to be verified.

Aim

In this chapter, I sought to further investigate the biological functions of Trib1 in macrophages, using effective knockdown of Trib1 or Trib1 overexpression to explore the biological role of Trib1 in cell migration, cell cycle progression and the regulation of apoptosis.

5.2 Materials, methods and experimental design

The experimental design is summarised in Figure 5.1 but detailed methodologies are presented in the Chapter 2.

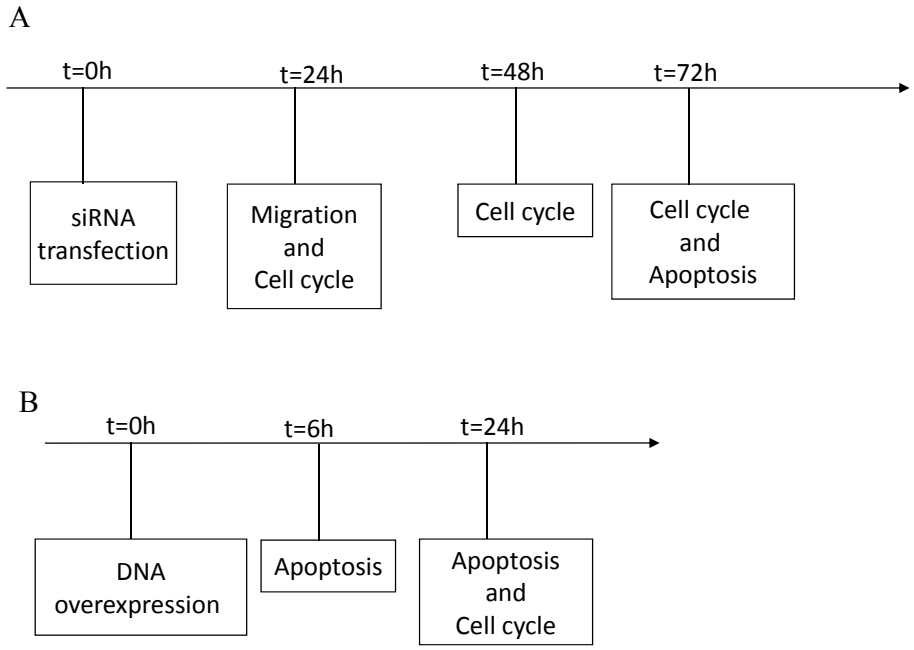

Figure 5.1. The experimental design in this chapter. (A) Trib1 siRNA experiments and (B) Trib1gain-of-function experiments.

5.2.1 Optimisation of Trib1 expression plasmid

Optimal conditions for transfection of the Trib1 expression into RAW264.7 cells were determined and transfection efficiency was measured by fluorescence microscopy and flow cytometry as described in section 2.3.1. Transfections were performed in duplicate wells of a six well plate using three different Trib1 plasmid concentrations (0.5 µg, 1.0 µg and 2.0 µg) and empty plasmid was used as a negative control. The electroporation protocol is described in detail in section 2.3.1. In short, RAW264.7 cells were harvest and 2×10^6 cells were placed into a 1.5 ml microcentrifuge tube with an appropriate concentration of Trib1 plasmid. The

positive control pmaxGFP plasmid was co-transfected with the Trib1 plasmid in parallel by electroporation as described in section 2.3.1. Transfection efficiency was analysed by counting GFP-positive cells using FACS and overexpression efficiency was analysed at the mRNA level by qPCR.

5.3 Results

5.3.1 Trib1 knockdown inhibits macrophage migration

In the previous chapter (Figs. 4.11A), I showed that Trib1 silencing increases C/EBPβ protein expression, indicating that Trib1 inhibits C/EBPβ, and that Trib1 function may be related to cell migration via C/EBPβ (Rorth *et al.*, 2000). Here, I extend these studies and firstly investigate whether Trib1 alters macrophage migration.

After Trib1 knockdown overnight, chemokinesis (random movement, medium control) and chemokine-mediated RAW264.7 cell migration was assayed (Fig. 5.2). Untransfected and scrambled groups showed a standard migration pattern in the absence of chemokines. Reduced Trib1 expression resulted in few cells exhibiting a chemokinesis response (Fig.5.2A).

The addition of MCP-1 (200 ng/ml) increased the numbers of cells migrating toward the lower wells, particularly in the untransfected and scrambled siRNA groups (Fig. 5.2B). Interestingly, following Trib1 knockdown, RAW264.7 cells exhibited a similar migratory pattern as medium controls (Figs. 5.2A and 5.2B).

A quantitative analysis of chemokine-mediated cell migration revealed that this only happened in the untransfected and scrambled siRNA groups, but not in the Trib1-silenced group (Fig. 5.2C). Migration in the two control groups was significantly greater than in the Trib1-silenced group after MCP-1-treatment ($p < 0.001$). However, the level of MCP-1-induced migration in Trib1 knockdown cells

was the same result as in controls lacking MCP-1 ($p = 0.989$).

Thus, Trib1 knockdown inhibits both chemokinesis and MCP-1 induced cell migration.

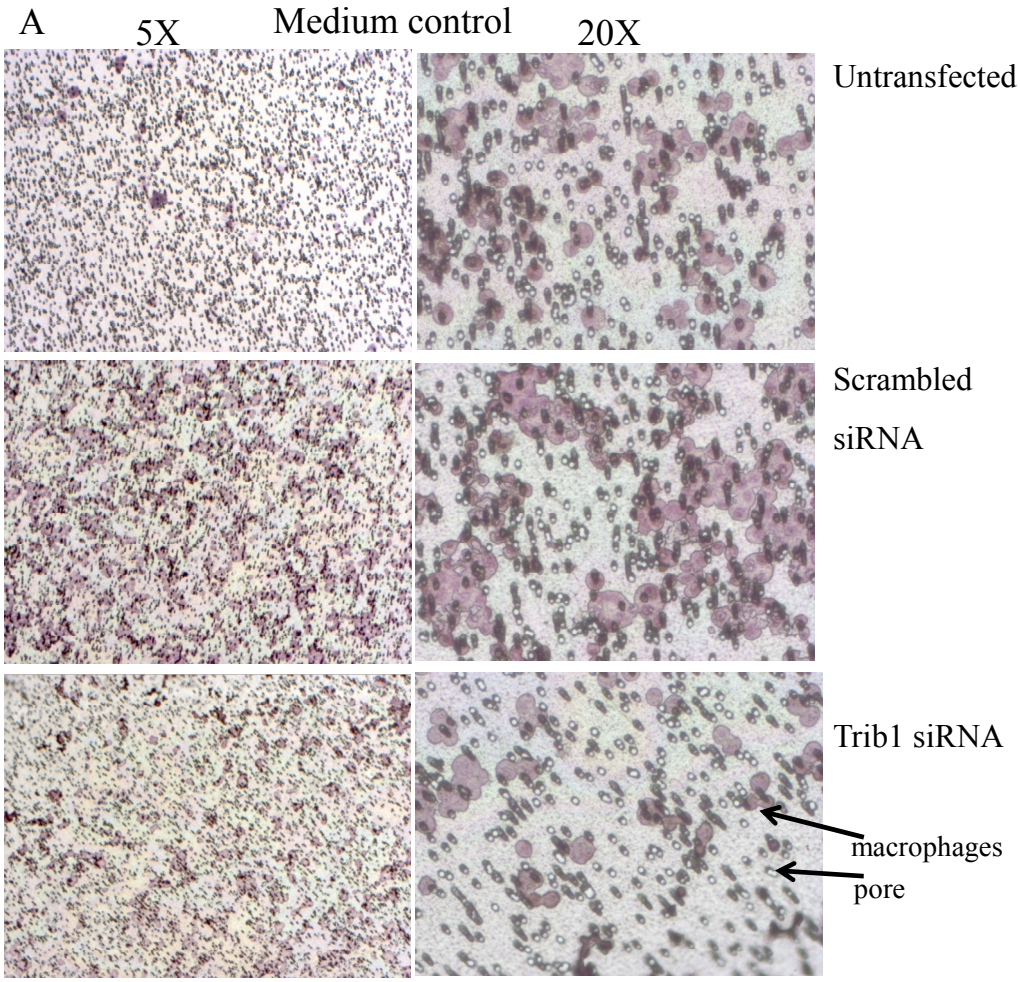

Figure 5.2A. Trib1 silencing inhibits RAW264.7 cell migration. Trib1 knockdown reduced cell migration compared to untransfected and scrambled siRNA controls. Appearance of a representative micropore membrane with medium only in the lower well of the chamber. After 90 min, cells trapped in the filter pores or adhering to the underside of the membrane were fixed and stained with haematoxylin. Arrows indicate cells trapped in the pores; low (left, 5×) and high (right, 20×) power fields are shown.

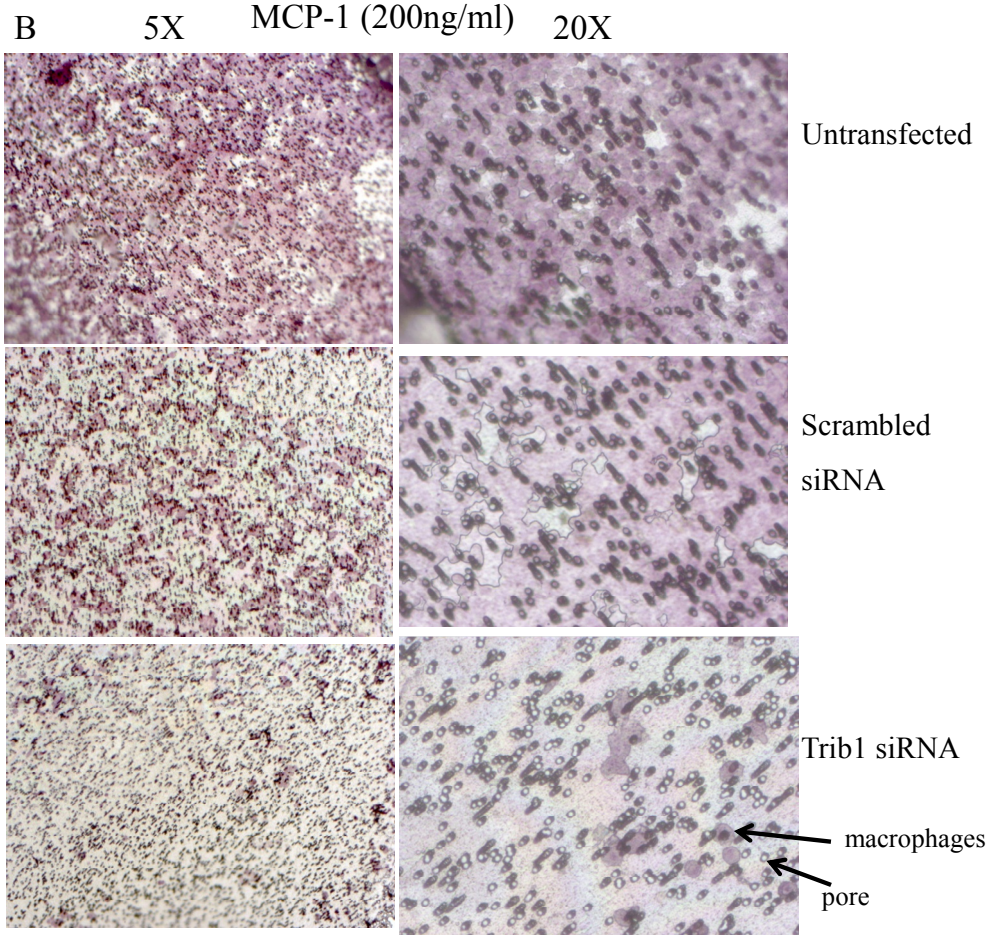

Figure 5.2B. Trib1 silencing inhibits RAW264.7 cell migration. Trib1 knockdown reduced cell migration compared to untransfected and scrambled siRNA controls following MCP-1 (200 ng/ml) treatment. Appearance of a representative micropore membrane with MCP-1 (200 ng/ml) was in the lower well of the chamber. After 90 min, cells trapped in the filter pores or adhering to the underside of the membrane were fixed and stained with haematoxylin. Arrows indicate cells trapped in the pores; low (left, 5×) and high (right, 20×) power fields are shown.

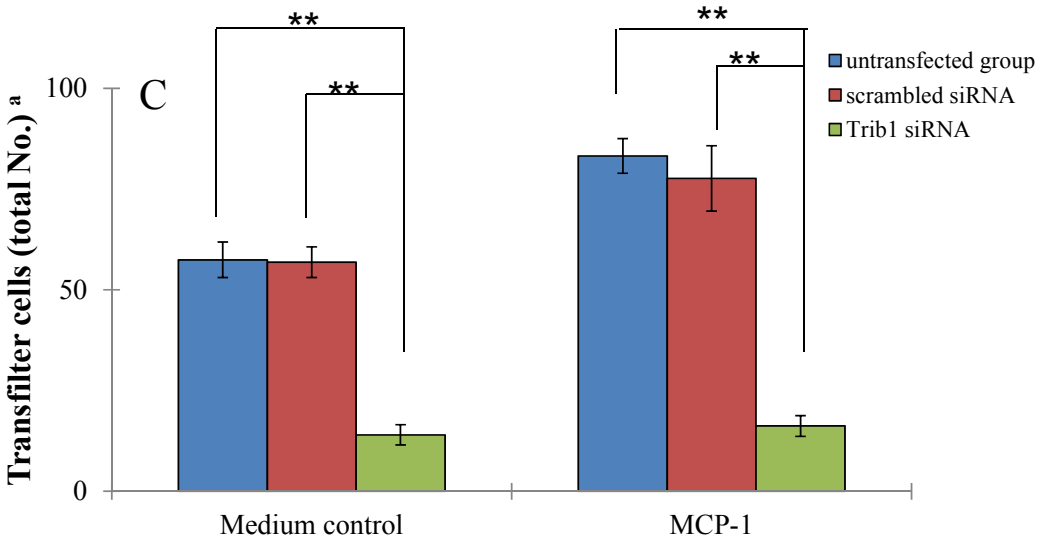

Figure 5.2C. Transfilter cell migration assay showing the effect of Trib1 silencing on MCP-1-mediated migration. Cells were counted in in 10 randomly selected high power fields under microscopy (20×). Statistical analysis was determined as described in sections 2.8. Generalised LME models were used for the analysis of cell count data in this chapter. Migrated cell counts were fitted to the Poisson process. p <0.05 was considered to indicate statistical significance; **, p <0.001 comparing untransfected and scrambled groups with Trib1 siRNA group.

5.3.2 Effect of Trib1 knockdown on cell cycle progression and apoptosis

Trib function in the cell cycle was first studied in *Drosophila*; however, whether Trib1 regulates the cell cycle in mammalian systems has not been investigated. Flow cytometric analysis of the cell cycle showed no difference in G_0/G_1 and S phase populations between the scrambled siRNA and Trib1 silenced groups up to 72 hr after transfection (p >0.1; Figs. 5.3A, B; Table 5.1).

Conversely, the Trib1 silencing group showed a reduction in G_2/M phase progression from 24 hr to 72 hr relative to the scrambled siRNA group, and this difference reached statistical significance at the 48 hr and 72 hr time points (p = 0.051, p = 0.028, p = 0.002, from 24 hr to 72 hr, respectively) (Fig. 5.3C, Table 5.1). Therefore, macrophage Trib1, similar to *Drosophila*, is involved in G_2/M cell cycle progression.

A typical cell cycle distribution profile is seen in the scrambled group after 72 hr; in contrast, in the Trib1-silenced group after 72 hr, there was a larger proportion of G_2 phase cells than in the scrambled siRNA group (Figs. 5.4A, B; Table 5.1). Under these conditions, the number of apoptotic cells (M4) was very small; consequently, a more accurate measurement of apoptosis was done using annexin V staining.

The numbers of late apoptotic cells (upper right, annexin V^+/PI^+) were significantly higher in the scrambled siRNA group (approximately 2 fold) than in the Trib1-knockdown group after 72 hr (p = 0.004) (Figs. 5.4C, D; Table 5.1). These experiments indicate that Trib1 postpone apoptosis in macrophages.

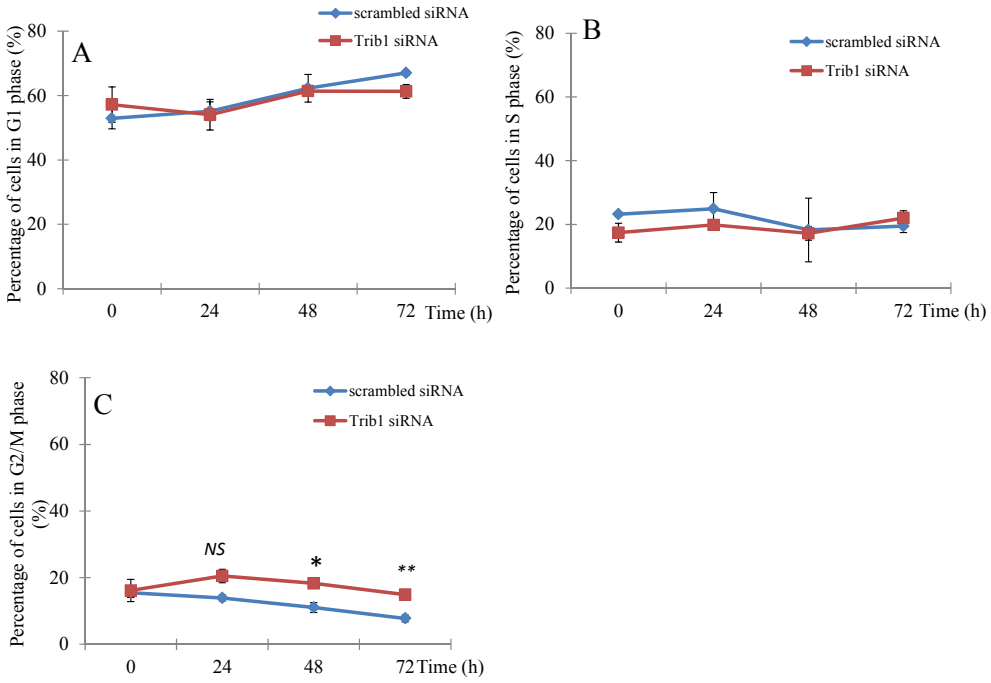

Figure 5.3. Timecourse profiles of cell cycle analysis. A typical cell cycle distribution profile, comprising G1 phase (A), S phase (B) and G2/M phase (C), in scrambled siRNA and Trib1 siRNA groups 0, 24, 48 and 72 hr after transfection. Data are expressed as the mean ± SD of two culture wells and two independent experiments. Statistical analysis was described section 2.8. For cell cycle analysis, the binomial process used the percentage of cells in $G_1/S/G_2M$ phase identified by FACS sorting. The analysis examined the proportion of cells in $G_1/S/G_2M$ phases by group (scrambled siRNA vs.Trib1 knockdown), random effects were defined as wells within an experiment and subsets were at different time points. p <0.05 was considered to indicate statistical significance; *, p <0.05; **, p <0.01 compared with the scrambled group; NS, not significant.

Table 5.1. Analysis of the cell cycle profile and apoptosis in RAW264.7 cells 72 hr post-transfection

Cell phase (%)	**Scrambled siRNA**	**Trib1 siRNA**	**Binomial analysis**
G_0/G_1	67.0 ± 0.7	61.3 ± 2.1	$p = 0.10$
S	19.5 ± 2.0	22.0 ± 2.3	$p = 0.657$
G_2/M	7.8 ± 1.1	14.9 ± 0.7	$p = 0.002$
Apoptosis (annexin V staining)	38.0 ± 2.9	15.9 ± 4.8	$p = 0.004$

p <0.05 was considered to indicate statistical significance.

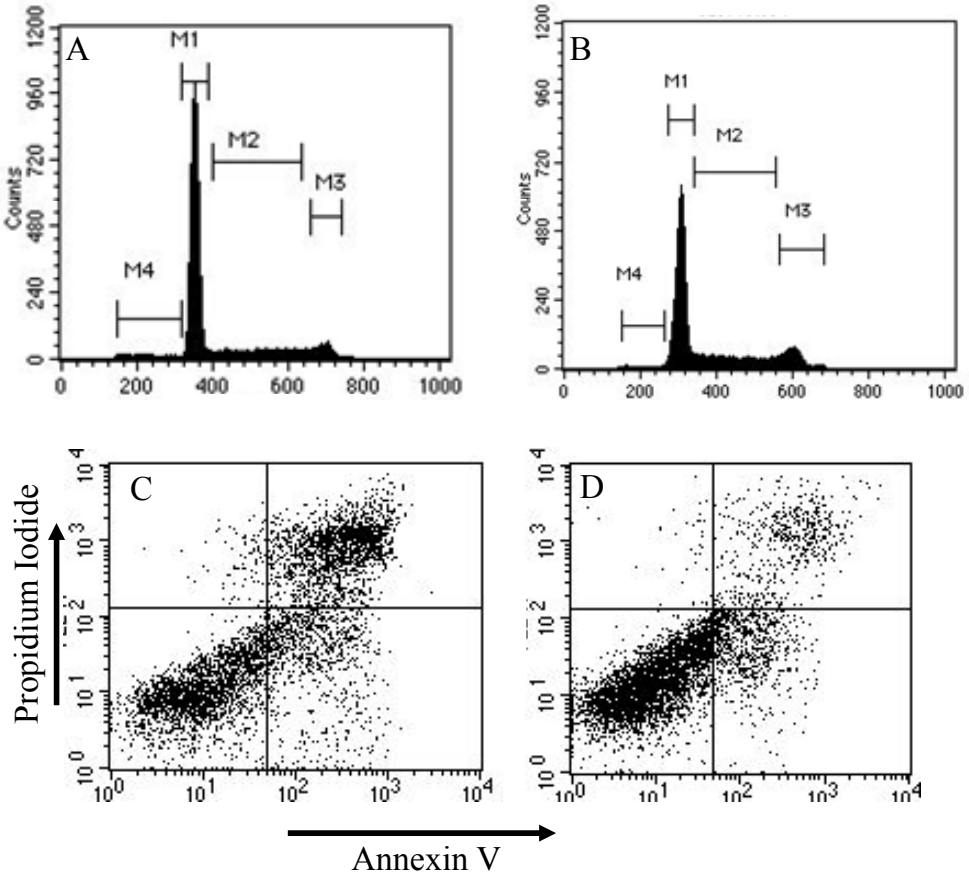

Figure 5.4. Trib1 knockdown disturbs the cell cycle and inhibits apoptosis. RAW264.7 cells were transfected with scrambled siRNA (A, C) or Trib1 siRNA (B, D) and examined after 72 hr. The values in Table 5.2 represent the percentage of cells in G_0/G_1 (M1), S (M2), G_2/M (M3) phases of the cell cycle. As numbers of apoptotic cells (M4) were low, annexin V was used to investigate changes in apoptosis (Figs. 5.4C, D). Data are represented as the mean ± SD of three independent experiments.

5.3.3 Optimisation of Trib1 expression plasmid concentration for transfection

As Trib1 siRNA–mediated knockdown experiments suggested that Trib 1 may function in cell cycle progression, I next evaluated the effect of Trib1 overexpression of cell cycle parameters using a commercial Trib1 expression plasmid.

Trib1 expression in the empty vector control group was similar to the untransfected group, which was normalised to a value of 1 (100%) (Fig. 5.5). RAW264.7 cells were transfected with increasing amounts of Trib1 vector. Relative *Trib1* expression increased by 50% following transfection with 0.5 µg vector (significance, p <0.001). However, when the amount of Trib1 vector was increased from 1.0 µg to 2.0 µg, relative Trib1 expression failed to increase over the baseline levels in the vector control group (1.0 µg DNA, p = 0.057) or was lower than the vector control group (2.0 µg DNA, p = 0.001; Fig. 5.5). Therefore, the 0.5 µg of Trib1 vector was used for subsequent Trib1 overexpression experiments.

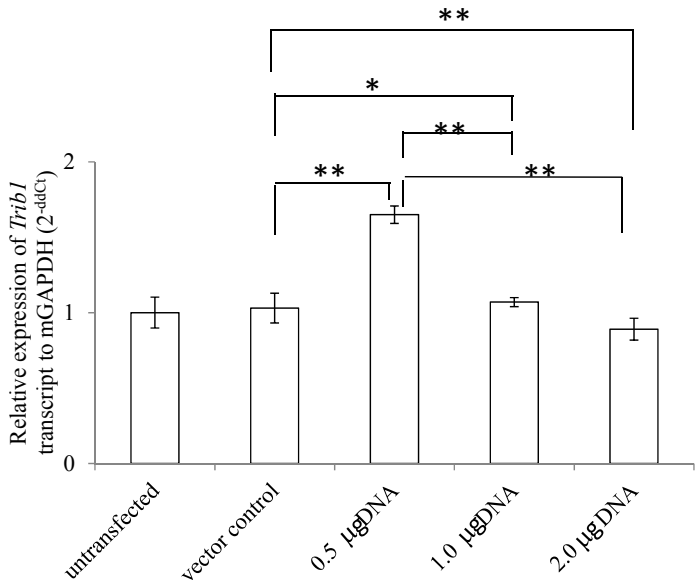

Figure 5.5. Optimisation of Trib1 plasmid concentrations for transfection. *Trib1* expression was measured by qPCR. The values represent the mean ± SD of two separate experiments. Statistical analysis was described in sections 2.8. LME methods were used for statistical analysis. Fixed effects were defined as vector control for the comparison of three Trib1 plasmid concentrations and random effects were defined as wells within an experiment. This data required Log2 transformation to normalise the residuals before analysis. A standard *post-hoc* (*Tukey*) test was used to carry out pair-wise comparisons of all groups. In all cases, p <0.05 when comparing experimental groups was considered to indicate a statistically significant difference.* p <0.05 compared with the vector control group was considered to indicate statistical significance; ** p <0.001.

The same experimental design was used as described for the siRNA-mediated gene knockdown experiment. Twenty-four hr after transfection, the proportion of live cells in the vector control and Trib1-transfected groups were 45.5% and 28.8%, respectively (Figs. 5.6A, B).

As there were more dead cells in the Trib1-transfected group, the cell cycle was only assessed at 24 hr and the time points for assaying apoptosis were 6 hr and 24 hr.

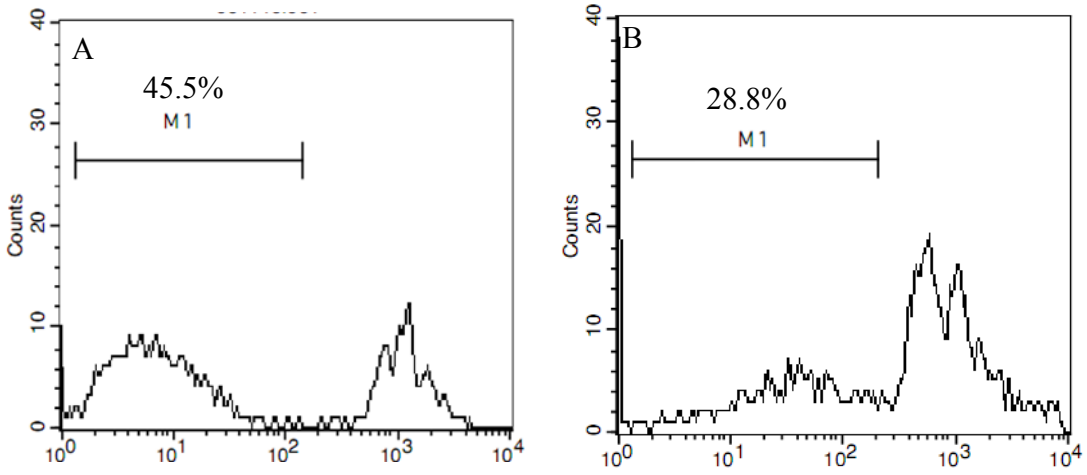

Figure 5.6. Viability of Trib1 transfected cells. PI staining and FACS were used to examined the viability of RAW264.7 cells 24 hr after transfection with (A) empty vector control and (B) Trib1 expression vector. M1 represents the live cell population. Two separate experiments showed similar results.

5.3.4 Effect of Trib1 overexpression on cell cycle progression and apoptosis

The experimental design of Trib1 overexpression was referred to Fig. 5.1B. In contrast to the Trib1 knockdown data, Trib1overexpression resulted in a significant accumulation of cells in the G_1 phase, and a reduced proportion of cells in the S and G_2/M phases compared to the vector control group (Table 5.2 and Fig. 5.7C). The empty vector controls showed the same cell cycle profiles as untreated RAW264.7 cells (Table 5.2, Figs. 5.7B and A, respectively). Thus, excess Trib1 causes macrophages to arrest at the G_1 transition.

Table 5.2. Cell cycle analysis of RAW264.7 cells 24 hr post-transfection

Cell phase (%)	Empty vector	Trib1 vector (0.5 µg)	Pearson's Chi-squared test
G_0/G_1	63.04 ± 0.3	74.46 ± 0.9	$p = 0.045$
S	18.31 ± 1.0	15.18 ± 1.0	$p = 0.613$
G_2/M	12.19 ± 0.2	7.31 ± 0.6	$p = 0.17$

Relative to the vector control group; $p < 0.05$ was considered to indicate statistically significant.

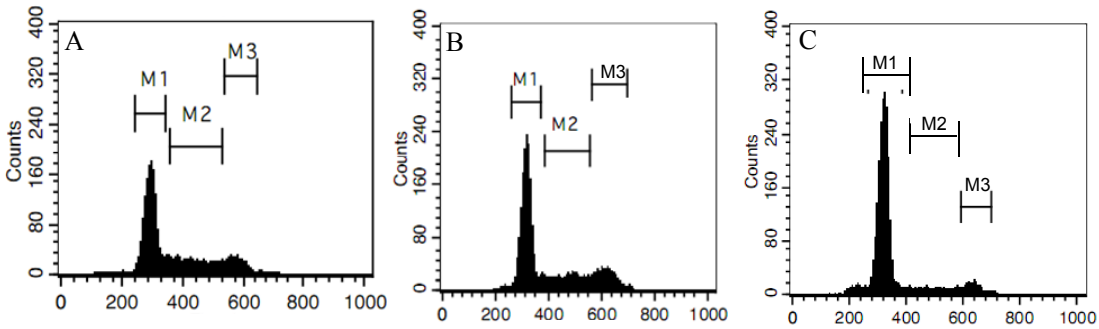

Figure 5.7. Trib1 overexpression disturbs the cell cycle. Untreated RAW 264.7 cells (A) and cells transfected with empty vector control (B) or Trib1 expression vector (C) after 24 hr. The values in Table 5.2 represent the percentage of cells in G_0/G_1 (M1), S (M2), G_2/M (M3) phases of the cell cycle. Data are represented as the mean ± SD of two independent experiments.

I previously showed that Trib1 silencing postpones RAW264.7 cell apoptosis after 72 hr (Figs. 5.4C, D). I compared over- and under-expression of Trib1 in RAW264.7 cells at 6 hr and 24 hr after transfection. After 6 hr, there was no significant increase in apoptosis in either gain-of-function or knockdown experiments (Table 5.3, upper row). Numbers of apoptotic cells were much higher in the Trib1 overexpression group than in the empty vector at 24 hr and this was statistically significant (Fig. 5.8A, B; Table 5.3, lower row; $p = 0.031$). However, there was no difference in apoptosis levels in the Trib1 knockdown experiment after 24 hr (Fig. 5.8C, D; Table 5.3, lower row; $p = 0.157$).

Interestingly, comparing 6 hr and 24 hr time points in the Trib1 overexpression groups showed a significant increase in apoptosis in Trib1 plasmid groups but no significance in the empty vector controls ($p = 0.001$ and $p = 0.064$, respectively). Nevertheless, There was no significant difference in apoptosis levels in the Trib1 knockdown group between 6 and 24 hr ($p > 0.1$).

Conversely, compared with the gain-of-function experiment, levels of apoptosis in the Trib1 siRNA group decreased after 24 hr (Table 5.3; Fig. 5.8B and D; $p < 0.001$). These data indicate that Trib1 plays a role in controlling cell apoptosis.

Table 5.3. Levels of apoptosis in RAW264.7 cells 6hr and 24 hr post-transfection with a Trib1 expression vector

	Vector control	Trib1 DNA (0.5 µg)	Pearson's Chi-squared test*	Scrambled siRNA	Trib1 siRNA	Pearson's Chi-squared test**
Apoptosis (6 hr)	50.6 ± 1.6	56.1 ± 0.3	$p = 0.395$	47.2 ± 0.9	48.7 ± 0.2	$p = 0.998$
Apoptosis (24 hr)	61.7 ± 0.7	73.5 ± 1.9	$p = 0.031$	54.5 ± 1.9	47.1 ± 1.4	$p = 0.157$

*Compared with the vector control group; ** compared with the scrambled control group; $p < 0.05$ was considered statistically significant.

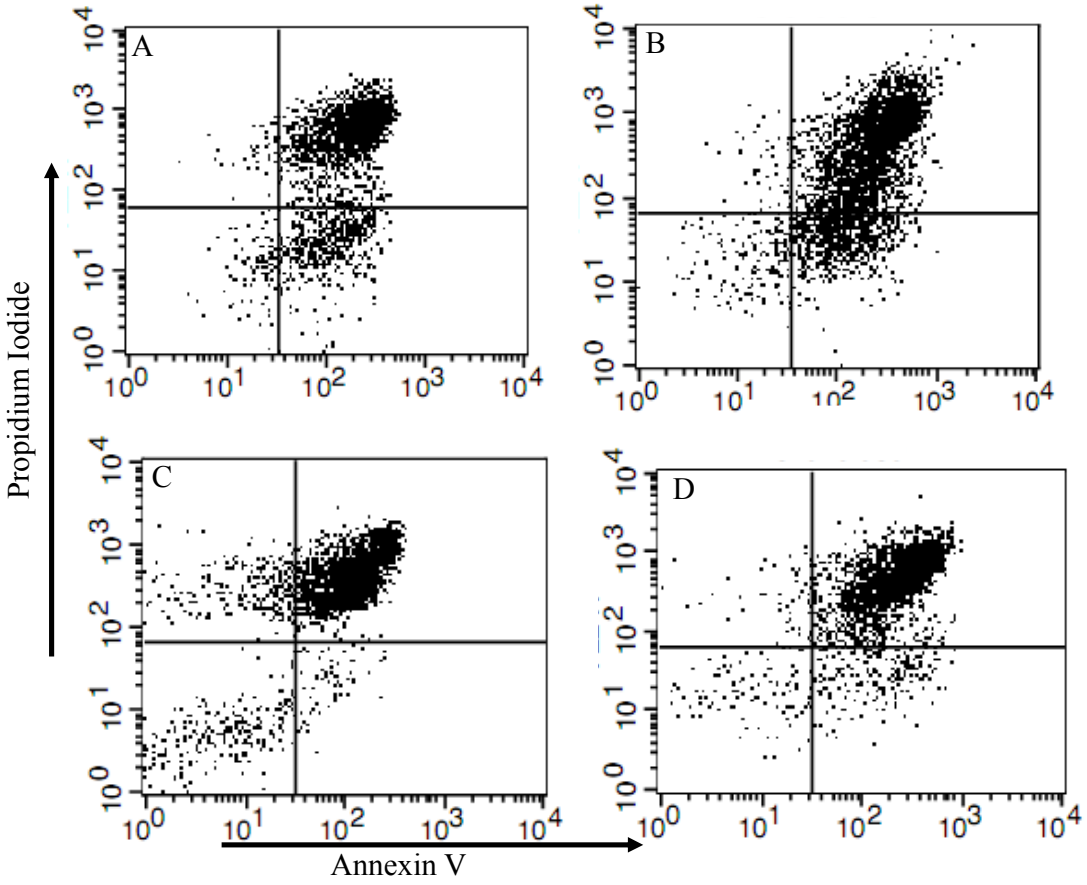

Figure 5.8. The effect of Trib1 gain- or loss-of-function on apoptosis levels. RAW264.7 cells were transfected with (A) empty vector, (B) Trib1 expression plasmid, (C) scrambled siRNA or (D) Trib1 siRNA and levels of apoptosis were determined using annexin V after 24 hr.

5.4 Discussion

The finding that reduced expression of Trib1 in RAW264.7 cells results in reduced cell adhesion (Chapter 4), prompted me to investigate the biological function of Trib1 in macrophage recruitment /migration. By overexpressing or reducing levels of Trib1, I demonstrated that Trib1 has an influential role in macrophage migration, G_2/M transition and delaying apoptosis.

It was reported that Trib negatively regulates Slbo in *Drosophila* cell migration (Rorth *et al.*, 2000). Here, I have also demonstrated that diminished expression of Trib1 reduces macrophage migration (Fig. 5.2). MCP-1, also named CCL2, is a key chemokine in regulating the recruitment and migration of monocytes/macrophages to sites of active inflammation (Ajuebor *et al.*, 1998; Sozzani *et al.*, 1993). In the untransfected and scrambled siRNA groups, MCP-1-treated macrophages showed strong chemokinesis activity. However, the numbers of migrating macrophages were unchanged in the Trib1-silenced group. Thus, this result suggests that Trib1 expression is associated with macrophage migration. Moreover, this result is consistent with a report that suppression of human Trib2 protein in melanoma cells decreases cell migration (Zanella *et al.*, 2010). Furthermore, MCP-1 activates the p42/p44 MAPK pathway (Sodhi and Biswas, 2002) and my results showed that Trib1 regulates ERK1/2 and inhibits C/EBPβ expression (Fig. 4.10 and Fig. 4.11). A previous report indicating that Trib1 functions as an adaptor between the ERK pathway and C/EBPα degradation also support my data (Yokoyama *et al.*, 2010). Collectively, the published literature together with my observations suggests that Trib1 regulates macrophage migration via the p42/44 MAPK (ERK1/2) pathway and

C/EBPβ inhibition in response to MCP-1 *in vitro*. Therefore, in this chapter, I demonstrated that loss of Trib1 is associated with macrophage dysfunction, such as in reduced migration.

As demonstrated in Chapter 4, a consequence of Trib1 silencing is altered macrophage morphology (Fig. 4.5C, D). It is unclear how this result relates to studies in *Drosophila*, although the link may be through Trib1 altering Snail expression or signalling (Grosshans and Wieschaus, 2000). Snail protein is a marker of macrophage migration during inflammation and early wound healing (Hotz *et al.*, 2010), which raises the possibility that Trib1 modulates cell migration through its interaction with Snail.

Multiple signalling pathways, such as Akt and MEK1/MKK7 (MAPK), can induce macrophage apoptosis, and Trib3 has been reported to have the same function (Fernández-Hernando C, 2007; Han S, 2006; Shang *et al.*, 2009). Moreover, Trib3-silenced macrophages showed decreased apoptosis (Shang *et al.*, 2009), consistent with my result for Trib1. In the present study, I demonstrated that Trib1 reduced the apoptotic of macrophages (Fig. 5.4C, D; Table 5.1). It is reasonable to suggest that Trib1 has a novel role in protecting from cell death, similar to Trib3. Moreover, Trib1 has been suggested to influence cell proliferation in human vascular smooth muscle cells and Trib3 has a similar function in macrophage (Shang *et al.*, 2009; Sung *et al.*, 2007). Hence, Trib1 may influence macrophage proliferation. In order to confirm this result, the effect of Trib1 overexpression was analysed.

Not surprisingly, overexpression of Trib1 caused a marked increase in apoptosis. This finding is similar to Trib3 overexpression, which caused an increase in apoptotic macrophages (Shang *et al.*, 2009). Here, I examined two time points, 6 hr and 24 hr, in the gain-of-function experiments. Even with the vector control, it was clear that electroporation killed approximately 50% cells after 6 hr. Furthermore, analysis of GFP expression (data not shown) showed that gene expression had not occurred to detectable levels in RAW 264.7 cells by 6 hr, therefore, confirming that the early apoptosis was due to the electroporation technique. Additionally, there was no significant increase in apoptosis in the vehicle controls (empty vector and scrambled siRNA, $p > 0.1$). However, 24 hr after transfection, Trib1 overexpression induces apoptosis and a reduced expression of Trib1 leads to reduced apoptosis (Table 5.3). Signal transduction pathways that control apoptosis in macrophages are complex. Therefore, my results suggest that Trib1 may control macrophage apoptosis as Trib3 does (Shang *et al.*, 2009). The precise mechanism needs to be evaluated in the future.

In *Drosophila*, Trib acts as a brake on the cell cycle, especially at the G_2/M transition phase (Seher and Leptin, 2000). Furthermore, Trib3 can slow cell cycle progression in G_2/M in human T cells (Selim *et al.*, 2007). Interestingly, Trib1 silencing had the same result (Fig. 5.4B; Table 5.1), but Trib1 overexpression resulted in G_1 arrest (Table 5.2; Fig. 5.7C). Although my Trib1 overexpression data is inconsistent with the fruit fly study, it was consistent with the report that Snail overexpression results in G_0/G_1 arrest (Vega *et al.*, 2004). Therefore, it can be concluded that Trib1 and Snail have similar functions in controlling the cell cycle. Furthermore, there are discrepancies between this study and those reported for

Drosophila Trib. For example, Trib1 activity may be cell-type specific (Kiss-Toth *et al.*, 2004; Sung *et al.*, 2006).

However, why are gain and loss of function results contradictory? It is possible that high expression of the Trib1 protein due to the CMV promoter cannot be efficiently post-translationally modified and that the excess Trib1 protein results in cell cycle disruption.

In summary, I have shown that Trib1 plays a role in the regulation of macrophage function. Trib1 silencing in macrophages causes a loss of migration (Fig. 5.2), delays cell entry into G_2/M and delays apoptosis (Figs. 5.3, 5.4 and 5.8). Combined with the results from Chapter 4, a novel role is postulated for Trib1 in modulation of ERK1/2 phosphorylation in macrophages (Fig. 4.10), as well as in C/EBPβ inhibition (Fig. 4.11) to modulate downstream functions, such as migration (Fig. 5.9).

In conclusion, this chapter achieved the aim of demonstrating that Trib1 displays novel biological functions and has an influence on macrophage biology.

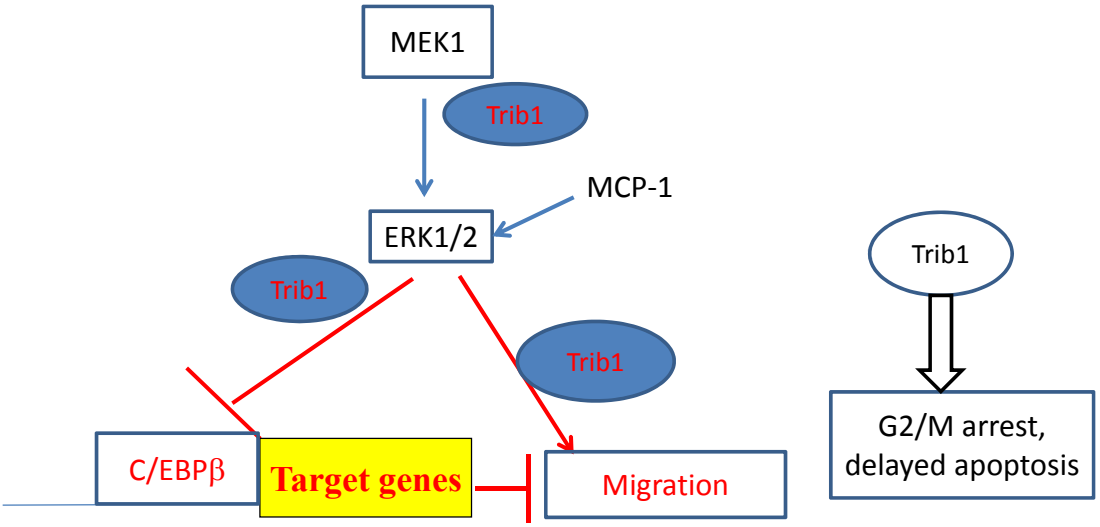

Figure 5.9. Schematic illustration of the possible signalling pathways interacting with Trib1 in RAW264.7 cells. Trib1 functions as a scaffold protein linking the MEK1/ERK1/ERK2 pathway and C/EBPβ. MCP-1 induces ERK1/2 phosphorylation and triggers chemokinesis. Trib1 interacts with MEK1 and enhances ERK1/2 phosphorylation that might control cell migration. Conversely, ERK1/2 inhibits C/EBPβ and Trib1 medicates cell movement. Further, Trib1 plays a role in modulating the cell cycle in macrophages by inducing G_2/M arrest and delaying apoptosis.

Chapter 6: General discussion

6.1 Introduction

When Trib was identified in *Drosophila*, it was reported to function as a regulator of the cell cycle, cell proliferation, and morphogenesis (Mata *et al.*, 2000; Seher and Leptin, 2000). In mammalian systems, more specific functions have been demonstrated for Trib2 and Trib3, such as the contribution of Trib2 to AML and human lung cancer through C/EBPα down-regulation (Dedhia *et al.*, 2010; Grandinetti *et al.*, 2011; Keeshan *et al.*, 2010; Keeshan *et al.*, 2006; Keeshan *et al.*, 2008). Trib3 function is connected with nutrient metabolism (Du *et al.*, 2003; Iynedjian, 2005; Koo *et al.*, 2004; Okamoto *et al.*, 2007; Qi *et al.*, 2006), and both Trib2 and Trib3 are involved in atherosclerosis (Deng *et al.*, 2009; Shang *et al.*, 2009). Compared with Trib2 and Trib3, there is very little information on the role of Trib1. Although the major functions of Trib1 remain unclear, possible roles for Trib1 have been discovered in this thesis.

In the *in vivo* system, it was demonstrated that Trib1-deficient female mice are infertile (Yamamoto *et al.*, 2007). Moreover, female fruit flies overexpressing *Trib* have smaller ovaries with fewer egg chambers than wild-type flies (Mata *et al.*, 2000). Trib1 knockdown in macrophages *in vitro* does not cause cell death (Fig. 4.6D). Thus, although absence of Trib1 causes female infertility, these results indicate it is a non-essential protein.

My observations in Chapters 4 and 5 show that silencing macrophage Trib1 up-regulates TNF-α production following treatment with immune modulators (Fig. 4.9)

and that macrophage migration is inhibited via ERK1/2 and C/EBPβ regulation (Figs. 4.10 and 4.11).

In the innate immune response, macrophage functions include phagocytosis and antigen presentation to activate T cells (Janeway *et al.*, 2001). Therefore, migration of macrophages to inflammatory tissue is necessary. However, Trib1-deficient macrophages failed to migrate, so I suspect that Trib1 protein influences macrophage migration (Fig. 5.2). This result is consistent with the fruit fly study, which indicated that *Drosophila* loss of Trib down-regulates border cell migration (Rorth *et al.*, 2000).

Here, I demonstrated that the murine Trib1 displays similar functions to that of fruit flies, such as controlling G_2/M transition (Figs. 5.3C, 5.4B). Moreover, Trib1 delayed apoptosis in macrophages (Figs. 5.4C and D) as was previously reported for human Trib3 (Shang *et al.*, 2009). Further, loss of macrophage function during inflammation leads to disease, including atherosclerosis. Although I do not provide enough evidence to verify the relationship between Trib1 and atherosclerosis, my findings suggest that a link may exist. Thus, I suggest that Trib1 has a potential role in atherosclerosis and future experiments will aim to investigate this possibility.

There are inconsistencies between my present results and those reported for *Drosophila* Trib and by Kiss-Toth's group. The unique feature of mammalian Trib proteins is that they are cell-type specific; therefore, similar treatments may have contrasting results in different tissues (Kiss-Toth *et al.*, 2004; Sung *et al.*, 2006). I found this characteristic in my apoptosis and cell cycle experiments (Figs. 5.3, 5.4,

5.7 and 5.8). The present study showed G_2/M arrest in Trib knockdown cells and delayed G_1/S following Trib1 overexpression (Fig. 5.7). These findings contradict those of *Drosophila* Trib. However, Kiss-Toth's group found no effect on cell cycle progression in HeLa cells by either overexpression or with antisense silencing of either Trib1 or Trib3. Further evidence suggests that Trib1 function following overexpression in primary bone marrow derived macrophages (BMMs) (Yamamoto *et al.*, 2007) and immortalised macrophage cell line are different (Chapter 4). Therefore, my results also demonstrate that Trib1 expression is cell-type specific.

TNF-α is a pro-inflammatory cytokine with an important role during inflammation. It is released quickly after infection and is an early mediator in inflamed tissue (Parameswaran and Patial, 2010). In this study, Trib1 knockdown caused up-regulation of TNF-α after stimulation with IFN-γ or TLR2L (Fig. 4.9). A study using Trib1 knockout mice demonstrated that *Trib1* is a pro-inflammatory gene that regulates TNF-α production and controls NF-κB activity (Ostertag *et al.*, 2010). This information provides strong evidence to support my findings of Chapter 4. However, TNF-α is also associated with macrophage apoptosis (Flad *et al.*, 1999). My observation of increased TNF-α production associated with delayed apoptosis following Trib1 knockdown indicates that the Trib1-induced delay in macrophage apoptosis is TNF-α independent.

Overall, Trib1 functions and my research findings have been fully discussed in the previous chapters of this thesis. In addition to the aforementioned functions, I would like to propose three possible roles for this novel protein in the following sections.

6.1.1 Trib1 signalling pathways

Kiss-Toth's group was the first to propose an interaction between Trib and certain signalling pathways, mainly the MAPK pathway. Both Trib over- and under-expression were reported to inhibit MAPK. Firstly, Trib3 interacts with the MEK1 and MKK7 upstream components of the MAPK pathway (Kiss-Toth *et al.*, 2004). Secondly, Trib2 negatively regulates MEK1 and MKK7 in monocytes (Eder *et al.*, 2008). My study confirmed that Trib1 positively regulates ERK1/ERK2 (MAPK) and downstream biological functions, such as macrophage migration (Fig. 5.2). Moreover, Trib1 inhibits C/EBPβ through an ERK1/ERK2 (MAPK) interaction (Figs. 4.10 and 4.11), consistent with Yokoyama's findings (2010). Furthermore, Trib2 has been reported to negatively regulate the C/EBP family via its conserved C-terminal-binding site for the E3 ubiquitin ligases (COP-1; (Keeshan *et al.*, 2010; Keeshan *et al.*, 2006). Surprisingly, Trib3 regulates lipid metabolism through the same pathway (Qi *et al.*, 2006), and the COP-1 binding motif is conserved in the C-terminus of all three mammalian Trib proteins. However, the results obtained in the current study do not provide direct evidence that Trib1 uses the same mechanism to regulate C/EBPβ. Taken together, all three members of Trib function as inhibitors of the C/EBP family. A report proposed that Trib1 is a scaffold protein between the MEK/ERK1/2 pathway and C/EBPα (Yokoyama and Nakamura, 2011), which supports my hypothesis. A series of downstream cellular events are triggered by Trib1 interaction with ERK1/2 and C/EBPβ, resulting in cell migration (Chapter 4). Whether or not Trib1 is involved in Akt and Notch pathways is unclear; however, some preliminary results indicated that Trib1 might be a downstream target of Notch pathway in RAW264.7 cells treated with γ-secretase inhibitors (GSIs). Table.6.1 summarises the signalling

pathways in which Trib1 is involved.

Table. 6.1. Summary of potential Trib1 signalling pathways identified in this thesis

	Trib1
MAPK	MEK1/MKK4 (Kiss-Toth *et al.*, 2004) a regulator of ERK1/2 (Chapter 4)
C/EBPβ	Inhibition (Yamamoto *et al.*, 2007) Inhibition (IFN-γ induced, Chapter 4)
IκB	May be an inhibitor (Chapter 4, indirect evidence from the TNF-α production)
Akt	Akt expression was very weak in RAW264.7 cells (preliminary results)
Notch	May be a downstream target (GSIs were treated, preliminary results)

6.1.2 Diverse roles for Trib proteins in cell differentiation and de-differentiation

Trib1 and Trib2 function with *HoxA9/Meis1* to induce AML (Jin *et al.*, 2007; Keeshan *et al.*, 2008). The *Hox* gene has a key role in haematopoiesis and regulates myeloid differentiation. Moreover, Trib1 is associated with early cell differentiation and has been reported to be involved in mammary epithelial cell differentiation (Perotti *et al.*, 2009). The possibility that Trib1 may have a role in differentiation prompts me to speculate that Trib1 may be associated with stem cell function. Interestingly, a recent report that human Trib2 may have a role in cancer stem cells supports this hypothesis (Grandinetti *et al.*, 2011).

RAW264.7 cells were used in the current study; however, my results using these cells differed from Yamamoto's findings in bone marrow derived macrophages. An explanation for this discrepancy may be that cell lines are relatively differentiated

and that Trib1 modulates downstream signalling pathways, such as ERK1/2, in activated macrophages (Fig. 4.11). Furthermore, bone marrow derived macrophages are classified as primary cells that may not be well differentiated; therefore, Trib1 may not function in regulating the MAPK pathway in these cells. As discussed in section 6.1, Trib1 plays diverse roles in different tissues. *Drosophila* studies reported contradictory results to my current study due to differences in developmental stage, i.e. developing vs. differentiated. Thus, it may be worthwhile examining the role of Trib1 in differentiation or in undifferentiated cells, such as stem cells or cancer stem cells, in the future.

6.1.3 The epithelial–mesenchymal transition and tumour-associated macrophages

After Trib1 siRNA electroporation and overnight culture, RAW264.7 morphology had changed to exhibit mainly monocyte-like features (Fig. 4.5D). Snail is involved in different stages of development, including the control of cell shape (Hemavathy *et al.*, 2000). Overexpression of Snail increases ERK1/2 activity (Vega *et al.*, 2004), consistent with Trib1 knockdown data in Chapter 4. Trib1, through its interaction with Snail, may modulate cell motility and cell cycle progression, and delay apoptosis by regulating ERK1/2.

The EMT is a fundamentally important, reversible cellular event that occurs during development and wound healing. It allows tightly anchored epithelial cells to lose their cellular adhesion and acquire migratory and invasive properties (Thiery *et al.*, 2009). Further, Snail transcriptional activation has a significant role in triggering

EMT (Kalluri, 2009; Thiery and Sleeman, 2006). EMT is a key step in cancer metastasis (Radisky, 2005). The morphology of Trib1 knockdown macrophages has some features in common with "EMT-like" cells (Table 6.2), although RAW264.7 cells are not epithelial cells. Features of Trib1-silenced cells are therefore similar to "EMT-like" features (caused by increasing Snail expression). Thus, it would be exciting to understand how Trib interacts with Snail. Intriguingly, Snail has been reported to mediate the migration of activated macrophages during TGF-β-induced inflammation and wound healing (Hotz *et al.*, 2010). I therefore speculate that Trib1 may function in the EMT through Snail.

Table 6.2. Comparison of Trib1 silencing cell features and EMT-like features (caused by increased Snail expression)

	EMT-like features (overexpression of Snail in murine melanoma cell line) (Kudo-Saito *et al.*, 2009)	**Trib1 silencing features in murine macrophages (my findings)**
Cell shape	Spindle, dendritic like	Round, monocyte-like
Cell proliferation	Decreased	ND[ab]
Cell adhesion	Decreased	Decreased
Cell migration	Not mentioned	Decreased
EMT markers	E-cadherin decreased Fibronectin increased	ND[a]

[a], experiment has not been done; [b], decreased apoptosis in Trib1-silenced cells.

As tumours progress, however, macrophages receive further differentiation signals, perhaps from the tumour itself, and begin to produce anti-inflammatory cytokines. TAMs and their anti-inflammatory cytokines can induce a series of immunosuppression signals that prevent tumour rejection. Thus, in cancer, the responses of macrophages to their microenvironment can determine disease progression (Mosser, 2003).

Trib1 has been reported to be a myeloid oncogene (Jin *et al.*, 2007). My results using a macrophage cell line did not clarify whether macrophage function in this cell line was different from primary macrophages. For instance, the adherence of following Trib1 silencing, RAW264.7 cells become less and less than the scrambled siRNA group. Therefore, these cells may have transformed into an undefined type of macrophage, which have lost typical macrophage characteristics, such as migration (Chapter 5), adhesion and cell shape (Chapter 4). Yamamoto's microarray results indicate that prostaglandin E synthase, lipocalin-2 (24p3), arginase type II and plasminogen activator inhibitor type II were highly up-regulated in Trib1-deficient macrophages (Yamamoto *et al.*, 2007), and this phenotype is similar to that of M2 macrophages. However, the classification of TAMs is more specifically M2c type (Mantovani and Sica, 2010; Mantovani *et al.*, 2002; Sica *et al.*, 2008). This evidence indicates that Trib1 deficiency induces macrophages to develop a TAM-like phenotype. IL-10 treatment *in vitro* leads to the development of an M2c phenotype and deactivates macrophages (Mantovani *et al.*, 2004). An attractive hypothesis suggests that C/EBPβ influences macrophage polarisation to form TAMs (He *et al.*, 2009), and my results demonstrate that Trib1 knockdown causes enhances C/EBPβ expression. Therefore, Trib1 might be involved in TAMs differentiation through C/EBPβ. TAMs are key producers of TNF-α (Pollard, 2004). Interestingly, I found that Trib1-silenced macrophages stimulated by TLR2L/IFN-γ produced higher levels of TNF-α that controls (Fig. 4.9). Although the present study did not include further experiments to observe the phenotype of Trib1-defiencent macrophages, if Trib1 is involved in transforming normal macrophages into TAMs, it may become a biomarker for use in tumour immunology. Manipulating the responses of Trib1 may

provide a therapeutic tool to reverse or prevent diseases.

Finally, the following illustration is proposed to summarise the role of Trib1 in activated macrophages (Fig. 6.1).

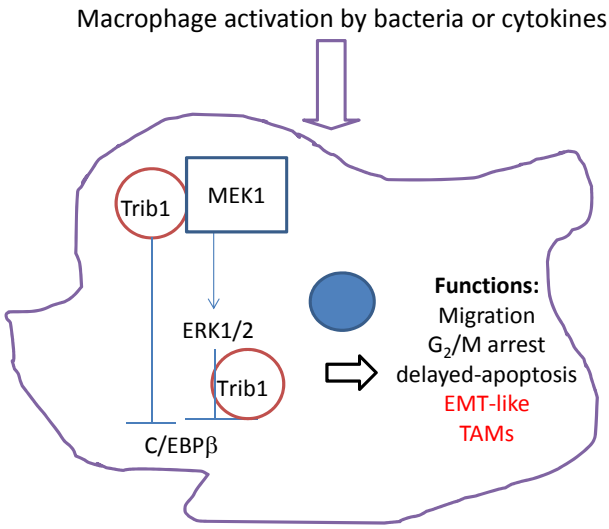

Figure 6.1. The proposed mechanism of Trib1 function in activated macrophages. When macrophages are activated by bacteria or inflammatory cytokines, Trib1 either interacts with ERK1/2 or directly inhibits C/EBPβ expression, resulting in downstream events, such as TNF-α production. Furthermore, Trib1 regulates a series of macrophage functions, such as migration and cell cycle disruption, and may cause transformation to tumour-associated macrophages.

6.2 Future work on Trib1

In this thesis, I left some important unanswered questions regarding direct evidence for Trib1 in C/EBPβ regulation, the relationships between Trib1 and EMT, and also between Trib1 with TAMs. Additionally, the disease profiles of bacterial infection should be investigated as Smith *et al.* (2011) have done for Trib3. Moreover, direct evidence of a role for Trib1 in atherosclerosis should be defined. The most significant and remarkable question of all will be whether Trib1 is involved in EMT. If Trib1 has a role in EMT, Trib1 could be a new therapeutic target for the prevention of cancer progression or metastasis in tumour immunology. Furthermore, Trib1 is also reported to be expressed in human $CD4^{+}CD25^{+}$ regulatory T cells (Pfoertner *et al.*, 2006). A lack of Treg cells that express $CD4^{+}CD25^{+}$ results in severe autoimmunity in both mice and humans (Buckner, 2010). Therefore, it will be worthwhile exploring the functional role of Trib1 in autoimmune diseases. Finally, all studies in this thesis were done using RAW264.7 cells; however, it would be useful to verify Trib1 function in primary BMMs. As Trib1 is a myeloid oncogene, Trib1-silencing in primary BMMs may provide more compelling evidence of Trib1 function. This would provide a comprehensive assessment of the roles of Trib1 both *in vitro* and *ex vivo*.

Appendix A

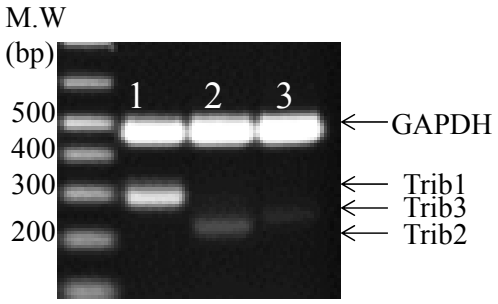

Figure 7.1. Expression of *Tribs* transcripts in splenocytes. The expression profiles of *Trib1* (lane 1; 294 bp), *Trib2* (lane 2; 221 bp) and *Trib3* (lane 3; 246 bp) transcripts were check that all *Tribs* primers were functional. A housekeeping gene (GAPDH, 472 bp) was used as an internal control.

Appendix B

Solutions and buffers

Agarose gels: 2% small (35 ml) and large gels (100–120 ml) are made by adding 2g agarose to 100 ml 1× TAE buffer and heating by microwave until dissolved. The solution is allowed to cool, and nucleic acid labelling solutions are added before the agarose solution is poured into moulds and allowed to set.

β-phosphatase inhibitor: 1 M β-phosphatase (β-GPP, Merck, MW= 306.1). β-GPP (15.3 g) is added to 50 ml dH_2O to make a 1 M solution. Then, 1 ml of 1M β-GPP solution is added to 100 ml blocking solution or PBS and final concentration is 10mM.

Freezing medium: 10% DMSO in FBS

Luria broth base (Miller's LB broth base, Invitrogen): Powder (25 g) is dissolved in 1 L of distilled water, autoclaved and allowed to cool. Ampicillin (250 µl) at a concentration of 100 mg/ml is added to 250 ml LB broth. Typical formula per litre: 10 g Peptone 140, 5 g Yeast Extract, 10 g NaCl.

Phosphate-buffered saline (PBS) (10x): Purchased as 10× concentrate and is made up to a 1× solution by adding 100 ml 10× solution to 900 ml distilled water. Typical formula per litre: 8 g NaCl, 0.2 g KCl, 1.44 g Na_2HPO_4 and 0.24 g KH_2PO_4.

PBS Tween-20 (PBST): PBS and 0.1 % Tween-20, pH 7.4.

PBST blocking buffer: 5% (w/v) skimmed milk powder in PBST.

Propidium Iodide: A 10 mg/ml stock solution is made in water and stored in 20 µl aliquots at -20°C. The working solution of 200 µg/ml is made by adding 980 µl PBS to a frozen aliquot, covered in foil and stored at 4°C.

Resolving gel

Ingredient/percentage	12%
dH_2O	3.3 ml
30 %, 37.5:1 Ratio Acrylamide/Bis-acrylamide (Protigel)	4.0 ml
1.5 M Tris, pH 8.8	2.5 ml
10 % SDS	100 µl
10 % Ammonium persulphate (APS)(Sigma, UK)	100 µl
N, N, N′, N′-tetramethylethylenediamine (TEMED)(Sigma, UK)	5 µl
Total (For 2 gels)	10 ml

SDS sample Buffer (2×): 120 mM Tris-HCl pH 6.8, 4% (w/v) SDS, 20% (v/v) glycerol, 200 mM DTT, 0.04% (w/v) bromophenol blue.

SDS-PAGE running buffer (5×)

Ingredient	
Trizma base (Sigma, UK)	125 mM
Glycine (Sigma, UK)	1.25 M
SDS (Sigma, UK)	0.5 %
Add dH_2O to final volume	1 L
	Adjust to pH 8.3

Stacking gel

Ingredient	
dH_2O	2.77 ml
30%, 37.5:1 Ratio Acrylamide/Bis-acrylamide (ProtiGel)	830 µl
0.5 M Tris, pH 6.8	1.26 ml
10% SDS	50 µl
10% APS	50 µl
TEMED	5 µl
Total (For 2 gels)	5 ml

TAE electrophoresis buffer (50×)

Ingredient	
Trizma base (Sigma, UK)	2 M
Glacial acetic acid (Sigma, UK)	1 M
EDTA (Sigma, UK)	50 mM
Add dH_2O to final volume	1 L
	Adjust to pH 7.0

Transfer buffer (1x)

Ingredient	
Trizma base (Sigma, UK)	25 mM
Glycine (Sigma, UK)	192 mM
20% (v/v) methanol	200 ml
Add dH_2O to final volume	1 L

Tris-buffered saline (TBS, 1×): 20mM Tris-HCl, 0.15M NaCl.

Tris-buffered saline Tween-20 (TBST): 20mM Tris-HCl, 0.15M NaCl, 0.1% Tween-20.

TBST blocking buffer: 5% 5% (w/v) skimmed milk powder in TBST.

Western blotting enhanced chemiluminescence (ECL) detection solution:

Solution 1

Ingredient	
250 mM Luminol (Sigma, UK)	1 ml
90 mM Coumaric acid (Sigma, UK)	440 µl
1M Tris, pH 8.5	10 ml
Add dH_2O to final volume	100 ml

Solution 2

Ingredient	
30 % Hydrogen peroxide (H_2O_2)(Sigma, UK)	64 µl
1M Tris, pH 8.5	10 ml
Add dH_2O to final volume	100 ml

References:

Adib-Conquy, M., and Cavaillon, J.-M. (2002). Gamma interferon and granulocyte/monocyte colony-stimulating factor prevent endotoxin tolerance in human monocytes by promoting interleukin-1 receptor-associated kinase expression and its association to MyD88 and not by modulating TLR4 expression. *J Biol Chem. 277*, 27927-27934.

Ajuebor, M.N., Flower, R.J., Hannon, R., Christie, M., Bowers, K., Verity, A., and Perretti, M. (1998). Endogenous monocyte chemoattractant protein-1 recruits monocytes in the zymosan peritonitis model. *J Leukoc Biol. 63*, 108-116.

Akira, S. (2003). Toll-like Receptor Signaling. *J Biol Chem. 278*, 38105-38108.

Akira, S., Isshiki H, Sugita T, Tanabe O, Kinoshita S, Nishio Y, Nakajima T, Hirano T, and T., K. (1990). A nuclear factor for IL-6 expression (NF-IL6) is a member of a C/EBP family. *EMBO J. 9*, 1897-1906.

Akira, S., and Kishimoto, T. (1997). NF-IL6 and NF-κB in cytokine gene regulation. *Adv Immunol. 65*, 1-46.

Akira, S., Takeda, K., and Kaisho, T. (2001). Toll-like receptors: critical proteins linking innate and acquired immunity. *Nat Immunol. 2*, 675-680.

Akira, S., Uematsu, S., and Takeuchi, O. (2006). Pathogen recognition and innate immunity. *Cell. 124*, 783-801.

Alan, A. (2001). Role of Toll-like receptors in inflammatory response in macrophages. *Crit Care Med. 7 Suppl*, S16-18.

Anastasov, N., Bonzheim, I., Rudelius, M., Klier, M., Dau, T., Angermeier, D., Duyster, J., Pittaluga, S., Fend, F., Raffeld, M., and Quintanilla-Martinez, L. (2010). C/EBPβ expression in ALK-positive anaplastic large cell lymphomas is required for cell proliferation and is induced by the STAT3 signaling pathway. *Haematologica. 95*, 760-767.

Argiropoulos, B., and Humphries, R.K. (2007). Hox genes in hematopoiesis and leukemogenesis. Oncogene *26*, 6766-6776.

Ashkar, A.A., and Rosenthal, K.L. (2002). Toll-like receptor 9, CpG DNA and innate immunity. *Curr Mol Med. 2*, 545-556.

Ashton-Chess, J., Giral, M., Mengel, M., Renaudin, K., Foucher, Y., and Gwinner, W., *et, al.* (2008). Tribbles-1 as a novel biomarker of chronic antibody-mediated rejection. *J Am Soc Nephrol. 19*, 1116-1127.

Bailey, D.P., Kashyap, M., Bouton, L.A., Murray, P.J., and Ryan, J.J. (2006). Interleukin-10 induces apoptosis in developing mast cells and macrophages. *J Leukoc Biol. 80*, 581-589.

Balmanno, K., and Cook, S.J. (2008). Tumour cell survival signalling by the ERK1/2 pathway. *Cell Death Differ. 16*, 368-377.

Banchereau, J., and Steinman, R.M. (1998). Dendritic cells and the control of immunity. Nature *392*, 245-252.

Barbalat, R., Lau, L., Locksley, R.M., and Barton, G.M. (2009). Toll-like receptor 2 on inflammatory monocytes induces type I interferon in response to viral but not bacterial ligands. *Nat Immunol. 10*, 1200-1207.

Belvin, M.P., and Anderson, K.V. (1996). A conserved signaling pathway: the Drosophila toll-dorsal pathway. *Annu Rev Cell Dev Biol. 12*, 393-416.

Boldrick, J.C., Alizadeh, A.A., Diehn, M., Dudoit, S., Liu, C.L., Belcher, C.E., Botstein, D., Staudt, L.M., Brown, P.O., and Relman, D.A. (2002). Stereotyped and specific gene expression programs in human innate immune responses to bacteria. *Proc Natl Acad Sci U S A. 99*, 972-977.

Bonjardim, C.A., Ferreira, P.C.P., and Kroon, E.G. (2009). Interferons: Signaling, antiviral and viral evasion. Immunology letters *122*, 1-11.

Bowers, A.J., Scully, S., and Boylan, J.F. (2003). SKIP3, a novel Drosophila tribbles ortholog, is overexpressed in human tumors and is regulated by hypoxia. *Oncogene. 22*, 2823-2835.

Briscoe, J., Rogers, N.C., Witthuhn, B.A., Watling, D., Harpur, A.G., Wilks, A.F., Stark, G.R., Ihle, J.N., and Kerr, I.M. (1996). Kinase-negative mutants of JAK1 can sustain interferon-γ-inducible gene expression but not an antiviral state. *EMBO J. 15*, 799-809.

Buckner, J.H. (2010). Mechanisms of impaired regulation by CD4+CD25+FOXP3+ regulatory T cells in human autoimmune diseases. *Nat Rev Immunol. 10*, 849-859.

Calkhoven, C.F., Muller, C., and Leutz, A. (2000). Translational control of C/EBPα and C/EBPβ isoform expression. Genes & Development *14*, 1920-1932.

Chammas, R., Taverna, D., Cella, N., Santos, C., and Hynes, N.E. (1994). Laminin and tenascin assembly and expression regulate HC11 mouse mammary cell differentiation. Journal of Cell Science *107*, 1031-1040.

Chatterjee-Kishore, M., Wright, K.L., Ting, J.P.Y., and Stark, G.R. (2000). How Stat1 mediates constitutive gene expression: a complex of unphosphorylated Stat1 and IRF1 supports transcription of the LMP2 gene. The EMBO journal *19*, 4111-4122.

Christian, B. (2000). The function of type I interferons in antimicrobial immunity. *Curr Opin Immunol. 12*, 419-424.

Coccia, E.M., Russo, N.D., Stellacci, E., Testa, U., Marziali, G., and Battistini, A. (1999). STAT1 activation during monocyte to macrophage maturation: role of adhesion molecules. *Int Immunol. 11*, 1075-1083.

Colonna, M., Trinchieri, G., and Liu, Y.-J. (2004). Plasmacytoid dendritic cells in immunity. *Nat Immunol. 5*, 1219-1226.

Corcoran, C.A., Luo, X., He, Q., Jiang, C., Huang, Y., and Sheikh, M.S. (2005). Genotoxic and endoplasmic reticulum stresses differentially regulate TRB3 expression. *Cancer Biol Ther. 4*, 1063-1067.

Crouch, D.H., Fincham, V.J., and Frame, M.C. (1996). Targeted proteolysis of the focal adhesion kinase pp125 FAK during c-MYC-induced apoptosis is suppressed by integrin signalling. *Oncogene. 12*, 2689-2896.

Csoka, B., Nemeth, Z.H., Virag, L., Gergely, P., Leibovich, S.J., and Pacher, P., *et, al.* (2007). A2A adenosine receptors and C/EBPβ are crucially required for IL-10 production by macrophages exposed to Escherichia coli. *Blood. 110*, 2685-2695.

Dalton, D.K., Pitts-Meek, S., Keshav, S., Figari, I.S., Bradley, A., and Stewart, T.A. (1993). Multiple defects of immune cell function in mice with disrupted interferon-γ genes. *Science. 259*, 1739-1742.

Darlington, G.J., Ross, S.E., and MacDougald, O.A. (1998). The Role of C/EBP Genes in Adipocyte Differentiation. *J Biol Chem. 273*, 30057-30060.

Decker, T., Kovarik, P., and Meinke, A. (1997). GAS elements: a few nucleotides with a major impact on cytokine-induced gene expression. *J Interferon Cytokine Res. 17*, 121-134.

Dedhia, P.H., Keeshan, K., Uljon, S., Xu, L., Vega, M.E., and Shestova, O., *et, al.* (2010). Differential ability of Tribbles family members to promote degradation of C/EBP{alpha} and induce acute myelogenous leukemia. *Blood. 116*, 1321-1328.

Deng, J., James, C.H., Patel, L., Smith, A., Burnand, K.G., Rahmoune, H., Lamb, J.R., and Davis, B. (2009). Human tribbles homologue 2 is expressed in unstable regions of carotid plaques and regulates macrophage IL-10 in vitro. *Clinical Science. 116*, 241-248.

Draper, D.W., Bethea, H.N., and He, Y.W. (2006). Toll-like receptor 2-dependent and -independent activation of macrophages by group B streptococci. *Immunol Lett. 102*, 202-214.

Du, K., Herzig, S., Kulkarni, R.N., and Montminy, M. (2003). TRB3: a tribbles homolog that inhibits Akt/PKB activation by insulin in liver. *Science. 300*, 1574-1577.

Eder, K., Guan, H., Sung, H.Y., Ward, J., Angyal, A., Janas, M., Sarmay, G., Duda, E., Turner, M., Dower, S.K.*, et al.* (2008). Tribbles-2 is a novel regulator of inflammatory activation of monocytes. *Int Immunol. 20*, 1543-1550.

Elbashir, S.M., Harborth, J., Lendeckel, W., Yalcin, A., Weber, K., and Tuschl, T. (2001). Duplexes of 21-nucleotide RNAs mediate RNA interference in cultured mammalian cells. Nature *411*, 494-498.

Farrar, M.A., and Schreiber, R.D. (1993). The molecular cell biology of interferon-γ and its receptor. *Annu Rev Immunol. 11*, 571-611.

Fernández-Hernando C, A.E., Yu J, Suárez Y, Murata T, Iwakiri Y, Prendergast J, Miao RQ, Birnbaum MJ, Sessa WC. (2007). Loss of Akt1 leads to severe atherosclerosis and occlusive coronary artery disease. Cell Metab. *6*, 446-457.

Flad, H.D., Grage-Griebenow, E., Petersen, F., Scheuerer, B., Brandt, E., Baran, J., Pryjma, J., and Ernst, M. (1999). The role of cytokines in monocyte apoptosis. *Pathobiology. 67*, 291-293.

Friedl, P. (2004). Prespecification and plasticity: shifting mechanisms of cell migration. *Curr Opin Cell Biol. 16*, 14-23.

Funami, K., Matsumoto, M., Oshiumi, H., Akazawa, T., Yamamoto, A., and Seya, T. (2004). The cytoplasmic 'linker region' in Toll-like receptor 3 controls receptor localization and signaling. *Int Immunol. 16*, 1143-1154.

Gade, P., Roy, S.K., Li, H., Nallar, S.C., and Kalvakolanu, D.V. (2008). Critical role for transcription factor C/EBPβ in regulating the expression of death-associated protein kinase 1. *Mol Cell Biol. 28*, 2528-2548.

Gazzinelli, R.T., Ropert, C., and Campos, M.A. (2004). Role of the Toll/interleukin-1 receptor signaling pathway in host resistance and pathogenesis during infection with protozoan parasites. *Immunol Rev. 201*, 9-25.

Gordon, S. (2003). Alternative activation of macrophages. *Nat Rev Immunol. 3*, 23-35.

Gordon, S., and Taylor, P.R. (2005). Monocyte and macrophage heterogeneity. *Nat Rev Immunol. 5*, 953-964.

Gortz, B., Hayer, S., Tuerck, B., Zwerina, J., Smolen, J., and Schett, G. (2005). Tumour necrosis factor activates the mitogen-activated protein kinases p38α and ERK in the synovial membrane in vivo. *Arthritis Res Ther. 7*, R1140 - R1147.

Gough, D.J., Sabapathy, K., Ko, E.Y.-N., Arthur, H.A., Schreiber, R.D., and Trapani, J.A., *et, al.* (2007). A Novel c-Jun-dependent signal transduction pathway necessary for the transcriptional activation of Interferon γ response genes. *J Biol Chem. 282*, 938-946.

Grandinetti, K.B., Stevens, T.A., Ha, S., Salamone, R.J., Walker, J.R., Zhang, J., Agarwalla, S., Tenen, D.G., Peters, E.C., and Reddy, V.A. (2011). Overexpression of TRIB2 in human lung cancers contributes to tumorigenesis through downregulation of C/EBP[alpha]. *Oncogene.*

Grosshans, J., and Wieschaus, E. (2000). A genetic link between morphogenesis and cell division during formation of the ventral furrow in Drosophila. *Cell. 101*, 523-531.

Haddad, J.J., Saade, N.E., and Safieh-Garabedian, B. (2003). Interleukin-10 and the regulation of mitogen-activated protein kinases: are these signalling modules targets for the anti-inflammatory action of this cytokine? *Cell Signal. 15*, 255-267.

Hallman M, R.M., Ezekowitz RA (2001). Toll-like receptors as sensors of pathogens. *Pediatr Res. 50*, 315-321.

Han S, L.C., DeVries-Seimon T, Ranalletta M, Welch CL, Collins-Fletcher K, Accili D, Tabas I, Tall AR. (2006). Macrophage insulin receptor deficiency increases ER stress-induced apoptosis and necrotic core formation in advanced atherosclerotic lesions. Cell Metab. *3*, 257-266.

He, M., Xu, Z., Ding, T., Kuang, D., and Zheng, L. (2009). MicroRNA-155 regulates inflammatory cytokine production in tumor-associated macrophages via targeting C/EBPβ. *Cell Mol Immunol. 6*, 343-352.

Hegedus, Z., Czibula, A., and Kiss-Toth, E. (2006). Tribbles: novel regulators of cell function; evolutionary aspects. *Cell Mol Life Sci. 63*, 1632-1641.

Hegedus, Z., Czibula, A., and Kiss-Toth, E. (2007). Tribbles: a family of kinase-like proteins with potent signalling regulatory function. *Cell Signal. 19*, 238-250.

Hemavathy, K., Ashraf, S.I., and Ip, Y.T. (2000). Snail/Slug family of repressors: slowly going into the fast lane of development and cancer. *Gene. 257*, 1-12.

Henson, P.M., Bratton, D.L., and Fadok, V.A. (2001). Apoptotic cell removal. *Curr Biol. 11*, R795-R805.

Hickman, S.P., Chan, J., and Salgame, P. (2002). Mycobacterium tuberculosis induces differential cytokine production from dendritic cells and macrophages with divergent effects on naive T cell polarization. *J Immunol. 168*, 4636-4642.

Hotz, B., Visekruna, A., Buhr, H.-J., and Hotz, H. (2010). Beyond epithelial to mesenchymal transition: a novel role for the transcription factor Snail in inflammation and wound healing. *J Gastrointest Surg. 14*, 388-397-397.

Hu, J., Roy, S.K., Shapiro, P.S., Rodig, S.R., Reddy, S.P.M., and Platanias, L.C., *et, al.* (2001). ERK1 and ERK2 activate CCAAAT/enhancer-binding proteinβ-dependent gene transcription in response to interferon-γ. *J Biol Chem. 276*, 287-297.

Hu, J.H., Chen, T., Zhuang, Z.-H., Kong, L., Yu, M.-C., Liu, Y., Zang, J.-W., and Ge, B.-X. (2007a). Feedback control of MKP-1 expression by p38. *Cell Signal. 19*, 393-400.

Hu, X., Chakravarty, S.D., and Ivashkiv, L.B. (2008). Regulation of interferon and Toll-like receptor signaling during macrophage activation by opposing feedforward and feedback inhibition mechanisms. *Immunol Rev. 226*, 41-56.

Hu, X., Chen, J., Wang, L., and Ivashkiv, L.B. (2007b). Crosstalk among Jak-STAT, Toll-like receptor, and ITAM-dependent pathways in macrophage activation. *J Leukoc Biol. 82*, 237-243.

Hu, X., Paik, P.K., Chen, J., Yarilina, A., Kockeritz, L., and Lu, T.T., *et, al.* (2006). IFN-γ suppresses IL-10 production and synergizes with TLR2 by regulating GSK3 and CREB/AP-1 proteins. *Immunity. 24*, 563-574.

Imai, Y., Kuba, K., Neely, G.G., Yaghubian-Malhami, R., Perkmann, T., van Loo, G., Ermolaeva, M., Veldhuizen, R., Leung, Y.H.C., Wang, H*., et al.* (2008). Identification of oxidative stress and Toll-like receptor 4 signaling as a key pathway of acute lung injury. Cell *133*, 235-249.

Imajo, M., and Nishida, E. (2010). Human Tribbles homolog 1 functions as a negative regulator of retinoic acid receptor. *Genes to Cells. 15*, 1089-1097.

Iynedjian, P.B. (2005). Lack of evidence for a role of TRB3/NIPK as an inhibitor of PKB-mediated insulin signalling in primary hepatocytes. *Biochem J. 386*, 113-118.

Janeway, C.A., Travers, P., Walport, M., and Shlomchik, M.J., eds. (2001). Immunobiology, 5th, 5th edn (New York: Garland Science).

Jaramillo, M., Naccache, P.H., and Olivier, M. (2004). Monosodium urate crystals synergize with IFN-γ to generate macrophage nitric oxide: involvement of extracellular signal-regulated kinase 1/2 and NF-κB. *J Immunol. 172*, 5734-5742.

Jin, G., Yamazaki, Y., Takuwa, M., Takahara, T., Kaneko, K., and Kuwata, T., *et, al.* (2007). Trib1 and Evi1 cooperate with Hoxa and Meis1 in myeloid leukemogenesis. *Blood. 109*, 3998-4005.

Johnston, L.A. (2000). Cell cycle: The trouble with tribbles. *Curr Biol. 10*, 502-504.

Jongeneel, C. (1994). Regulation of the TNF-α gene. *Prog Clin Biol Res. 388*, 367-381.

Juliano, R.L., and Haskill, S. (1993). Signal transduction from the extracellular matrix. *J Cell Biol. 120*, 577-585.

Kaisho, T., and Akira, S. (2001). Toll-like receptors and their signaling mechanism in innate immunity. *Acta odontologica Scandinavica. 59*, 124-130.

Kaisho, T., and Akira, S. (2006). Toll-like receptor function and signaling. *J Allergy Clin Immunol. 117*, 979-987.

Kalluri, R. (2009). EMT: When epithelial cells decide to become mesenchymal-like cells. *J Clin Invest*. *119*, 1417-1419.

Kaminska, B. (2005). MAPK signalling pathways as molecular targets for anti-inflammatory therapy--from molecular mechanisms to therapeutic benefits. *Biochim Biophys Acta. 1754*, 253-262.

Kanellis, J., Bick, R., Garcia, G., Truong, L., Tsao, C.C., Etemadmoghadam, D., Poindexter, B., Feng, L., Johnson, R.J., and Sheikh-Hamad, D. (2004). Stanniocalcin-1, an inhibitor of macrophage chemotaxis and chemokinesis. *Am J Physiol Renal Physiol. 286*, F356-362.

Kato, H., Sato, S., Yoneyama, M., Yamamoto, M., Uematsu, S., Matsui, K., Tsujimura, T., Takeda, K., Fujita, T., Takeuchi, O., and Akira, S. (2005). Cell type-specific involvement of RIG-I in antiviral response. Immunity *23*, 19-28.

Keeshan, K., Bailis, W., Dedhia, P.H., Vega, M.E., Shestova, O., Xu, L., Toscano, K., Uljon, S.N., Blacklow, S.C., and Pear, W.S. (2010). Transformation by Tribbles homolog 2 (Trib2) requires both the Trib2 kinase domain and COP1 binding. *Blood. 116*, 4948-4957.

Keeshan, K., He, Y., Wouters, B.J., Shestova, O., Xu, L., and Sai, H., *et, al.* (2006). Tribbles homolog 2 inactivates C/EBPα and causes acute myelogenous leukemia. *Cancer Cell. 10*, 401-411.

Keeshan, K., Shestova, O., Ussin, L., and Pear, W.S. (2008). Tribbles homolog 2 (Trib2) and HoxA9 cooperate to accelerate acute myelogenous leukemia. *Blood Cells Mol Dis. 40*, 119-121.

Kimbrell, D.A., and Beutler, B. (2001). The evolution and genetics of innate immunity. *Nat Rev Genet. 2*, 256-267.

Kiss-Toth, E., Bagstaff, S.M., Sung, H.Y., Jozsa, V., Dempsey, C., Caunt, J.C., Oxley, K.M., Wyllie, D.H., Polgar, T., Harte, M.*, et al.* (2004). Human tribbles, a protein family controlling mitogen-activated protein kinase cascades. *J Biol Chem. 279*, 42703-42708.

Kiss-Toth, E., Wyllie, D.H., Holland, K., Marsden, L., Jozsa, V., Oxley, K.M., Polgar, T., Qwarnstrom, E.E., and Dower, S.K. (2005). Functional mapping of Toll/interleukin-1 signalling networks by expression cloning. *Biochem Soc Trans. 33*, 1405-1406.

Kiss-Toth, E., Wyllie, D.H., Holland, K., Marsden, L., Jozsa, V., Oxley, K.M., Polgar, T., Qwarnstrom, E.E., and Dower, S.K. (2006). Functional mapping and identification of novel regulators for the Toll/Interleukin-1 signalling network by transcription expression cloning. *Cell Signal. 18*, 202-214.

Koo, S.H., Satoh, H., Herzig, S., Lee, C.H., Hedrick, S., and Kulkarni, R., *et, al.* (2004). PGC-1 promotes insulin resistance in liver through PPAR-alpha-dependent induction of TRB-3. *Nat Med. 10*, 530-534.

Krishnan, J., Selvarajoo, K., Tsuchiya M, Lee G, and S, C. (2007). Toll-like receptor signal transduction. *Exp Mol Med. 39*.

Kudo-Saito, C., Shirako, H., Takeuchi, T., and Kawakami, Y. (2009). Cancer metastasis is accelerated through immunosuppression during Snail-induced EMT of cancer cells. *Cancer Cell. 15*, 195-206.

Kurt-Jones, E.A., Popova, L., Kwinn, L., Haynes, L.M., Jones, L.P., Tripp, R.A., Walsh, E.E., Freeman, M.W., Golenbock, D.T., Anderson, L.J., and Finberg, R.W. (2000). Pattern recognition receptors TLR4 and CD14 mediate response to respiratory syncytial virus. Nature immunology *1*, 398-401.

Lang, R. (2005). Tuning of macrophage responses by Stat3-inducing cytokines: molecular mechanisms and consequences in infection. *Immunobiology. 210*, 63-76.

Lang, R., Rutschman, R.L., Greaves, D.R., and Murray, P.J. (2002). Autocrine deactivation of macrophages in transgenic mice constitutively overexpressing IL-10 under control of the human CD68 promoter. *J Immunol. 168*, 3402-3411.

Lee, J.C., Laydon, J.T., McDonnell, P.C., Gallagher, T.F., Kumar, S., Green, D., McNulty, D., Blumenthal, M.J., Keys, J.R., Land vatter, S.W*., et al.* (1994). A protein kinase involved in the regulation of inflammatory cytokine biosynthesis. *Nature. 372*, 739-746.

Li, H., Gade, P., Xiao, W., and Kalvakolanu, D. (2007). The interferon signaling network and transcription factor C/EBP-beta. *Cell Mol Immunol. 4*, 407-418

Lin, K.-R., Lee, S.-F., Hung, C.-M., Li, C.-L., Yang-Yen, H.-F., and Yen, J.J.Y. (2007). Survival factor withdrawal-induced apoptosis of TF-1 cells involves a TRB2-Mcl-1 axis-dependent pathway. *J Biol Chem. 282*, 21962-21972.

Lin, Y.-C., Huang, D.-Y., Chu, C.-L., and Lin, W.-W. (2010). Anti-inflammatory actions of Syk inhibitors in macrophages involve non-specific inhibition of toll-like receptors-mediated JNK signaling pathway. *Mol Immunol. 47*, 1569-1578.

Liu, P.T., Stenger, S., Li, H., Wenzel, L., Tan, B.H., and Krutzik, S.R., *et, al.* (2006). Toll-like receptor triggering of a vitamin D-mediated human antimicrobial response. *Science. 311*, 1770-1773.

Lp, Y.T., and Gridley, T. (2002). Cell movements during gastrulation: Snail dependent and independent pathways. *Curr Opin Genet Dev. 12*, 423-429.

Lu, Y.C., Kim, I., Lye, E., Shen, F., Suzuki, N., and Suzuki, S., et, al (2009). Differential role for c-Rel and C/EBPβ/δ in TLR-mediated induction of proinflammatory cytokines. *J Immunol. 182*, 7212-7221.

Mantovani, A., and Sica, A. (2010). Macrophages, innate immunity and cancer: balance, tolerance, and diversity. *Curr Opin Immunol. 22*, 231-237.

Mantovani, A., Sica, A., Sozzani, S., Allavena, P., Vecchi, A., and Locati, M. (2004). The chemokine system in diverse forms of macrophage activation and polarization. *Trends Immunol. 25*, 677-686.

Mantovani, A., Sozzani, S., Locati, M., Allavena, P., and Sica, A. (2002). Macrophage polarization: tumor-associated macrophages as a paradigm for polarized M2 mononuclear phagocytes. *Trends Immunol. 23*, 549-555.

Mark, M., Ghyselinck, N.B., and Chambon, P. (2006). Function of retinoid nuclear receptors: lessons from genetic and pharmacological dissections of the retinoic acid signaling pathway during mouse embryogenesis. In *Annu Rev Pharmacol Toxicol.*, pp. 451-480.

Martin, S.E., and Caplen, N.J. (2007). Applications of RNA interference in mammalian systems. In Annual Review of Genomics and Human Genetics (Annual Reviews), pp. 81-108.

Martinez, F., Sica A., Mantovani A., and M., L. (2008). Macrophage activation and polarization. *Front Biosci 13*, 453-461.

Mata, J., Curado, S., Ephrussi, A., and Rorth, P. (2000). Tribbles coordinates mitosis and morphogenesis in Drosophila by regulating string/CDC25 proteolysis. *Cell. 101*, 511-522.

Matsusaka, T., Fujikawa, K., Nishio, Y., Mukaida, N., Matsushima, K., Kishimoto, T., and Akira, S. (1993). Transcription factors NF-IL6 and NF-κB synergistically activate transcription of the inflammatory cytokines, interleukin 6 and interleukin 8. *Proc Natl Acad Sci USA. 90*, 10193-10197.

Mayumi-Matsuda, K., Kojima, S., Suzuki, H., and Sakata, T. (1999). Identification of a novel kinase-like gene induced during neuronal cell death. *Biochem Biophys Res Commun. 258*, 260-264.

McBride, A., Bhatt, K., Salgame, P. (2010). Development of Secondary Immune Response to Mycobacterium tuberculosis is independent of Toll-like receptor 2. *Infect Immun.*, 1076-1083.

McCoy, C.E., and O'Neill, L.A. (2008). The role of toll-like receptors in macrophages. *Front Biosci. 13*, 62-70.

Medzhitov, R. (2001). Toll-like receptors and innate immunity. *Nat Rev Immunol. 1*, 135-145.

Mills, C.D., Kincaid, K., Alt, J.M., Heilman, M.J., and Hill, A.M. (2000). M-1/M-2 macrophages and the Th1/Th2 paradigm. *J Immunol. 164*, 6166-6173.

Montoya, M., Schiavoni, G., Mattei, F., Gresser, I., Belardelli, F., Borrow, P., and Tough, D.F. (2002). Type I interferons produced by dendritic cells promote their phenotypic and functional activation. Blood *99*, 3263-3271.

Moore, K.W., de Waal Malefyt, R., Coffman, R.L., and O'Garra, A. (2001). Interleukin-10 and the interleukin-10 receptor. In *Annu Rev Immunol.* (Annual Reviews), pp. 683-765.

Mosser, D.M. (2003). The many faces of macrophage activation. *J Leukoc Biol. 73*, 209-212.

Murphy, K., Travers, P., and Walport, M., eds. (2011). Janeway's Immunobiology, 8th, 5th edn (New York: Garland Science).

Murray, P.J. (2006). Understanding and exploiting the endogenous interleukin-10/STAT3-mediated anti-inflammatory response. *Curr Opin Pharmacol. 6*, 379-386.

Muzio, M., Bosisio, D., Polentarutti, N., D?amico, G., Stoppacciaro, A., Mancinelli, R., van?t Veer, C., Penton-Rol, G., Ruco, L.P., Allavena, P., and Mantovani, A. (2000). Differential expression and regulation of toll-like receptors (TLR) in human leukocytes: selective expression of TLR3 in dendritic cells. *J Immunol. 164*, 5998-6004.

Naiki, T., Saijou, E., Miyaoka, Y., Sekine, K., and Miyajima, A. (2007). TRB2, a mouse Tribbles ortholog, suppresses adipocyte differentiation by inhibiting AKT and C/EBPβ. *J Biol Chem. 282*, 24075-24082.

O'Neill, L.A.J. (2004). TLRs: Professor Mechnikov, sit on your hat. *Trends Immunol. 25*, 687-693.

Okamoto, H., Latres, E., Liu, R., Thabet, K., Murphy, A., Valenzeula, D., Yancopoulos, G.D., Stitt, T.N., Glass, D.J., and Sleeman, M.W. (2007). Genetic deletion of Trb3, the mammalian Drosophila tribbles homolog, displays normal hepatic insulin signaling and glucose homeostasis. *Diabetes. 56*, 1350-1356.

Ord D, and Ord, T. (2003). Mouse NIPK interacts with ATF4 and affects its transcriptional activity. *Exp Cell Res. 286*, 308-320.

Ostertag, A., Jones,A., Rose, A.J. Liebert, M., Kleinsorg, S., Reimann, A., Vegiopoulos, A., Diaz, M.B., Strzoda, D., Yamamoto, M., Satoh, T., Akira, S., and Herzig, S. (2010). Control of Adipose Tissue Inflammation Through TRB1. *Diabetes. 59*, 1991-2000.

Pabst, T., and Mueller, B.U. (2007). Transcriptional dysregulation during myeloid transformation in AML. Oncogene *26*, 6829-6837.

Pai, S.I., Lin, Y.Y., Macaes, B., Meneshian, A., Hung, C.F., and Wu, T.C. (2005). Prospects of RNA interference therapy for cancer. Gene Ther *13*, 464-477.

Parameswaran, N., and Patial, S. (2010). Tumor necrosis factor-α signaling in macrophages. *Crit Rev Eukaryot Gene Expr. 20*, 87-103.

Pasare, C., and Medzhitov, R. (2004). Toll-like receptors and acquired immunity. *Semin Immunol. 16*, 23-26.

Paterson S, and Lello J (2003). Mixed models: getting the best use of parasitological data. Trends Parasitol *19*, 370-375.

Perotti, C., Wiedl, T., Florin, L., Reuter, H., Moffat, S., and Silbermann, M., *et, al.* (2009). Characterization of mammary epithelial cell line HC11 using the NIA 15k gene array reveals potential regulators of the undifferentiated and differentiated phenotypes. *Differentiation. 78*, 269-282.

Pestka, S., Kotenko, S.V., Muthukumaran, G., Izotova, L.S., Cook, J.R., and Garotta, G. (1997). The interferon gamma receptor: a paradigm for the multichain cytokine receptor. *Cytokine & Growth Factor Reviews 8*, 189-206.

Pfaffl, M. (2001). A new mathematical model for relative quantification in real-time RT-PCR. Nucleic Acids Res. *1*, e45.

Pfoertner, S., Jeron, A., Probst-Kepper, M., Guzman, C., Hansen, W., Westendorf, A., Toepfer, T., Schrader, A., Franzke, A., Buer, J., and Geffers, R. (2006). Signatures of human regulatory T cells: an encounter with old friends and new players. *Genome Biol. 7*, R54.

Pifer, R., Benson, A., Sturge, C.R., and Yarovinsky, F. (2011). UNC93B1 is essential for TLR11 activation and IL-12-dependent host resistance to Toxoplasma gondii. *J Biol Chem. 286*, 3307-3314.

Pilipuk, G.P., Galigniana, M.D., and Schwartz, J. (2003). Subnuclear Localization of C/EBPβ Is Regulated by Growth Hormone and Dependent on MAPK. *J Biol Chem. 278*, 35668-35677.

Poli, V. (1998). The role of C/EBP isoforms in the control of inflammatory and native immunity functions. *J Biol Chem. 273*, 29279-29282.

Pollard, J.W. (2004). Tumour-educated macrophages promote tumour progression and metastasis. *Nat Rev Cancer. 4*, 71-78.

Pradervand, S., Maurya, M., and Subramaniam, S. (2006). Identification of signaling components required for the prediction of cytokine release in RAW 264.7 macrophages. *Genome Biol. 7*, R11.

Pujol, N., Cypowyj, S., Ziegler, K., Millet, A., Astrain, A., Goncharov, A., Jin, Y., Chisholm, A.D., and Ewbank, J.J. (2008). Distinct innate immune responses to infection and wounding in the C. elegans epidermis. *Curr Biol. 18*, 481-489.

Qi, L., Heredia, J.E., Altarejos, J.Y., Screaton, R., Goebel, N., Niessen, S., Macleod, I.X., Liew, C.W., Kulkarni, R.N., Bain, J., *et al.* (2006). TRB3 links the E3 ubiquitin ligase COP1 to lipid metabolism. *Science. 312*, 1763-1766.

Radisky, D.C. (2005). Epithelial-mesenchymal transition. *J Cell Sci. 118*, 4325-4326.

Ramana, C.V., Gil, M.P., Han, Y., Ransohoff, R.M., Schreiber, R.D., and Stark, G.R. (2001). Stat1-independent regulation of gene expression in response to IFN-γ. *Proc Natl Acad Sci USA. 98*, 6674-6679.

Raschke, W.C., Baird, S., Ralph, P., and Nakoinz, I. (1978). Functional macrophage cell lines transformed by abelson leukemia virus. *Cell. 15*, 261-267.

Ray, A., Tatter, S.B., Santhanam, U., Helfgott, D.C., May, L.T., and Sehgal, P.B. (1989). Regulation of expression of Interleukin-6. *Annals of the New York Academy of Sciences. 557*, 353-362.

Roberts, P.J., and Der, C.J. (2007). Targeting the Raf-MEK-ERK mitogen-activated protein kinase cascade for the treatment of cancer. Oncogene *26*, 3291-3310.

Robinson, M.J., and Cobb, M.H. (1997). Mitogen-activated protein kinase pathways. *Curr Opin Cell Biol. 9*, 180-186.

Rorth, P., Szabo, K., and Texido, G. (2000). The level of C/EBP protein is critical for cell migration during Drosophila oogenesis and is tightly controlled by regulated degradation. *Molecular Cell. 6*, 23-30.

Rosetto, M., Engstrom, Y., Baldari, C.T., Telford, J.L., and Hultmark, D. (1995). Signals from the IL-1 Receptor Homolog, Toll, Can Activate an Immune Response in a Drosophila Hemocyte Cell Line. *Biochem Biophys Res Commun. 209*, 111-116.

Roy, S.K., Wachira, S.J., Weihua, X., Hu, J., and Kalvakolanu, D.V. (2000). CCAAT/enhancer-binding protein-β regulates interferon-induced transcription through a novel element. *J Biol Chem. 275*, 12626-12632.

Sabroe, I., Parker, L.C., Dower, S.K., and Whyte, M.K.B. (2008). The role of TLR activation in inflammation. *J Pathol. 214*, 126-135.

Santos-Sierra, S., Deshmukh, S.D., Kalnitski, J., Kuenzi, P., Wymann, M.P., Golenbock, D.T., and Henneke, P. (2009). Mal connects TLR2 to PI3Kinase activation and phagocyte polarization. *EMBO J. 28*, 2018-2027.

Scherer, L.J., and Rossi, J.J. (2003). Approaches for the sequence-specific knockdown of mRNA. Nat Biotech *21*, 1457-1465.

Schnare, M., Barton, G.M., Holt, A.C., Takeda, K., Akira, S., and Medzhitov, R. (2001). Toll-like receptors control activation of adaptive immune responses. *Nat Immunol. 2*, 947-950.

Schroder, K., Sweet, M.J., and Hume, D.A. (2006). Signal integration between IFN-γ and TLR signalling pathways in macrophages. *Immunobiology. 211*, 511-524.

Sebastian, T., and Johnson, P.F. (2006). Stop and go: anti-proliferative and mitogenic functions of the transcription factor C/EBPbeta. *Cell Cycle. 5*.

Seger, R., and Krebs, E.G. (1995). The MAPK signaling cascade. *FASEB J. 9*, 726-735.

Seher, T.C., and Leptin, M. (2000). Tribbles, a cell-cycle brake that coordinates proliferation and morphogenesis during Drosophila gastrulation. *Curr Biol. 10*, 623-629.

Selim, E., Frkanec, J.T., and Cunard, R. (2007). Fibrates upregulate TRB3 in lymphocytes independent of PPAR[alpha] by augmenting CCAAT/enhancer-binding protein[beta] (C/EBP[beta]) expression. Mol Immunol. *44*, 1218-1229.

Shang, Y.Y., Wang, Z.H., Zhang, L.P., Zhong, M., Zhang, Y., Deng, J.T., and Zhang, W. (2009). TRB3, upregulated by ox-LDL, mediates human monocyte-derived macrophage apoptosis. *FEBS J. 276*, 2752-2761.

Sica, A., Larghi, P., Mancino, A., Rubino, L., Porta, C., Totaro, M.G., Rimoldi, M., Biswas, S.K., Allavena, P., and Mantovani, A. (2008). Macrophage polarization in tumour progression. *Semin Cancer Biol. 18*, 349-355.

Simitsopoulou, M., Roilides, E., Paliogianni, F., Likartsis, C., Ioannidis, J., Kanellou, K., and Walsh, T.J. (2008). Immunomodulatory effects of voriconazole on monocytes challenged with Aspergillus fumigatus: differential role of Toll-Like receptors. *Antimicrob Agents Chemother 52*, 3301-3306.

Sing, A., Roggenkamp, A., Geiger, A.M., and Heesemann, J. (2002). Yersinia enterocolitica evasion of the host innate immune response by V antigen-induced IL-10 production of macrophages is abrogated in IL-10-deficient mice. *J Immunol. 168*, 1315-1321.

Smallie, T., Ricchetti, G., Horwood, N.J., Feldmann, M., Clark, A.R., and Williams, L.M. (2010). IL-10 inhibits transcription elongation of the human TNF gene in primary macrophages. *J Exp Med. 207*, 2081-2088.

Smith, S.M., Moran, A.P., Duggan, S.P., Ahmed, S.E., Mohamed, A.S., Windle, H.J., and et, a. (2011). Tribbles 3: A Novel Regulator of TLR2-Mediated Signaling in Response to Helicobacter pylori Lipopolysaccharide. *J Immunol.*

Sodhi, A., and Biswas, S.K. (2002). Monocyte chemoattractant protein-1-induced activation of p42/44 MAPK and c-Jun in murine peritoneal macrophages: a potential pathway for macrophage activation. *J Interferon Cytokine Res. 22*, 517-526.

Solinas, G., Germano, G., Mantovani, A., and Allavena, P. (2009). Tumor-associated macrophages (TAM) as major players of the cancer-related inflammation. *J Leukoc Biol. 86*, 1065-1073.

Sozzani, S., Molino, M., Locati, M., Luini, W., Cerletti, C., Vecchi, A., and Mantovani, A. (1993). Receptor-activated calcium influx in human monocytes exposed to monocyte chemotactic protein-1 and related cytokines. *J Immunol. 150*, 1544-1553.

Steinman, R., and Cohn, Z. (1973). Identification of a novel cell type in peripheral lymphoid organs of mice. I. Morphology, quantitation, tissue distribution. *J Exp Med. 137*, 1142-1162.

Sung, H.Y., Francis, S.E., Crossman, D.C., and Kiss-Toth, E. (2006). Regulation of expression and signalling modulator function of mammalian tribbles is cell-type specific. *Immunol Lett. 104*, 171-177.

Sung, H.Y., Guan, H., Czibula, A., King, A.R., Eder, K., and Heath, E., *et, al.* (2007). Human tribbles-1 controls proliferation and chemotaxis of smooth muscle cells via MAPK signaling pathways. *J Biol Chem. 282*, 18379-18387.

Takeda, K., Kaisho, T., and Akira, S. (2003). Toll-like receptors. *Annu Rev Immunol. 21*, 335-376.

Takeuchi, O., and Akira, S. (2010). Pattern Recognition Receptors and Inflammation. *Cell. 140*, 805-820.

Takeuchi, O., Kawai, T., Muhlradt, P.F., Morr, M., Radolf, J.D., Zychlinsky, A., Takeda, K., and Akira, S. (2001). Discrimination of bacterial lipoproteins by Toll-like receptor 6. International immunology *13*, 933-940.

Tamai, R., Sugawara, S., Takeuchi, O., Akira, S., and Takada, H. (2003). Synergistic effects of lipopolysaccharide and interferon-γ in inducing interleukin-8 production in human monocytic THP-1 cells is accompanied by up-regulation of CD14, Toll-like receptor 4, MD-2 and MyD88 expression. *J Endotoxin Res. 9*, 145-153.

Thiery, J.P., Acloque, H., Huang, R.Y.J., and Nieto, M.A. (2009). Epithelial-mesenchymal transitions in development and disease. Cell *139*, 871-890.

Thiery, J.P., and Sleeman, J.P. (2006). Complex networks orchestrate epithelial-mesenchymal transitions. *Nat Rev Mol Cell Biol. 7*, 131-142.

Tournier, C., Hess, P., Yang, D.D., Xu, J., Turner, T.K., Nimnual, A., Bar-Sagi, D., Jones, S.N., Flavell, R.A., and Davis, R.J. (2000). Requirement of JNK for stress-induced activation of the cytochrome c-mediated death pathway. *Science. 288*, 870-874.

Trinchieri, G. (2010). Type I interferon: friend or foe? *J Exp Med. 207*, 2053-2063.

Ubol, S., and Halstead, S.B. (2010). How innate immune mechanisms contribute to antibody-enhanced viral infections. *Clin Vaccine Immunol. 17*, 1829-1835.

Uematsu, S., and Akira, S. (2007). Toll-like receptors and Type I interferons. Journal of Biological Chemistry *282*, 15319-15323.

Valledor, A.F., Borras, F.E., Cullell-Young, M., and Celada, A. (1998). Transcription factors that regulate monocyte/macrophage differentiation. *J Leukoc Biol. 63*, 405-417.

Varshavsky, A. (1997). The ubiquitin system. *Trends Biochem Sci. 22*, 383-387.

Vega, S., Morales, A.V., Ocana, O.H., Valdes, F., Fabregat, I., and Nieto, M.A. (2004). Snail blocks the cell cycle and confers resistance to cell death. *Genes Dev. 18*, 1131-1143.

Vila-del Sol, V., Carmen Punzo ´n, and Manuel Fresno (2008). IFN-γ -induced TNF-α expression is regulated by interferon regulatory factors 1 and 8 in mouse macrophages. *J Immunol. 181*, 4461–4470.

Wan, Y., Kim, T.W., Yu, M., Zhou, H., Yamashita, M., Kang, Z., Yin, W., Wang, J.-a., Thomas, J., Sen, G.C.*, et al.* (2011). The dual functions of IL-1 receptor-associated kinase 2 in TLR9-mediated IFN and proinflammatory cytokine production. *J Immunol. 186*, 3006-3014.

Wen, Z., Zhong, Z., and Darnell, J.E. (1995). Maximal activation of transcription by statl and stat3 requires both tyrosine and serine phosphorylation. *Cell. 82*, 241-250.

Wessells, J., Yakar, S., and Johnson, P.F. (2004). Critical prosurvival roles for C/EBPβ and insulin-like growth factor I in macrophage tumor cells. *Mol Cell Biol. 24*, 3238-3250.

Widmann, C., Gibson, S., Jarpe, M.B., and Johnson, G.L. (1999). Mitogen-activated protein kinase: conservation of a three-kinase module from yeast to human. *Physiol Rev. 79*, 143-180.

Wilkin, F., Savonet, V., Radulescu, A., Petermans, J., Dumont, J.E., and Maenhaut, C. (1996). Identification and characterization of novel genes modulated in the thyroid of dogs treated with methimazole and propylthiouracil. *J Biol Chem. 271*, 28451-28457.

Wilkin, F., Suarez-Huerta, N., Robaye, B., Peetermans, J., Libert, F., Dumont, J.E., and Maenhaut, C. (1997). Characterization of a phosphoprotein whose mRNA is regulated by the mitogenic pathways in dog thyroid cells. *Eur J Biochem. 248*, 660-668.

Wouters, B.J., Jorda, M.A., Keeshan, K., Louwers, I., Erpelinck-Verschueren, C.A.J., and Tielemans, D., *et, al.* (2007). Distinct gene expression profiles of acute myeloid/T-lymphoid leukemia with silenced CEBPA and mutations in NOTCH1. *Blood. 110*, 3706-3714.

Wu, Y., and Zhou, B.P. (2010). TNF-α/NF-κB/Snail pathway in cancer cell migration and invasion. *Br J Cancer. 102*, 639-644.

Yamamoto, M., Uematsu, S., Okamoto, T., Matsuura, Y., Sato, S., and Kumar, H., *et, al.* (2007). Enhanced TLR-mediated NF-IL6 dependent gene expression by Trib1 deficiency. *J Exp Med. 204*, 2233-2239.

Yokoyama, T., Kanno, Y., Yamazaki, Y., Takahara, T., Miyata, S., and Nakamura, T. (2010). Trib1 links the MEK1/ERK pathway in myeloid leukemogenesis. *Blood. 119*, 246-264.

Yokoyama, T., and Nakamura, T. (2011). Tribbles in disease: Signaling pathways important for cellular function and neoplastic transformation. *Cancer Sci. 102*, 1115-1122.

Yong, H.-Y., Koh, M.-S., and Moon, A. (2009). The p38 MAPK inhibitors for the treatment of inflammatory diseases and cancer. *Expert Opin Investig Drugs. 18*, 1893-1905.

Zahnow, C.A. (2009). CCAAT/enhancer-binding protein β: its role in breast cancer and associations with receptor tyrosine kinases. *Expert Rev Mol Med. 11*, 1-29.

Zahnow, C.A., Cardiff, R.D., Laucirica, R., Medina, D., and Rosen, J.M. (2001). A role for CCAAT/enhancer binding protein β-liver-enriched inhibitory protein in mammary epithelial cell proliferation. *Cancer Res. 61*, 261-269.

Zanella, F., Renner, O., Garcia, B., Callejas, S., Dopazo, A., and Peregrina, S. (2010). Human TRIB2 is a repressor of FOXO that contributes to the malignant phenotype of melanoma cells. *Oncogene. 29*, 2973-2982.

Zhang, S.-Y., Boisson-Dupuis, S., Chapgier, A., Yang, K., Bustamante, J., Puel, A., Picard, C., Abel, L., Jouanguy, E., and Casanova, J.-L. (2008). Inborn errors of interferon (IFN)-mediated immunity in humans: insights into the respective roles of IFN-α/β, IFN-γ, and IFN-λ in host defense. *Immunol Rev. 226*, 29-40.

Zhang, X., and Mosser, D.M. (2008). Macrophage activation by endogenous danger signals. *J Pathol. 214*, 161-178.